EVALUATION OF PERFORMANCE OF EPOXY BASED COATINGS FOR CORROSION INHIBITION IN REINFORCING BARS

A Thesis submitted in fulfilment of the requirement for the award of the degree of

MASTERS OF ENGINEERING
IN
STRUCTURAL ENGINEERING

Submitted by:

NIKHIL SHARMA

Roll No: - 801724019

Under the supervision of

DR. SHRUTI SHARMA

Associate Professor, CED,
TIET, Patiala

DR. RAJEEV MEHTA

Professor, CHED
TIET, Patiala

CIVIL ENGINEERING DEPARTMENT

THAPAR INSTITUTE OF ENGINEERING AND TECHNOLOGY
(A DEEMED TO BE UNIVERSITY), PATIALA, PUNJAB
JULY, 2019

DECLARATION

I, Nikhil Sharma hereby declare that the work presented in this thesis entitled "**EVALUATION OF PERFORMANCE OF EPOXY BASED COATINGS FOR CORROSION INHIBITION IN REINFORCING BARS**", in fulfilment of the requirement for the award of the degree of **Masters of Engineering** in **Structural Engineering** submitted at Civil Engineering Department (CED), Thapar Institute of Engineering & Technology (Deemed to be University), Patiala, is an authentic record of work carried out under the supervision of **Dr. Shruti Sharma** (Associate professor, CED, TIET, Patiala) and **Dr. Rajeev Mehta** (Professor, CHED, TIET, Patiala) from June 2018- July 2019. The matter presented in this thesis has not been submitted either in part or full to any other university or institute for the award of any other degree.

Date: 31/7/2019

(NIKHIL SHARMA)

(801724019)

CERTIFICATE

This is to certify that the above declaration made by the student concerned is correct according to the best of my knowledge and belief.

Date: - 31/7/2019

Dr. Shruti Sharma
Associate Professor
Civil Engineering Department (CED)
Thapar Institute of Engineering & Technology (A Deemed to Be University), Patiala, Punjab

Date: - 31/7/2019

Dr. Rajeev Mehta
Professor
Chemical Engineering Department (CHED)
Thapar Institute of Engineering & Technology (A Deemed to Be University), Patiala, Punjab

ACKNOWLEDGEMENT

This acknowledgment is meant to be credited to all those individuals who were directly or indirectly engaged in my dissertation work.

First of all, I want to convey my gratitude and indebtedness to my Supervisor, Dr. Shruti Sharma, Associate Professor of Civil Engineering Department and Co-Supervisor, Dr. Rajeev Mehta, Professor, Chemical Engineering Department, Thapar Institute of Engineering & Technology (Deemed to be University), Patiala for their profound participation, invaluable and ongoing encouragement throughout this work. I am very grateful to them for always being there whenever I need them.

I prob will not discover enough words to convey my sentiment of gratitude to the entire professors and staff of the Civil Engineering Department of Thapar Institute of Engineering & Technology (Deemed to be University), Patiala for their assistance, encouragement and personal support that helped me to complete my thesis successfully.

Similar, profound gratitude goes to PhD scholars Mr. Sunil Garhwal, Mr. Anil Garhwal for devoting their precious time as well as extending constant support and encouragement which helps me in the completion of project.

The cheerful support of my friend and colleagues is sincerely appreciated. Special words of appreciation go to Mr. Hitesh Bhardwaj, Mr. Manreet Sidhu, and other laboratory staff, who helped me in my experimental work.

I also ackNowledge the support of Structure Health Monitoring Lab and SAI Lab, TIET, Patiala for testing.

Finally, I would like to dedicate this project work to my parents who have always been an excellent source of inspiration and help, particularly in all my academic efforts.

ABSTRACT

Corrosion of reinforcing steel in concrete structures is a huge problem facing by the construction industry. Corrosion of reinforcing steel leads to a catastrophic failure of structures. Recently, to inhibit the corrosion of concrete structures either self-healing concrete or different epoxy coatings for reinforcing bars were used. In this study, three different types of epoxy based self-healing coatings: Nano-clay based, Tung-oil microcapsules based and hybrid of both epoxy coatings were proposed to inhibit the corrosion of reinforcing bars in concrete. Coatings were tested on plain mild steel rebar and rebar in concrete. Also coatings were initially damaged and tested to evaluate the self-healing performances of the coatings. Non-destructive testing used to evaluate the performances of all coatings and further destructive testing was done to quantify the non-destructive results. Pull-out strength testing was done to evaluate the effect of coatings on the bond strength between steel and concrete.

Various tests revealed that, all the proposed coatings showed significant delay in corrosion as compared with conventional epoxy coatings whereas tung-oil based micro-encapsulated coatings were most promising out of all the coatings. In tung-oil micro-encapsulated epoxy coatings, self-healing effect was observed which was triggered by the damage of coatings either initially induced or due to corrosion initiation and achieved by the polymerization reaction of tung-oil. By introducing tung-oil microcapsules in epoxy, mass loss due to corrosion was 65% less and residual tensile strength was 63% more in comparison with conventional epoxy coatings. Pull-out strength barely affected by these coatings in comparison with conventional epoxy coatings.

TABLE OF CONTENTS

LIST OF FIGURES

LIST OF TABLES

CHAPTER – 1
INTRODUCTION

1.1 BACKGROUND

Concrete is one of the most widely used structural material in the world because of its versatility, high compressive strength, durability and locally availability but it also have some limitations. It is vulnerable to many sources of damages like internal cracks in initial stage or major cracks at later stages. Initially concrete has internal damages due to factors like extreme heat and cold, sudden extreme loads, etc. which may not be seen until cracks become large and then major repair is needed. As concrete shrinks and expands with dissimilarities in moisture and temperature, cracks develop. Factors that can also affect concrete include design flaws, shrinkage and poor quality of construction materials used. Factors like corrosion of reinforcement steel, chemical attacks, etc. leads to a catastrophic failure of the structure during its service life. Structures affected by these factors either require major repair or needs to be rebuild to become serviceable again.

According to an American report *(ASCE, 2017)* world is going to face a rapidly growing infrastructure maintenance crisis. Over billions of dollars are required to uphold and recover the built environment in infrastructure industry and still this is not sufficient to retain infrastructure in a state of good repair. In 2013, the American Society of Civil Engineers (ASCE) estimated that $3.6 trillion will be required by 2020 to improve infrastructure of United States to an acceptable condition. Steel-reinforced concrete is the most widely used infrastructure material all over the world. The production of concrete is an energy-intensive process where in transportation, mining and processing are considered. About 2.35 billion metric tons of concrete are produced every year, which contributes to a shocking 10% of CO_2 emissions into the atmosphere. Secondly, concrete is a major contributor to environmental pollution primarily because of the production of its major component i.e. cement. Hence, any effort to improve the lifetime of concrete structures will indirectly improve the sustainability of the environment.

Corrosion of the reinforcement in concrete is one of the most critical causes of failure of concrete structures. In India, about $ 40 billion per year are spent on repair due to the corrosion in both infrastructure and industry segments. Cracks developed in concrete increases the permeability in the concrete, which allows the penetration of the aggressive media (like, carbon dioxide and chloride ions) into the concrete, accelerate the corrosion and reduce the durability and strength of

concrete. Thus, to protect the reinforcement steel from corrosion either a concrete with low permeability is the key, or reinforcement bars which are less susceptible to corrosion can be used.

1.2 CORROSION MECHANISM

Corrosion of steel occurs in concrete principally due to carbonation and chloride attacks (*Broomfield, 2007*). Initially, steel in concrete does not corrode just because of the alkalinity of the concrete which opposes the corrosion of reinforcement in early stages. Factors responsible for corrosion of rebar are:

- Chlorides, free chlorides or bound chlorides
- Carbon dioxide
- Type of steel
- Moisture
- Permeability of concrete
- Temperature
- Reduction of pore solution concentration in concrete
- Concrete resistivity

1.2.1 Corrosion in Absence of Chlorides (Oxide Corrosion)

Corrosion of rebar is an electrochemical process which includes transfer of electrons from a part of one material to another. In the presence of oxygen and water, anodic and cathodic reactions occurs leading to corrosion initiation. There is dissolution of Fe at anode and deposition of rust product at cathode. Anodic reaction leads to pitting in rebar and formation of voluminous rust product leads to cracking and spalling in concrete surrounding the rebar.

Anodic reaction: $Fe \longrightarrow Fe^{2+} + 2e^-$ [1.1]

Cathodic reaction: $2e^- + 1/2O_2 + H_2O \longrightarrow 2OH^-$ [1.2]

Formation of red rust: $Fe^{2+} + 2OH^- \longrightarrow Fe(OH)_2$ (Ferrous hydroxide) [1.3]

$4\,Fe(OH)_2 + O_2 + 2H_2O \longrightarrow 4\,Fe(OH)_3$ (Ferric hydroxide) [1.4]

$2\,Fe(OH)_3 \longrightarrow Fe_2O_3.3H_2O$ (hydrated Ferric oxide) [1.5]

(rust product)

1.2.2 Chloride Corrosion

Likely sources of chlorides in concrete are admixtures, aggregates, deicing chemicals, use of sea water for construction, mixing water and from marine environment. Corrosion of steel reinforcement due to chlorides initiates from anodic reaction where no oxygen is needed. In anodic reaction iron reacts with chloride ions and forms a complex iron-chloride. Further in cathodic reaction, this complex diffuses away towards higher concentration of oxygen or higher pH to react with hydroxyl ions and forms ferrous hydroxide (rust produced). Rate of corrosion in chloride mechanism is faster than oxide mechanism. Moreover, chloride corrosion leads to loss of significant properties of the bar like local weakening, reduction in ductility and significant loss of strength.

Anodic reaction: $Fe + 2Cl^- \longrightarrow (Fe^{2+} + 2Cl^-) + 2e^-$ [1.6]

Cathodic reaction: $(Fe^{2+} + 2Cl^-) + 2e^- + H_2O \longrightarrow Fe(OH)_2 + 2H^+ 2Cl^-$ [1.7]

(rust product)

So, it is important to look for measures to prevent or delay the initiation of corrosion at steel rebar itself. Otherwise maintenance of concrete would be regularly required to maintain structure durable or healthy, which is an expensive proposition. The construction industry uses various methods to delay or prevent corrosion:

- Use of low permeable concrete or rebar less susceptible to corrosion is key to control the corrosion.
- Use of Supplementary Cementitious Materials (SCM) and Epoxy Coated Rebar (ECR) are other methods to control corrosion by reducing permeability and making an impervious layer for rebar, respectively.
- Further, use of stainless steel rods, galvanized rebar etc., which are expensive, is also a method to delay or prevent corrosion.

Recently, construction industry has taken substantial interest in engineering concrete as a smart material, which reacts only when it is needed. Whenever cracks occur it will block the crack, reduce the permeability or protect the rebar from corrosion by using smart materials. They also reduce excessive routine maintenance, which helps in economic growth balance. This strategy is the use of Self-Healing Concrete.

1.3 SELF-HEALING CONCRETE

Self-healing means the process of recovery. Self-healing materials are a new class of smart materials that keep the ability to completely or partly recover a functionality that is facilitated by operational use. Specifically in civil engineering process of recovery of the cracks of structural elements. There are two functionality fatalities of structures i.e. local and global. Local functionality loss is defined as the condition when a section of a material or structure shows degraded performance when correlated with the rest of the material/structure. Global functionality loss is defined as the condition when the material or structure shows degraded performance when related to its properties prior to any exposure to working loads. Generally two types of healing mechanism exists: Intrinsic self-healing mechanism and Extrinsic self-healing mechanism.

- **Intrinsic self-healing:** In this mechanism materials are naturally able to restore its functionality without additives but sometimes system frequently requires an external trigger to initiate healing process. Triggers can be heat, sun-light, electrical, thermo-mechanical, etc.
- **Extrinsic self-healing:** In this mechanism healing material is not the part of the main material, they are separated from the surrounding material by microcapsules or vascular network and are triggered when the crack initiates in the structure and then healing agents react and allows the reestablishment of material functionalities by healing the structure.

Self-healing concrete is defined as a smart material involving self-healing agents, which automatically heals the structure when cracks occur during its serviceability. These self-healing agents are transferred in the structure through microcapsules, hollow fibers or even in the form of organic matter. Self-healing ability of concrete can be enhanced by the integration of biochemical and chemical strategies. Approaches to achieve self-healing in cementitious materials are illustrated in Figure 1.1.

1.3.1 Autogenous Healing

Autogenous healing is also referred to as intrinsic healing. Autogenous healing is the natural ability of the cementitious materials to repair or heal cracks whenever they occur. Its ability to do so depends upon the composition of the concrete. Healing of the cracks in concrete is done mainly by two mechanisms i.e. hydration of un-hydrated cementitious products present in the

matrix and carbonation of dissolved calcium hydroxide. Contribution of these two mechanisms depend on many factors like presence of water, age of concrete at cracking, crack width, temperature, etc. Apparently in autogenous healing, its healing capacity principally depends on the age of the concrete at the time of cracking. Due to un-hydrated cement particles hydration is main healing mechanism for young concrete. At later stage, calcium carbonate precipitates and becomes the major contributor to the healing mechanism (*Tittelboom et al., 2013*).

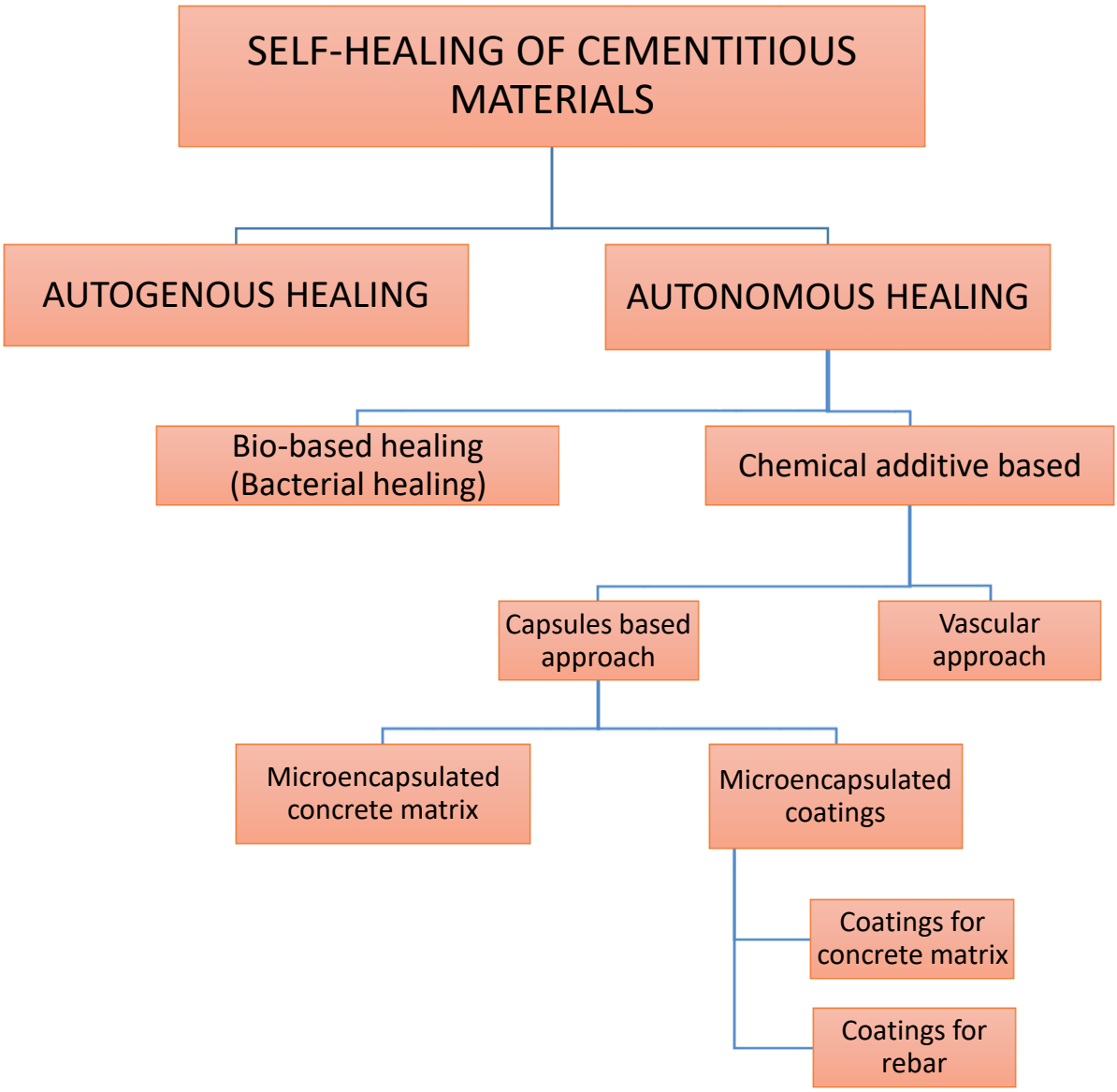

Figure 1.1: Approaches to self-healing in cementitious materials.

Background

Several reports lists the healing capability of autogenous healing. One of the main weakNess of this approach is the limitation related to crack width, and is mainly effective for narrow cracks. Different studies have been reported for crack widths of 5-10 µm *(Jacobsen et al. 1995) (Sahmaran et al. 2008),* 200 µm *(Edvardsen et al. 1999),* and 300 µm *(Clear et al. 1985),* and they concluded that the healing process is only effective for the narrow cracks, which healed completely by this approach. Wider cracks which affect the durability of concrete cannot be effectively healed by this approach. Further work has been done to improve the autogenous healing. *Ter Heide et al. (2007)* discovered that healing can be improved by applying compressive force to make crack faces contact each other. Besides, continuous water is required to support the hydration procedure so that cracks can be totally healed. The phenomenon of autogenous healing is more prominent in young concrete, whereas carbonate precipitation is more effective at later stages. From recent studies, it was seen that if the crack width is restricted then autogenous healing mechanism is more effective. The continuous supply of water improves the healing mechanism since hydration and crystallization process promotes autogenous self-healing. Some of the work on improved autogenous healing are discussed below:

- **Restriction of crack width:** *Li et al. (1998)* first proposed use of fiber reinforced strain hardening Engineered Cementitious Composite (ECC) to restrict crack width which is susceptible to autogenous self-healing. *Sakai et al. (2003)* and *Kuang et al. (2008)* suggested that cracks cannot restricted at the time of crack development but when the structure is unloaded cracks are closed due to the nature of shape memory alloys embedded in concrete. *Homma et al. (2009)* and *Nishiwaki et al. (2012)* compared efficiency of polypropylene, steel cord and PVA fibers to reduce crack widths. PVA fibers had shown maximum efficiency to restrict crack width and steel cord fibers showed slight crack closing as steel corroded inside cracks.

- **Water supply:** Several researchers examined the likelihood to mix Super Absorbent Polymers (SAP) into cementitious materials to offer additional water. SAP are cross-linked polymers that can engross a huge amount of liquid and swell significantly to form an insoluble gel. Their swelling capacity is depend upon the alkalinity and ionic concentration of the matrix. At the time of hydration, SAP releases the engrossed water and shrinks,

leaving behind some macro-pores. When cracks rise, they are expected to spread through the pores and entrance of moisture through the crack causes SAP to swell again. During dry periods, SAP releases the water content, encouraging autogenous healing. *Qian et al. (2010)* proposed that utilization of nano-clays as internal water reservoir in ECC and concluded that water retaining capacity of clay provide internal water for future hydration process leading to autogeneous healing.

- **Hydration and Crystallization:** Alternative attempts involve use of Supplementary Cementitious Materials (SCM) which promotes crystal deposition inside the cracks. Materials like fly ash and blast furnace slag which hydrate at slower rate than cement and consequently, un-hydrated particles of such minerals encourage autogenous healing mechanism at later stage of concrete. *Ahn et al. (2008)* concluded that autogenous crack healing can be acquired when 10% replacement of the cement content by a mixture of expansive agents, chemical agents and geo-materials. *Jonkers (2007)* suggested that it would be beneficial to custom $CaCO_3$ precipitating bacterial spores. But bacteria will die once the cells are surround by $CaCO_3$ crystals and the bacterial action will also stop when all nutrients are spent. It was concluded that even the bacterial method will not allow an infinite recurrence of the healing process.

1.3.2 Autonomous Healing

Autonomous healing is also referred to as extrinsic healing. To repair structure autonomously healing agents are used with chemical composition different from the concrete constituents, and remains enclosed in a polymer which make them non-reactive until they needed. The effectiveness of this healing mechanism is depend upon the properties of the healing agents used. The autonomous healing broadly classified into two categories:

Bio-Based Healing

The concept of self- healing of cracks by biological resources is receiving great attention among researchers, since it is a natural method and is environmental friendly. *Achal et al. (2010),* self-healing capability of concrete has been enhanced by the amalgamation of bacteria, which encourage precipitation of calcium carbonate through their metabolic action. These precipitates form an effective closure against crack related water entrance. Biological healing of concrete is extremely necessary in complex underground structures and dangerous liquid containers. The

usage of bacteria is a durable method for structural restoration and there are several types of bacteria which have been used to crop bio-based self-healing concrete materials. From the studies *(Achal et al. 2010)* it also has been established that biological healing agents not only heal the structural elements but also enhances the strength and durability of the concrete. Bacteria are fed by micro-nutrients of different forms due to which calcite is constantly precipitating and transformed into insoluble limestone which further solidifies on the cracked surface. This phenomenon is called the Microbiologically Induced Calcite Precipitation (MICP). Bacterial concrete leads to calcite precipitation in concrete, which also improves the compressive strength and reduces the permeability of water and other liquids in concrete. There are certain types of biological materials like Bacillus sp CT-5, Bacillus cereus, Bacillus pasteurii, Sporosarcina pasrteurii, Bacillus subtilis, Enterococcus sp, etc. which are used as healing agents and are used to enhance the mechanical and durability properties of concrete *(Jonkers et al. 2010)* and mortar *(Achal et al. 2010).* Hence biological self-healing agents not only repair cracks in concrete autonomously but they also increase the strength and durability properties of concrete. There are certain approaches by which bio-based self-healing is put into application:

- By spraying/injection of bacteria on the damaged region of concrete or in bacterial nature curing of concrete been done.
- By direct addition of bacteria into the concrete mix.
- By encapsulation of bacteria in concrete matrix.

It was, however evident from the studies that it is very difficult to provide food to bacteria for a long period of time in concrete, which limits its usage. Life span of the bacteria in concrete is very small and also due to the typical nature of concrete reactions like high temperature at the time of hydration process, high alkalinity, selection of the bacteria becomes tougher task and the issue of longevity of the bacteria still needs to be resolved.

Chemical Additive Based Healing

When self-healing is achieved through the reaction of certain chemical agents it is called chemical based self-healing of cementitious materials. Direct chemical based healing agents are used for the healing of structures. Two prime strategies exist to implement these agents into the structure:

- Capsules based

- Vascular network based

These vascular networks and capsules rupture when crack appears, there by releasing the healing agents into the structure and healing the damaged region. In bio-based healing it was found that bacteria in concrete remained viable only for maximum of 4-6 months and this limitation can easily be eliminated by chemical based approach. In chemical based approach, healing agents in the microcapsules and vascular tubes remain non-reactive until they needed by shell of healing agent (Urea-Formaldehyde shell), which manufactures at the time of synthesis process. These chemical based approaches are more promising than bio-based approaches for long-life of healing agents and consequent healing of the concrete structure.

1.4 CAPSULE BASED SELF-HEALING

In chemical based healing, capsules and vascular networks play a crucial role in healing of the structure. By effecting variations in the synthesis procedure of their capsules and vascular networks, the healing efficiency can be changed, significantly. In this section various methods involving chemical based healing and synthesis procedure of the capsules are discussed in brief. The vascular based approach is not described since it is beyond the scope of this work.

1.4.1 Concept and Methodology

In this approach, the capsules provide mechanical shield to the healing agents and when crack occurs, they get triggered and release the healing agents from the capsules, by rupturing or diffusion *(White et al., 2001)*. The external trigger to initiate the healing mechanism may be air or heat and change in pH or moisture. This is related to the nature or character of microcapsules prepared. In cases wherever cracking is the trigger tool, the capsules rupture and the healing agent is dragged into the crack by capillary action.

Encapsulation strategy enhances the healing capability and lifespan of healing agents by controlling their release into the concrete matrix. The major disadvantage of this approach is its repeatability over a long period. The amount of repair agent is limited and most of the healing agents capsules are shattered under a single loading sequence and hence repetitive healing over the long period is questionable. Depending on the capsulation method used, capsules either are tactically located at expected locations of failure or spread throughout the matrix homogeneously (*Tittelboom et al., 2013*). A schematic procedure of microcapsules healing is shown (Figure 1.2),

which shows crack initiation, healing and curing process. Healing process depends heavily on three sub-processes:

- Immediate rupture of inserted capsules
- Flow of healing agent into the crack location, and
- Satisfactory curing reactions

There are some factors on which the effectiveness of healing agent curing process is completely dependent:

- Curing time and its kinetics
- Capsules shell material and shell wall thickNess
- Composition of healing agents
- Accelerators / Catalyst
- Robustness throughout mixing with concrete matrix
- Probability of cracks meeting the capsules
- Effect of vacant capsules on concrete strength
- Controllability of release of agents
- Stability of healing agent
- Sealing ability
- Repeatability of action

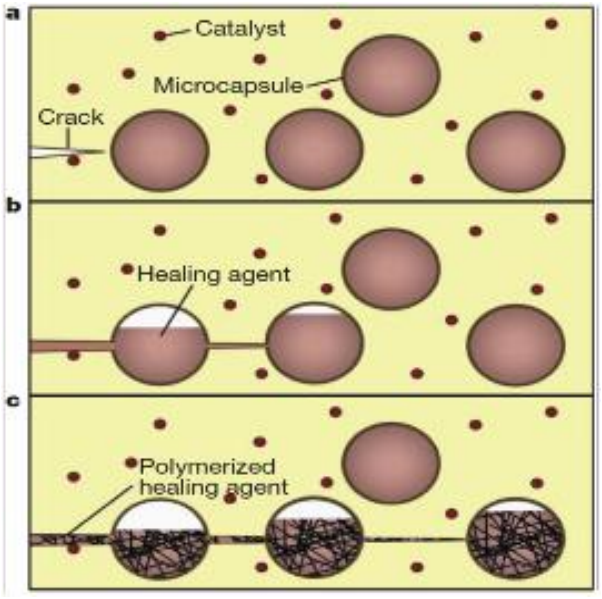

Figure 1.2: Healing mechanism of a microencapsulated system: (a) Initiation of crack; (b) releasing of healing agent; (c) Curing *(White et al., 2001).*

Encouraged by the self-repair polymeric materials, maximum of healing agents in encapsulated concrete are polymers. Polymers are capable with potential ability for crack healing, such as low viscosity, stress transfer capability, and fast polymerization kinetics. Healing agents are broadly divided into two categories i.e. Single component healing agents (without catalyst) and Multi-components healing agents (with catalyst) *(Xue et al. 2018)*. Examples of some self-healing agents are Cyanoacrylate, epoxy resin, sodium silicate, polyurethane, etc. Commonly these micro/Nano capsules are small elements containing a droplet of liquid, solid or gaseous core material enclosed by a film called shell in which 10-90 wt% is core material.

1.4.2 Microcapsules Synthesis Procedure

There are several methods used to synthesis chemical based microcapsules and there are interfacial polymerization, coacervation, *in-situ* polymerization, extrusion, sol-gel methods etc. Among all these methods, the most useful and easiest method is *in-situ* polymerization because it does not require high level of technology. Most common healing material used in self-healing processes is a liquid because of the requirement of free flow into the cracks through capillarity action and by gravity effect. In Urea-Formaldehyde (UF) and Melamine-Formaldehyde (MF) types of micro-encapsulation systems, *in-situ* polymerization technique involved is very comparable to interfacial coating. The distinctive characteristic of *in-situ* polymerization process is that reactants (aqueous phase constituents) are not involved in the core material. There are two phases in the synthesis process of microcapsules *(Ansari et al. 2017)*, an aqueous phase and a continuous phase. In aqueous phase, the constituents are used to control the behavior of prepared material and in continuous phase the polymerization reactions occur. All polymerization happens in the continuous phase only, rather than on the both sides of the interface i.e. between the continuous phase and the core material.

1.4.3 Methods to Introduce Microcapsules in Concrete

Most commonly adopted ways of introducing capsules based approach in cementitious materials are:

- **Micro-Encapsulated Concrete Matrix:** In this approach, self-healing microcapsules are used as a part of the concrete matrix composition. Microcapsules are prepared before the casting of cementitious material and at the time of casting in the mix, microcapsules are

mixed with the rest of the materials. This type of approach have been used as an alternative to autogenous healing approach in which healing capacity of self-healing concrete is increased by induced chemicals in the form of capsules into the concrete matrix. These capsules rupture when crack occurs to release healing agent to trigger the healing mechanism. Hence primary requirement of the microcapsules is brittleness. At the time of mixing or casting due to vibration or impact there is a high probability of rupturing brittle microcapsules.

An approach to save microcapsules from rupturing at the time of mixing was introduced. Where in wrapping of capsules with cord is done and shelter then with slight layer of mortar. In other method, a layer of cement paste is put into the molds and afterwards capsules are placed on it. The remaining mold is then filled with paste and vibrated. Alternatively, a layer of sand with epoxy resin before mixing can be used to shelter the microcapsules. Detailed discussion and literature review is presented in Section 2.2.

- **Micro-Encapsulated Coatings:** Another method of capsule based approach is the use of micro-encapsulated coatings for the self-healing of cementitious materials. These coatings were inspired from the field of organic coatings. In recent years, coatings are suggested for metals to save them from the toxic environments and similar have been suggested for concrete.

Coatings for concrete matrix: The coatings for concrete matrix were proposed *(Song et al. 2013)* since they are environmental friendly. Matrix coatings secured the surface of the concrete from deterioration. Cracks induced by the loading, triggers the healing mechanism and then healing occurs by polymerization of the healing agents. Further studies *(Yang et al. 2016* and *Kim et al. 2017)* have been reported to improve the crack limits, repeatability and effectiveness of coatings as per the environment of the structure. These coatings are very effective to use for bridge piers *(Yang et al. 2016)*.

Coatings for rebar: In reinforced concrete, steel bar has the most important part to play, they provide the desired ductility strength to the RC structures. But these reinforcing bars are susceptible to corrosion, which inhibits their serviceability. Researchers proposed

alternatives to save rebar from corrosion by creating an impervious layer of epoxy coatings *(Lau et al. 2007)*, stainless steel bars *(García-Alonso et al. 2007)*, galvanized rebar *(Fayala et al. 2013)*, etc. The brittleness of epoxy coatings leading to their damage at the time of their transportation and casting, reduces their effectiveness. Recently researchers proposed *(Chen et al. 2017)* self-healing organic epoxy coatings for rebar. The challenge is the appropriate thickNess of the self-healing coating on the rebar i.e. if it is too thin then aggressive media may enter easily and if it is too thick then bond strength between concrete and steel may be compromised and advantage of using rebar may be lost.

1.5 NON-DESTRUCTIVE MONITORING FOR SELF-HEALING

Monitoring of the concrete structures or different mechanism of self-healing been achieved by non-destructive testing in different fields. It includes course of inspecting, evaluating materials and testing without abolishing the serviceability of the system. These testing methods do not affect the utility of the testing systems only monitor the remaining health or strength of the systems. Non-destructive techniques (NDT) like, visual inspection, vibration measurements, radiography, acoustic emission, infrared thermography, ultrasonic guided waves, X-ray measurement, etc. are used to monitor the structures. Since corrosion of reinforced bars results in a catastrophic failure so their detection before it initiates and leads the structure to failure is very necessary. Techniques like, visual inspection, ultrasonic guided wave, corrosion current and acoustic emission (*(Sharma et al. 2018)* have been useful to monitor the corrosion in RC structure *(Sharma et al. 2011)*.

These NDT techniques have also been used to monitor the healing mechanism were like, ultrasonic guided waves, acoustic emission, X-ray micro-computed tomography, Digital image correlation etc. *In et al. (2013)* monitor the self-healing cracks in concrete by ultrasonic technique. *Dong et al. (2018)* studied the self-healing mechanism with X-Ray Micro-Computed Tomography (XCT) to evaluate the performance of self-healing microcapsules. With the images of XCT it was concluded that the self-healing agents delayed the corrosion process. Researchers (*Li et al., 2017* and *Tsangouri et al., 2013*) used Acoustic Emission (AE) and Digital Image Correlation (DIC) to monitor the healing of cracks in concrete effectively.

1.6 GAPS IN RESEARCH AREA

- Crack of limited width can be healed by autogenous self-healing. But new approaches need to be investigated for cracks larger than 300 μm.
- Brittleness of microcapsules is required to be optimized when, rupturing of microcapsules taken place and also at the time of mixing.
- Repeatability of the healing mechanism of capsules based approach needs to be explored.
- Reduction in the strength resulting by introduction of capsules remains to be explored.
- Self-healing coatings effect on the bond strength of concrete and steel is questionable.
- Very few reports are there on the NDT monitoring of self-healing coatings.

1.7 OBJECTIVES OF WORK

- Preparation of three different types of self-healing epoxy coatings for rebar, to be used in concrete for corrosion inhibition.
- Nano-clay based epoxy coatings, tung-oil microcapsules based epoxy coatings and hybrid of nano-clay and tung-oil microcapsules based epoxy coatings to be prepared and evaluated.
- Damage induced coatings to be prepared to analyze the self-healing efficiency as corrosion inhibition and correlated with the undamaged coatings.
- To do the non-destructive testing for corrosion protection evaluation of coated plain bars and coated bars reinforced in concrete.
- Destructive testing for the assessment of NDT to be done.
- Determination of rebar pullout strength testing was done to compare the bond strength between the interface of steel and concrete of coated bars.

1.8 LAYOUT OF THESIS

The thesis covers 5 chapters and each chapter has its own importance in the thesis.

Chapter 1: Characterizes the general introduction of self-healing of cementitious materials and techniques used to monitor the behavior of self-healing mechanism non-destructively along with the objective and scope of present work.

Chapter 2: Includes literature review of the self-healing approaches using chemical additives, corrosion protection using nano-clay and NDT monitoring.

Chapter 3: The methodology of the all experimental program used, procedure of the all experiments, the testing samples and characterization of samples explained in detail in this chapter.

Chapter 4: Deals with the experimental results and analysis of all results with significant discussions.

Chapter 5: Summary of test results and conclusions from the results with recommendations for future work.

CHAPTER – 2
LITERATURE REVIEW

2.1 GENERAL

This chapter presents a review of the studies on chemical based approach i.e. capsules based and vascular channel based, with focus on encapsulated concrete and encapsulated coatings to delay the corrosion of reinforced steel. Studies reported for the corrosion inhibition using nano-clay and corrosion monitoring using ultrasonic guided waves have also been discussed.

2.2 CHEMICAL BASED SELF-HEALING

It is well established that concrete has its own self-healing capability due to the hydration process of un-hydrated particles in initial stage of concrete and the carbonation on later stages. Due to the limitations of autogeneous healing, autonomic healing process was introduced in which biological and chemical based healing agents were used. In this section studies on chemical based approach are discussed.

Yang et al. (2011) studied microcapsules embedded in concrete matrix. The microcapsules prepared were having oil as core and silica gel as the shell material. Healing agent used was Methyl-Methacrylate (MMA) monomer and the catalyst was Triethyl-Borane (TEB), both in oil core phase in the system. Healing agents were microencapsulated through an interfacial self-assembly process and sol–gel reaction. With three types of carbon microfiber (2% by volume) and self-healing microcapsules (1.5% MMA and 0.03% TEB by weight of cement) mortar specimens were prepared and termed as Self-Healing Mortars (SHM), micro-fibers were used to control the thickNess of the crack at micro level. Also modified Sulphonated Poly-Styrene Mortars (SPSM) with admixture of sulphonated poly-styrene (0.15% by weight of cement) were prepared and control mortar with no admixtures were prepared and correlated with experimental results.

Gas permeability and fatigue tests were performed to evaluate the efficiency of SHM. Figure 2.1 shows the results of gas permeability tests. Among many techniques that might be executed to measure the permeability of mortar, in this study, gas permeability tests were performed using liquid methanol as the gas source, because it is one of the easiest and fastest method reported till date. Fatigue leads to progressive and permanent internal damage in a material subjected to repeated loading. This was accredited to the transmission of internal micro-cracks

which fallouts in a substantial increase of irrecoverable strain. Figure 2.2 represents the fatigue behavior of mortar specimen and reported that SHM performed best among all.

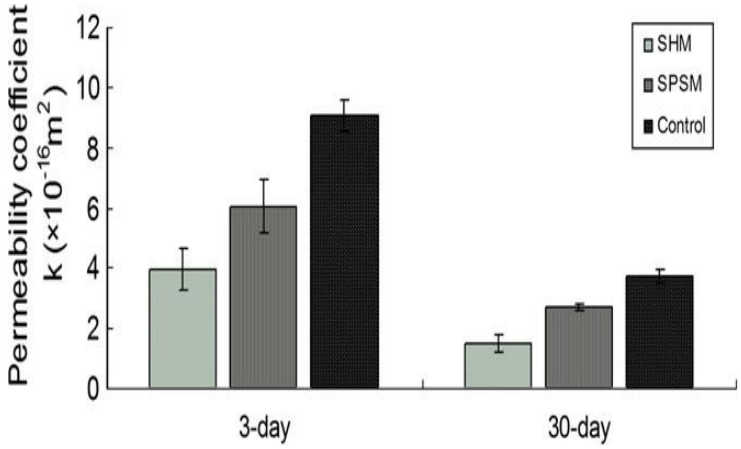

Figure 2.1: Permeability coefficients at different curing ages of cement mortar composite, at 3-day and 30-day, after being loaded under 80% of ultimate compressive strength and Afterwards set aside for 24 h *(Yang et al., 2011).*

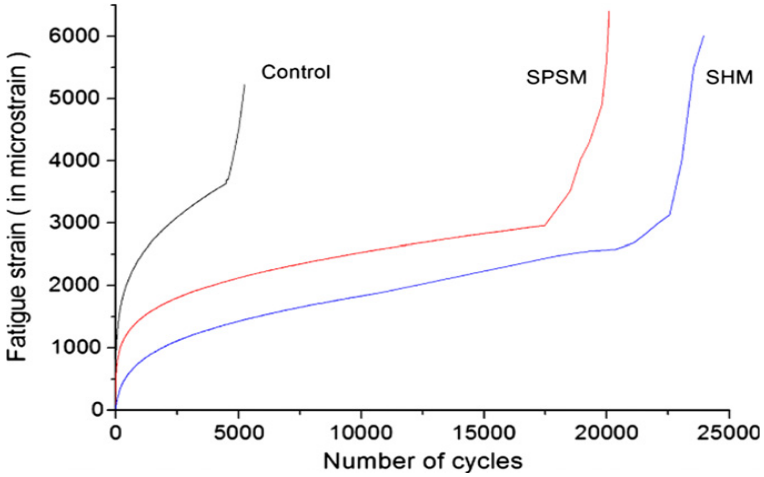

Figure 2.2: Fatigue strain and the number of cycles under uniaxial compression cyclic loading, for SHM, SPSM and for control mortar specimens *(Yang et al., 2011).*

Sangadji et al. (2012) reported a self-healing concrete structure using porous network concrete. The aim was to achieve the self-healing network by vascular self-healing technique. Approach used was to replicate the bone self-healing process by placing porous concrete inside the concrete structure to build a porous network like sponges' bone. When cracks occurred in structures and spotted by sensors, healing agent can be pervaded into the porous network so as to fill up voids and seal the cracks. In this study they introduced healing agent manually by injecting it into the porous network. Figure 2.3 shows a conceptual design of the idea.

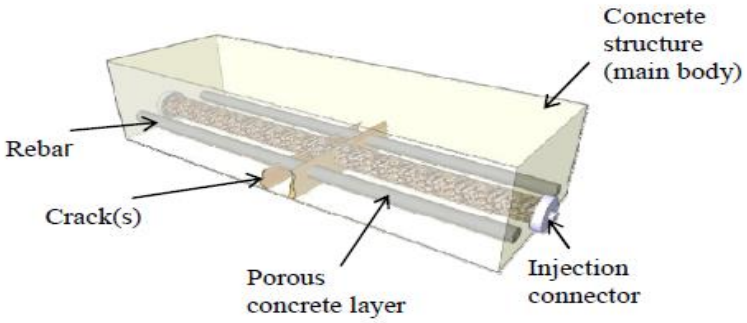

Figure 2.3: A conceptual design of porous network concrete *(Sangadji et al., 2012).*

Self-healing mechanism was tested on cylindrical and beam samples. A porous concrete core was placed in the medium strength self-compacting designed concrete casted for outer solid concrete. Uni-axial tensile load testing used for cylindrical samples and bending load testing for beams to create cracks. First crack was created on cylinder on and then provided with the healing agent, after the polymerization (healing process) when cylinders were once more loaded, then in tensile loading testing crack was formed at other location rather than on its first location shown in Figure 2.4. In testing of beams, first crack was created with the width of approximately 400µm and load was removed then the healing agent was introduced by porous network, after the healing process second load cycle was implemented and noted the regain of strength during second loading cycle shown in Figure 2.5. This method of self-healing or autonomic repair is extremely appropriate for situations that are challenging to repair from outside, for example when the cracks are not reachable or in situations where it is too unsafe to do a manual repair. In this study effect of introducing porous concrete to mechanical properties of concrete not been discussed.

Figure 2.4: Original and final crack pattern after healing and new crack surface due to healing effect *(Sangadji et al., 2012).*

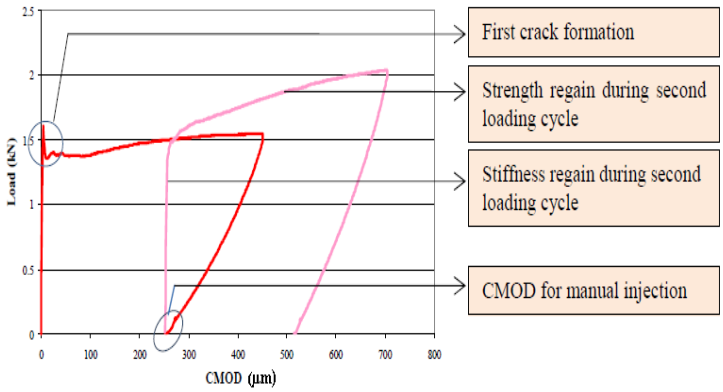

Figure 2.5: Load v/s Crack mouth opening displacement (CMOD) of porous network concrete beam *(Sangadji et al., 2012).*

Song et al. (2013) reported first self-healed microcapsules type protective coating for mortar which had sunlight induced self-healing capability (Figure 2.6). For self-healing, Methacryloxypropyl-Terminated Poly-Di-Methyl-Siloxane (MAT-PDMS) and Benzoin Isobutyl Ether (BIE) microcapsules were micro-encapsulated with urea-formaldehyde polymer as shell. Mean diameter and size distribution of the microcapsules were affected by the agitation rate. A coating matrix was prepared by sol−gel reaction of tetraethyl orthosilicate (TEOS) in the existence of a polysiloxane. Optical microscopy and SEM were used to confirm that, when the self-healing coating is scratched, the healing agent is released from the microcapsules and covers the damaged region and subsequently hardens by the photoreaction. The self-healing coating was assessed as protective coating for mortar, which was confirmed by water permeability and chloride ion penetration tests. It was the first example of capsule-type photo-induced self-healing system, and offered the advantage of catalyst-free, environmentally friendly, economical and practical healing. In Figure 2.7, water absorption test results are shown and it was concluded that uptake of water after cracking of coatings was minimum for self-healing micro-encapsulated coating. Limitation of the study is the healing process only been triggered when sunlight is available.

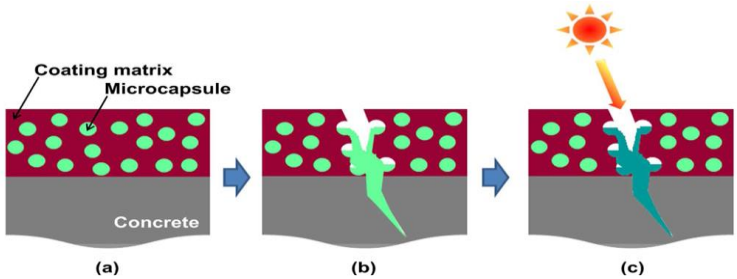

Figure 2.6: Self-healing mechanism of coatings: (a) Self-healing coating; (b) Rupturing of capsules and releasing of healing agent; (c) crack healing through sunlight *(Song et al., 2013).*

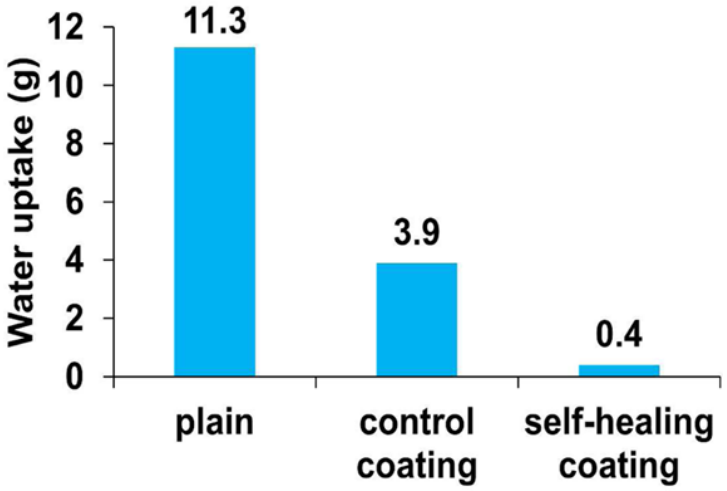

Figure 2.7: Water absorption test results, amount of water uptake in 24hours *(Song et al., 2013).*

Wang et al. (2013) reported self-healing microcapsules which were organic in nature. Microcapsules and catalyst were mixed with mortar blend to create self-healing mortar specimens. Compression and flexural strength were determined to evaluate the effect of microcapsules on strength parameters and permeability test was conducted to determine the healing efficiency or recovery rate of the mortar specimens. From the results it was concluded that with small amount of microcapsules, the strength of the mortar increased by 9 percent and correspondingly decreased with increase in the percentage of microcapsules in the mortar mixture. From permeability results it was seen that both recovery rate and the healing effect were nearly proportional to the amount of microcapsules used in the mortar. They concluded that the most economical or effective percentage of microcapsules in the mortar mixture was 3% (by weight of cement). After 3%, significant decrease in the strength parameters was detected. From these experiments it was concluded that volume of microcapsules in the matrix plays important role in strength recovery rate.

Dong et al. (2015) reported the smart releasing behavior of microcapsules in the cement matrix. In chemical based micro-encapsulated self-healing, the vital issue is how to release the healing agent and how to trigger the healing mechanism. The study focused on the releasing behavior of healing agent, and the results showed that smart releasing behavior can controlled by the thickNess of the wall of the microcapsules. Moreover the pH value affects the release rate of the healing agent i.e. the release rate unusually increases with the decrease in the pH value. At a pH of 13, there was no observable damage on the surface of the microcapsules. As the pH value was reduced,

surface damage became more and more apparent. In a neutral environment, at pH of 7, the surface of a microcapsule was completely destroyed after soaking. That confirmed that the environmental pH has a significant effect on the microcapsule release behavior, and can be used as a trigger mechanism for these types of self-healing system.

Yang et al. (2016) reported microcapsule type organo-gel based self-healing coating system that had secondary damage prevention capability. This study proposed to overcome limitations of an earlier study by *Song et al.* (2013), wherein it was reported that, microcapsules required UV-light to heal the structure and healing agent turned into a hard solid after healing reaction. That hard solid may effortlessly cracked by diminutive vibrations. Limitations of healing agent were overcome by attempts reported in this study. A mixture of an organogelator was introduced with, poor and good solvents for the gelator, was used as the healing agent. When the good solvent evaporated from the agent, a visco-elastic organo-gel was formed. The healing agent was microencapsulated with urea-formaldehyde polymer, and the resultant microcapsules were integrated into a polymer coating to prepare self-healing coatings. When the coatings were scratched, they self-healed the crack and covered the cracked region: after the healing process the coatings were subjected to vital vibration, by which they demonstrated that no secondary damage occurred in the healed region because of visco-elastic region formation after healing process. At the time of rupturing of microcapsules, huge amount of cyclohexane was evaporated within 2 minutes (Figure 2.8) and the gelation of coating initiated which prevents the secondary damage.

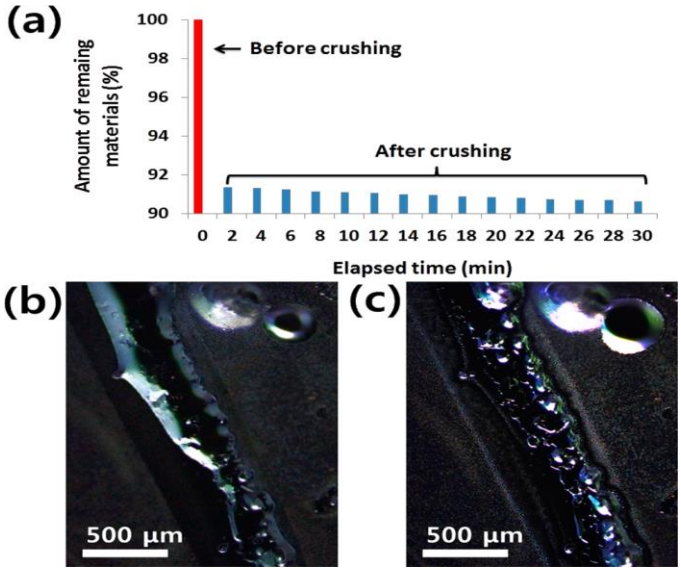

Figure 2.8: (a) Remaining materials v/s time after crushing the microcapsules. (b, c) Optical images: (b) just after scratching and (c) 2 min after scratching *(Yang et al., 2016).*

Ansari et al. (2017) proposed modification to the calcium nitrate microencapsulation procedure to minimize the concrete strength reduction due to microcapsules. Recently, *Hassan et al. (2016)* attempted to encapsulate calcium nitrate in urea-formaldehyde shell as an alternative healing agent due to its low cost, its reactivity with the cement matrix and its accelerated setting ability of un-hydrated cement particles. *Hassan et al. (2016)* reported that calcium nitrate microcapsules had satisfactory healing potentials but significantly reduced concrete compressive strength. *Ansari et al. (2017)* investigated its adverse effect and modified them to achieve good results. That modification comprised a partial replacement of the sulfonic acid catalyst with a low Hydrophilic-Lipophilic Balance (HLB) emulsifier for the preparation of the continuous phase of microcapsules while the aqueous phase composition was kept unaltered. In microcapsules synthesis, aqueous phase was added to the continuous phase drop-wise for a period of 10 minutes and then agitated.

Mortar samples were prepared with various microcapsule concentrations and tested for compressive and flexural strengths according to ASTM standards. Four different microcapsule concentrations were investigated i.e. 0.50%, 0.75%, 1.00% and 1.25% (by weight of cement) in addition to the control mix (without microcapsules). From the results it was concluded that this modification lowered both compressive and flexural strengths as compared to *Hassan et al. (2016)* report. The reduction in the 28-day strengths did not exceed 10% in compression and 17% in flexure. However, the optimal microcapsule concentration by weight of cement was selected in the range of 0.75% and 1.00%, as in these cases reduction in strengths was less than 10% and to achieve acceptable strength and elastic modulus, it was recommended to use microcapsule concentration of 0.75% by cement weight.

Chen et al. (2017) reported self-healing coating for steel reinforced concrete. This was for the first report on using self-healing coating was introduced for reinforcing bar in concrete. In this report, Epoxy Coated Rebar (ECR) method was used where tung-oil was selected as a healing agent. Epoxy coating matrix were prepared admixing tung-oil self-healing microcapsules and coated on rebar. Core material of the microcapsules prepared was tung-oil and urea-formaldehyde shell wall was formed for core material to behave them as non-reactive until crack is generated. Their goal of creating self-healing coatings was that it can endure construction site damage which contradicts the coatings ability to counterattack corrosion. Self-healing coatings microcapsules (10wt% by weight of epoxy) were mixed into epoxy in a centrifugal mixture. Control coatings were also prepared with the epoxy without tung oil microcapsules.

Mortar cylinders were prepared for the testing of self-healing capability of microcapsules, cylinders of 3inch x 6inch were used for accelerated corrosion testing and cylinders of 4inch x 8inch were used for rebar pullout strength test. From optical microscope images (Figure 2.9) it was concluded that coatings had self-healed significantly. These coatings showed no apparent differences in pullout bond strength as compared to conventional epoxy coatings (Figure 2.10). Self-healing coatings were performed significantly better than conventional epoxy coatings during accelerated corrosion testing and intentionally damaged coatings does not affect performance (Figure 2.11). In this way, a sustainable approach to improving the resiliency and sustainability of steel-reinforced concrete had been demonstrated.

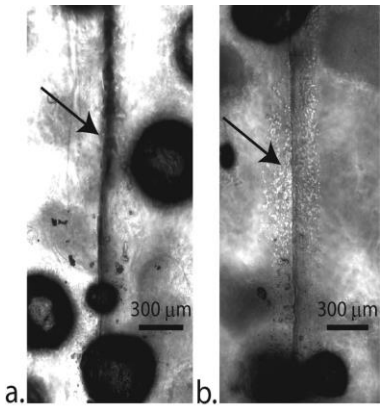

Figure 2.9: Optical microscope images of damaged coating. (a) At the day of damage (b) 5 days after damage *(Chen et al., 2017).*

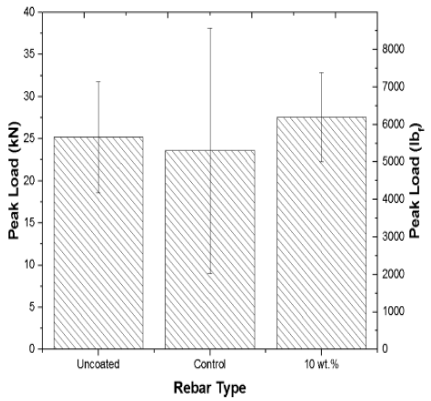

Figure 2.10: Pullout testing results, peak loads for unlike rebar surface conditions *(Chen et al., 2017).*

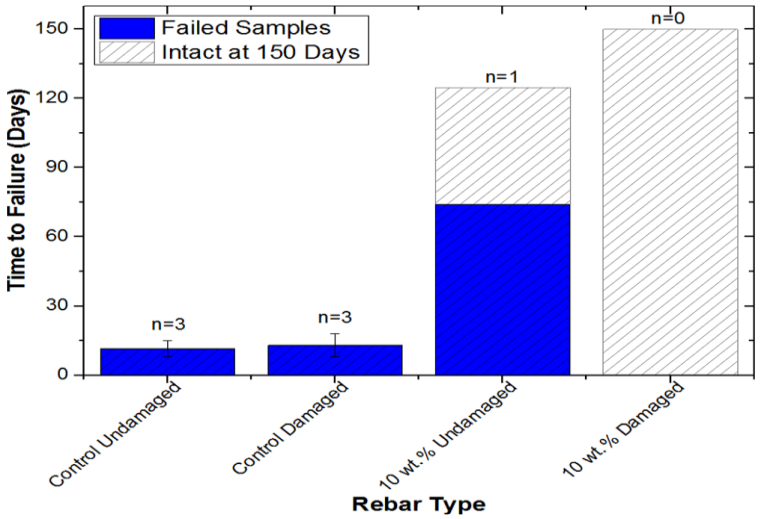

Figure 2.11: Accelerated corrosion testing results. Failed samples represents by solid bars, where n is the number of samples that failed. Hashed bars signifies the samples that were unharmed after 150 days of testing *(Chen et al., 2017).*

Kim et al. (2017) reported a different microcapsule type self-healing protective coating for cementitious composites with secondary crack prevention ability. *Yang et al. (2016)* reported that at the time of healing process the healing agent deficit very rapidly due to the evaporation of the solvent. This loss of agent and limitations of *Song et al.* (2013) report were controlled in this study. A microcapsule-type self-healing coating has been established using Silanol-Terminated Polydimethylsiloxane (STP) and Dibutyltin-Dilaurate (DD) healing agent. STP undergoes condensation reaction in the presence of DD to give a viscoelastic substance. STP and DD containing microcapsules were prepared separately by in-situ polymerization and interfacial polymerization methods, respectively. These microcapsules were incorporated into commercial enamel paint or epoxy coating, which applied on steel panels and mortar specimens to make dual-capsule based self-healing protective coatings. SEM images and water permeability test conducted to evaluate the efficiency of these microcapsules.

To prepare self-healing coatings the STP- and DD-containing microcapsules were mixed into the enamel paint or epoxy coating with a mass ratio of STP capsules: DD capsules: paint :: 19:6:75. The resulting coatings applied to the steel panel and mortar specimens, and dried for 3–4 days at room temperature. In a similar manner control coating samples were prepared without microcapsules. The applicability of the self-healing coating system to mortar specimen was successfully demonstrated by water permeability test results (Figure 2.12). It was confirmed from SEM images (Figure 2.13) that secondary crack does not occur in the healed region upon the application of vigorous vibration to the self-healing coating.

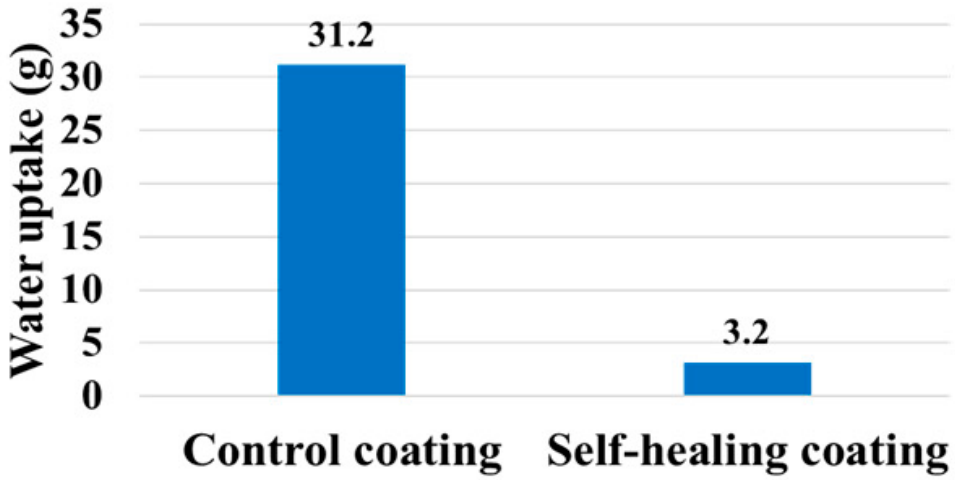

Figure 2.12: Water permeability test results: amount of water uptake in 48 hours *(Kim et al., 2017).*

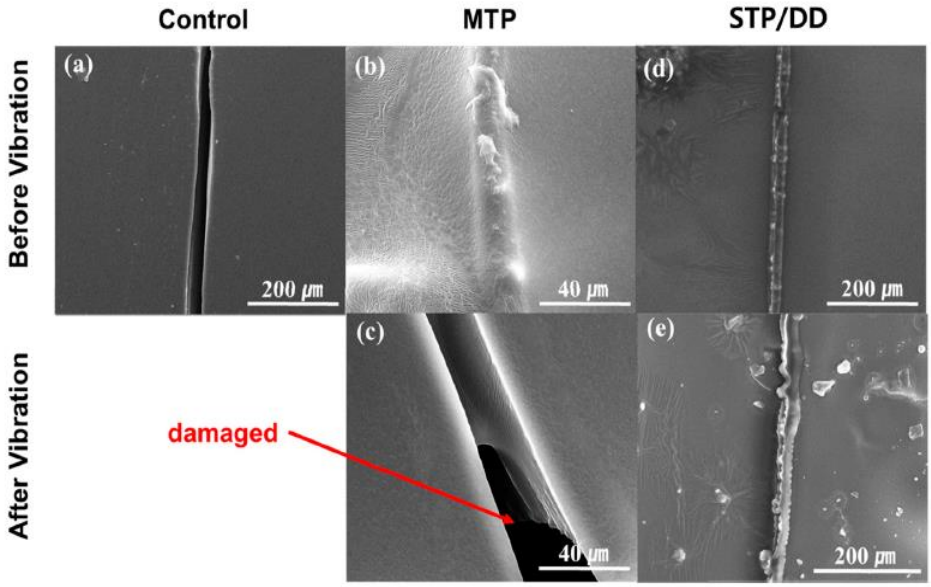

Figure 2.13: SEM images of the damaged region: (**a**) a control coating; (**b**) MTP-based coating after damaging and healing; (**c**) MTP-based coating after damaging, healing, and vibration; (**d**) STP/DD-based coating after damaging and healing; (**e**) STP/DD-based coating after damaging, healing and vibration *(Kim et al., 2017).*

Restuccia et al. (2017) reported new self-healing technique for cement based materials using two types of shells for self-healing microcapsules i.e. glass spheres and pharmaceutical capsules shells. Sodium silicate was used as healing agent encapsulated in shells and uniformly mixed in the cementitious matrix during preparation. Utilization of the materials already present in the market was done with an aim to reduce final cost of the self-healing concrete. Self-healing capsules were prepared and then to make their smooth surface rougher to make it stronger for mixing step, capsules were coated with epoxy resin and sand. Mortar beams were casted, two samples contained about 30 pharmaceutical capsules each, two samples contained approximately 35 hollow glass spheres each and one mixed sample with 15 glass spheres and 15 pharmaceutical capsules. Three point bending test conducted to create cracks, then understand the mechanism of self-healing microcapsules and again loaded to check the strength regain by the healing effect. It was shown that it was possible to use these kind of shells, crack breaks them and released healing agent to repair the cracks.

Dong et al. (2018) reported micro-encapsulated chemical based self-healing system for corrosion inhibition of rebar in concrete with two different kind of chemicals used for self-healing system with unique microcapsules. A system proposed which uses ethyl cellulose (EC) as shell of the

microcapsules with sodium nitrate ($NaNO_2$) and sodium monofluorophosphate (MFP) both used as healing agent or core material for microcapsules. Self-healing mechanism activated by pH reduction inside the concrete and mechanism of MFP/EC system was to protect the rebar by forming a protective layer against steel corrosion while $NaNO_2$/EC system focused on forming a passive layer on the surface of rebar. Three types of mortar specimens were prepared i.e. one control without microcapsules and two were of purposed system with each kind of microcapsules.

Results from wet-dry cycle accelerated corrosion testing revealed that the self-healing system postponed the initiation of the corrosion and blocked the corrosion rate after initiation. With an equivalent dosage, the $NaNO_2$/EC system had better performance for the passive film protection, while the MFP/EC system was decreased the rate of the corrosion process. Both kinds of the chemical self-healing systems was showed highly effective corrosion protection of rebar by delaying the de-passivation and the cracking caused by corrosion.

Weishaar et al. (2018) evaluated the self-healing capability of tung-oil micro-encapsulated epoxy coatings for corrosion protection with harsher environment. Steel coupons were coated with three different types of coatings, two without self-healing microcapsules of varying thickNess of plain epoxy coatings and other with micro-encapsulated coating. Reinforced mortar beams were casted for corrosion testing reinforcing with micro-encapsulated coated rebar and micro-encapsulated damaged coatings. Coatings were damaged with a kNife and impact.

Adhesion strength of coatings were evaluated using ASTM Standard and steel coupons subjected to aerated salt water baths to analyzed the corrosion initiation on coated coupons. Micro-encapsulated coatings were 42% thicker than plain coatings. Thin plain coatings showed better adhesion strength than thick plain coatings and micro-encapsulated coatings. Micro-encapsulated coatings showed poor adhesion strength due to the imperfections at the boundary of coating and coupon. Uncoated bars lasted for an average of approximately 1.5 days before through cracking of the concrete cover. Plain coated lasted for 12.5 days and micro-encapsulated coatings had only one failure after 60 days of corrosion. In damaged induced coatings, micro-encapsulated coatings had longest resistance against corrosion. These results confirmed that self-healing coatings were able to heal coating damage and prevent corrosion before embedding in mortar and after installation. Figure 2.14 shows the corrosion testing results of undamaged rebar, rebar of coating damaged by kNife and rebar of coating damaged by impact.

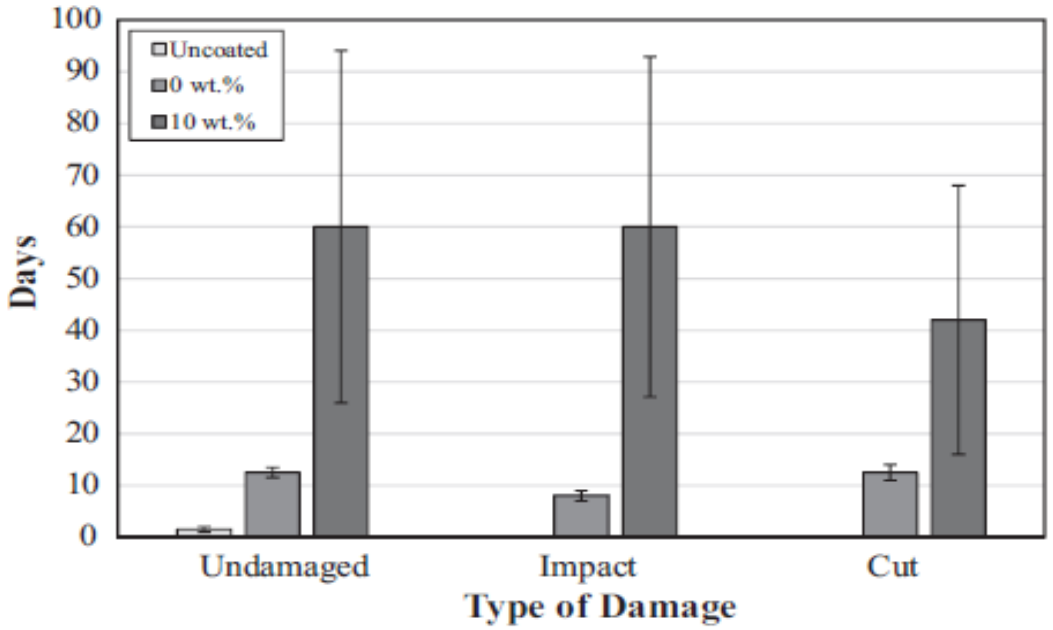

Figure 2.14: Results from corrosion testing of rebar embedded in mortar *(Weishaar et al., 2018).*

Du et al. (2019) presented microcapsules containing Toluene-Di-Isocyanate (TDI) as core material and paraffin as shell for the self-healing of concrete. Effect of agitation rate, temperature and paraffin/TDI mass ratio on core fraction of microcapsules at the time of preparation of microcapsules were studied. Effect of microcapsules percentage on self-healing ability of mortars was evaluated and the optimum values were selected for all parameters. Mortar specimens with microcapsules were casted with different percentage, 1.5%, 3%, 4%, 6% of microcapsules by mass ratio of cement and control specimen with no microcapsules was prepared. Compressive strength of mortar before and after pre-load damage was investigated, pre cracked using split tensile testing to evaluate the healing efficiency and concluded that the surface cracks of the mortar were self-healed completely by microcapsules.

Optimum preparation parameters of the microcapsules, which were suggested are agitation rate of 600 RPM at 75 ^{0}C and paraffin/TDI mass ratio of 1:2. From the SEM images it was seen that microcapsules were in regular spherical shapes and the thickNess was about 1/10 of the diameter. Compressive strength of the self-healing mortar with microcapsules percentage 3% (by mass of cement) noted 28.2% more than the control mortar (without microcapsules). Cracks with the width of less than 0.4 mm was successfully healed within 6 hours of cracking.

2.3 CORROSION PROTECTION USING NANO-CLAY

Shirehjini et al. (2016) reported the effect of nano-clay on corrosion protection of Zinc-rich Epoxy coatings on steel. Epoxy coatings were prepared containing nano-clay particles then their cathodic protection was evaluated with electrochemical impedance spectroscopy (EIS) and immersion test. Transmission electron microscopy (TEM) was used to observe the structure of the clay in the coating. The sacrificial protection of the coatings was deliberated by measuring the open circuit potential (OCP) values at unlike immersion time. The morphology of the zinc rich coatings was also studied by scanning electron microscopy (SEM) technique before and after immersion test. Four types of zinc rich coatings were prepared in which zinc content was 85% by the total weight of the coating. The clay contents were 0, 1%, 2% and 3% by weight of binder. Montmorillonite clay were used whose particle size was 0.5-5 μm and layer thickNess of 1 nm. Epoxy and clay was stirred at 1000 rpm for 3 hours then mixture was sonicated for 60 minutes. Zinc powder added to the mixture and stirred for 45 minutes then hardener was added and thoroughly mixed and sample ready for coating. Steel panels were coated with the prepared mixture and analyzed for the cathodic protection. EIS and immersion test results showed that 1 wt% clay led to better corrosion protection performance due to enhanced clay dispersion in coatings whereas more than 1% clay content could reduce the long term protective performance. Higher clay percentage caused decrease in intercalation of clay. May be due to supply of water molecule leading to corrosion at rebar surface (autogenous processes in which clay is used for supplying water for the cement matrix, *Qian et al., 2010).*

2.4 ULTRASONIC GUIDED WAVES FOR CORROSION MONITORING

Sharma et al. (2011) studied the effect of different environments on corrosion of reinforced bar using ultrasonic guided waves (UGW). Initiation and progress of rebar corrosion with corrosion rate is monitored by UGW in chloride and oxide environments. Surface seeking and core seeking wave modes were used for UGW monitoring and modes combination relate the differences in corrosion mechanism or rates. Concrete beams were casted with one steel bar reinforced at the center of the cross-section. Reinforced beams were accelerated corroded by impressed current corrosion in artificial maintained oxide and chloride environments. From the results they concluded that in core-seeking mode due to corrosion pitting the signal reduces in chloride

corrosion and very slow fall noted in oxide corrosion whereas in surface seeking mode signals strength rises in chloride corrosion indicating delamination followed by local damage of material and in oxide environment corrosion rate is slow and initial signal was fallen due to creation of corrosion products then bond deterioration rises the signal. In destructive testing of mass loss and tensile strength correlated the results with UGW results and concluded that corrosion product creates roughness at the surface of rebar which correspondingly improves the bond strength. From these successfully monitored and evaluated the corrosion behavior of RC beam with UGW and predict the level of deterioration with UGW.

Miller et al. (2013) studied a guided wave based technique for the monitoring of corrosion of reinforced steel in concrete. Signal strength of the guided waves affected by the bonding between sensors and the material, in this study bond affect was eliminated. Investigated the alteration in time of flight of spreading wave in loaded RC structures at different levels of corrosion. Reinforced beams were casted and subjected to corrosion then monitored with guided waves. Experimental results presented that recorded signal strength was increased when the delamination occurred at the bar-concrete interface.

Sharma et al. (2015) reported an ultrasonic guided waves *in-situ* monitoring technique for corrosion of reinforced bars in freshly poured concrete. Monitoring with UGW on steel reinforcing bars was done expressed curing and solidification of freshly poured concrete. When concrete solidified and cured signals received were attenuated. RC beams casted and monitored during first 24 hours of setting of poured concrete and destructive evaluation done by pullout strength and compressive strength testing. With the help of UGW early age properties of concrete were determined. Successfully recognized setting and bond development progression of young concrete with optimized guided wave mode. As concrete solidified with increase in compressive strength there was fall in voltage amplitude of ultrasonic waves. This study purposed the use of it for the final setting properties of concrete. Relationship founded between voltage and compressive strength was parabolic and also relationship between bond strength and concrete founded parabolic relationship. They successfully calibrated the early age concrete properties with the help of ultrasonic signals.

Sharma et al. (2015) reported corrosion monitoring of FRP wrapped concrete using ultrasonic guided waves. Studied a non-destructive monitoring technique for the corrosion initiation and progression in RC structures after repairing damaged structures with FRP sheets. Cylinders of concrete were casted with reinforcing bars embedded in it. Cylinders were accelerated corroded in chloride environment with impressed current corrosion after specific damage occurred due to corrosion those cylinders were repaired by CFRP and GFRP sheets. Core seeking and surface seeking guided modes were used to monitor the resistance presented by repaired sheets ultrasonically and results correlated with destructive parameters. FRP wrapped samples increased cell voltages indicated corrosion resistance increment. In wrapped GFRP or CFRP samples the rate of corrosion slow down to great extent measured by electrical resistance and concluded from resistance results that GFRP was more effective than CFRP. By monitoring with UGW in surface seeking mode signals were low initially and rises correspondingly with the delamination of rebar due to corrosion whereas in core seeking mode initially signals were high and fall correspondingly with the pitting or loss of area of rebar due to corrosion. In wrapped samples very slow rate of signal fall observed where as in their control specimen signals fall drastically. Wrapped samples showed lesser mass loss as compared to control specimen and higher pullout strength as compared to control specimen. Demonstrated that UGW can successfully monitor and evaluate the corrosion defense offered by FRP sheets.

Sharma et al. (2018) reported two different non-destructive monitoring techniques based on wave propagation. Ultrasonic guided waves and acoustic emission monitoring techniques were used and are active and passive techniques respectively. RC beams were casted and subjected to accelerated corrosion using impressed current corrosion at a constant voltage. Corrosion initiation and progression were studied with these two non-destructive techniques. Acoustic emission sensors recoded acoustic events due to corrosion and ultrasonic guided waves pulses passing through rebar was recorded as non-destructive parameter and related with electrochemical techniques. Half-cell potential measurements indicated the possibility of corrosion but does not provide any information about the damaged location and nature of damaged region. In UGW by selecting suitable guided waves mode like surface seeking or core seeking differentiation can done between surface and pitting corrosion. Initiation and progression of corrosion was well tracked by acoustic emission sensors in early stages and gave clear image of nature and location of damaged region affected by corrosion. AE gave information about damage and UGW gave extent and nature of corrosions.

They reported one advantage of UGW over AE was that AE sensors requirement was to be installed at all times of corrosion period whereas UGW devices only involved at the time of monitoring of corrosion extent. Reported that in initial phase AE was more reliable to track cracks and for pitting or surface loss manner of rebar UGW was more appropriate.

2.5 CLOSING REMARKS

The chapter has discussed several studies reported for the micro-encapsulated self-healing techniques using chemical additives, nano-clay based protection of metals from corrosion and the corrosion monitoring using non-destructive ultrasonic guided waves and acoustic emission.

CHAPTER - 3
EXPERIMENTAL PROGRAMME AND METHODOLOGY

3.1 GENERAL

This chapter outlines the research program followed in this thesis. The aim of the research is to prepare self-healing coatings for mild steel bar of reinforced concrete for corrosion protection. Three types of coatings were prepared: one self-healing tung-oil based microcapsules coatings, second was nano-clay based epoxy coatings and the third with both tung-oil microcapsules and nano-clay for rebar in concrete as corrosion protection. Non-destructive tests of visual inspection, ultrasonic guided waves and corrosion current were measured at different instants. Destructive tests of mass loss and residual tensile strength was also conducted to quantify the effect of corrosion on rebar and the effectiveness of coatings on rebar.

3.2 TEST PROGRAM

The test program for the same involved the following steps:

STEP 1: Preparation of three types of epoxy based coatings for rebar.

STEP 2: Microcapsules based coatings involving tung oil were prepared.

STEP 3: Nano-clay based epoxy coatings for rebar corrosion protection were prepared.

STEP 4: Microcapsules and nano-clay based epoxy coatings were prepared.

STEP 5: Application of coatings on the rebar of 300mm length and 12mm diameter. Undamaged coatings and damage induced coatings were also prepared.

STEP 6: Determination of elementary properties of constituent materials of concrete namely cement, fine and coarse aggregates as per IS specifications.

STEP 7: Casting of concrete cubes of size 150×150×150 mm of M20 grade.

STEP 8: Casting of RC beams of size 100×100×250 mm and cylinders of size 100×200 mm (diameter × length) using M20 grade of concrete.

STEP 9: Compression test conduct for the cubes to check the characteristic strength of M20 grade prepared.

STEP 10: Effect of coatings on the pullout strength of rebar in concrete cylinders to check the bond strength of coated rebar in concrete.

STEP 11: Accelerated corrosion testing on plain bars and bars reinforced in concrete.

STEP 12: During corrosion the effectiveness of coatings is evaluated by non-destructive parameters of visual inspection, corrosion current and ultrasonic guided waves.

STEP 13: Destructive parameters of mass loss and residual strength were measured after specific degree of corrosion.

The methodology is outlined in Figure 3.1 below:

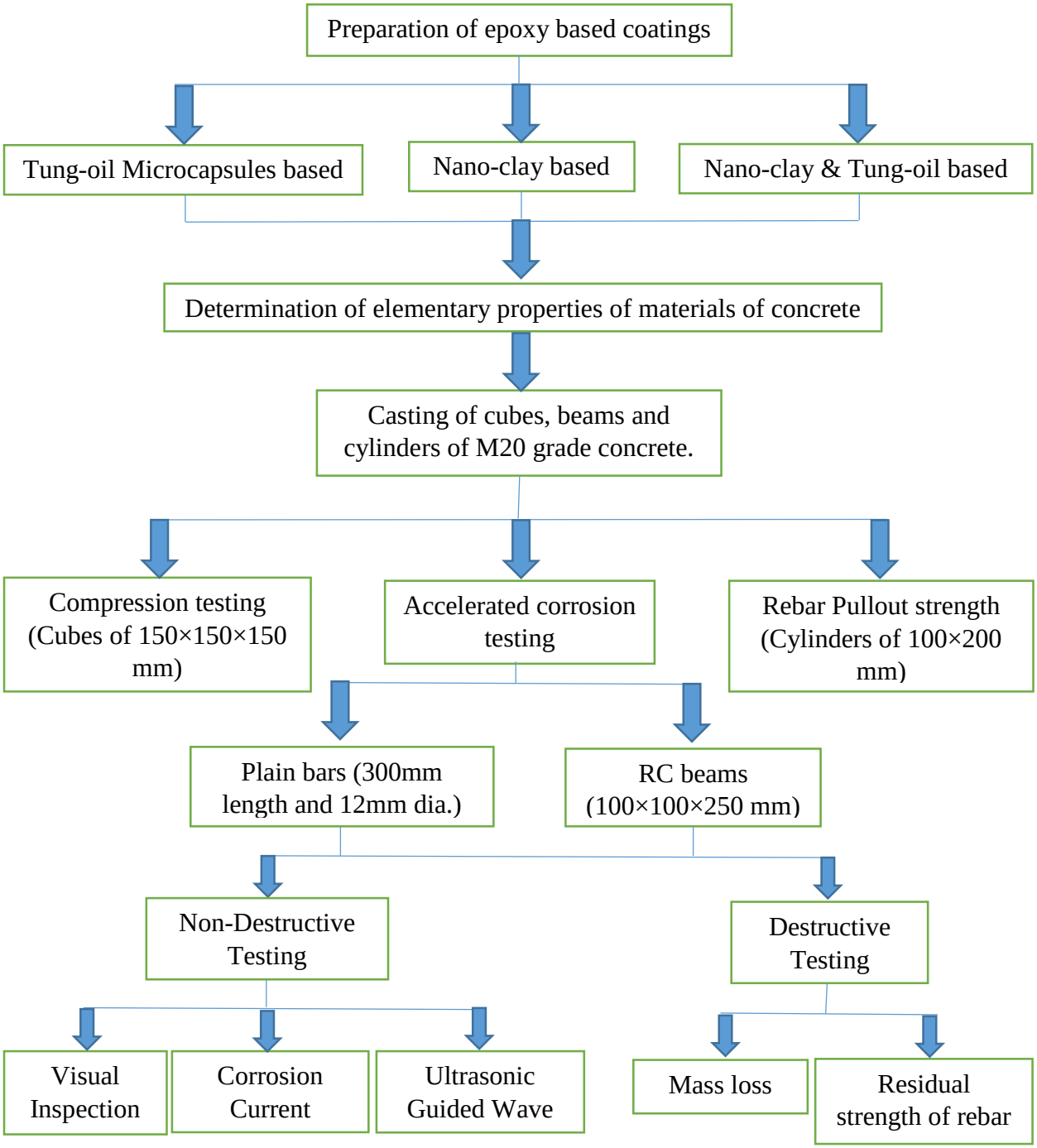

Figure 3.1: Flow chart of operational program.

3.3 MATERIALS

Chemicals such as dodecyl sulphate solution, urea, ammonium chloride, resorcinol and formaldehyde purchased locally and tung oil was purchased from Sigma Aldrich, were used to prepare tung-oil based microcapsules for epoxy coatings of rebar. Nano-clay Cloisite® 15A was used for the nano-clay based epoxy coatings. Two-part epoxy having resin of Araldite CY 230-1 and hardener of Aradur HY 951 was used. Cement, water, reinforcing steel, fine and coarse aggregates were purchased locally and used at the time of casting of RC structures.

Specifications and purpose (Figure 3.2-3.5) of the materials used for the synthesis of tung-oil based microcapsules are as discussed here. Dodecyl sulphate solution was used as surfactant which reduces surface tension. Urea was used to react with formaldehyde to form polymer shells and ammonium chloride provides pH buffer to the solution of microcapsules. Resorcinol stabilizes the solution and formaldehyde reacts with urea to form Urea-Formaldehyde shell which provided non-reactive surface for healing agent. Tung oil is drying oil used as oxidative healing agent in this study. For waterproof coatings and paints tung-oil has been used. Tung oil has the ability to dry quickly and polymerize into a tough, glossy and waterproof coatings.

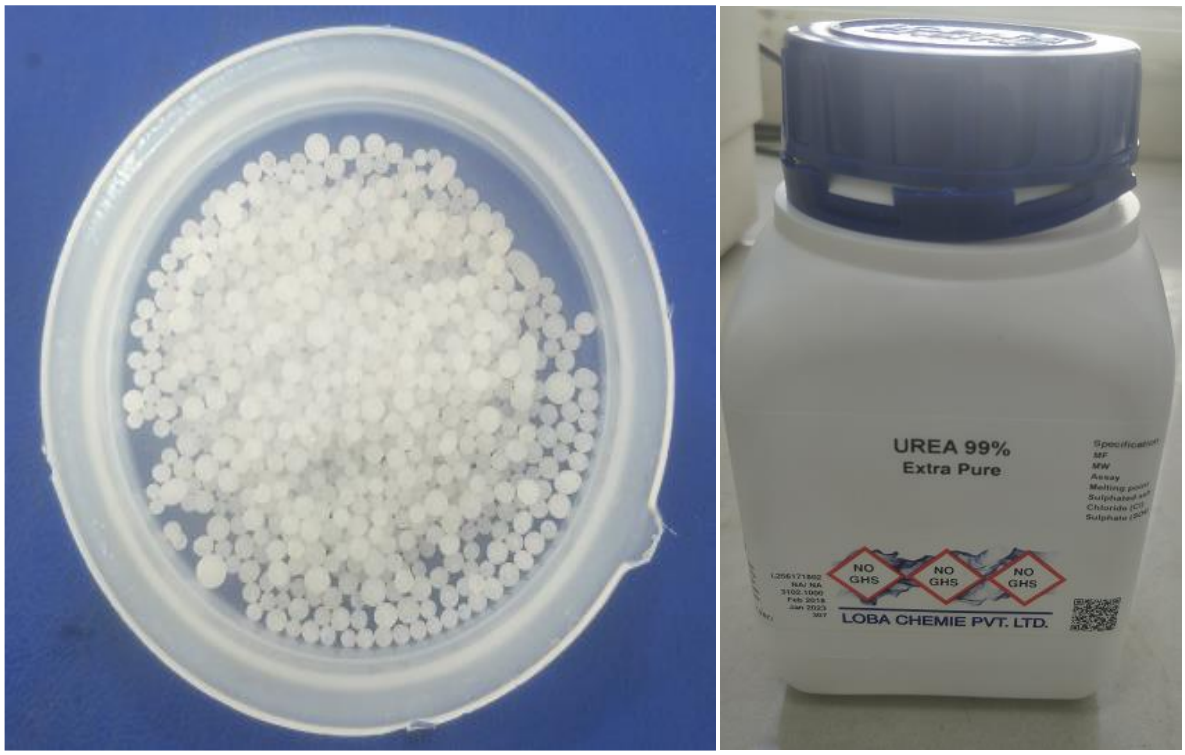

Figure 3.2: Urea, used in aqueous phase of microcapsules synthesis process.

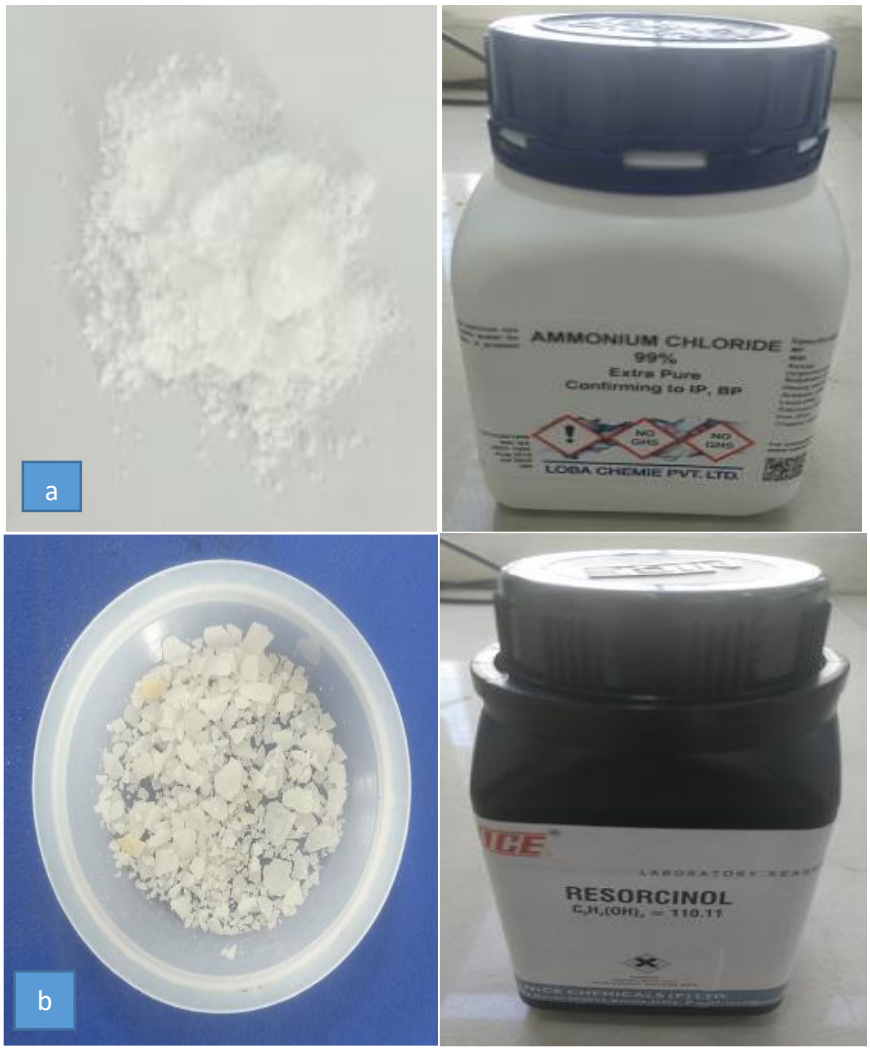

Figure 3.3: Chemicals used in aqueous phase; (a) Ammonium chloride, (b) Resorcinol.

Figure 3.4: Formaldehyde used in continuous phase.

Figure 3.5: Self-healing agent, tung oil used in continuous phase.

3.3.1 Cement: Ordinary Portland cement (43 grade) was used for the experimental work conforming to IS: 8112-1989 of BIS. Cement was of grey color with light greenish shade. Table 3.1 represents the summary of all tests conducted on cement. According to the IS: 8112-1989 all tests have been done.

3.3.2 Fine aggregates: For the investigational work locally available fine aggregates were used. Properties of aggregates shown in Table 3.2 and sand lies in Zone III.

Table 3.1: Properties of cement used.

S. No.	Properties	Value Obtained	Standard Values
1	Normal Consistency	33%	--
2	Initial Setting Time	47 min	Not less than 30 min
3	Final Setting Time	240 min	Not more than 600 min
4	Specific Gravity	3.12	--

5	Fineness	4.6%	--
6	Compressive strength		
	3 days	26.2 MPa	Min. 23 MPa
	7 days	34.8 MPa	Min. 33 MPa
	28 days	46 MPa	Min. 43 MPa

Table 3.2: Properties of fine aggregates used.

S. No.	Properties	Values Obtained
1	Grading Zone	Zone III
2	Fineness Modulus	2.62
3	Bulk Density	1.31 g/cm^3
4	Water Absorption	0.889%
5	Specific Gravity	2.55

3.3.3 Coarse aggregates: Locally available crushed stone aggregates of size 10 mm were used in this study. Aggregates were washed to remove dust and dried to surface dry conditions. Several tests conducted as per IS: 383-1970 and the properties of aggregates were given in Table 3.3.

Table 3.3: Properties of coarse aggregates used.

S. No.	Properties	Values Obtained
1	Type	Crushed
2	Fineness Modulus	6.78

3	Water Absorption	0.51%
4	Specific Gravity	2.57

3.3.4 Water: For the mixing and curing purpose of concrete tap water was used in this study and deionized water was used for the synthesis process of microcapsules. It does not have any organic matter, oil, sugar, silt or any acidic material present in it as per IS: 456-2000.

3.3.5 Epoxy used: Epoxy used for the preparation of coatings (Figure 3.6) was made by mixing resin and hardener in the ratio of 10:1. Mixing was done for five minutes to thoroughly disperse all the components.

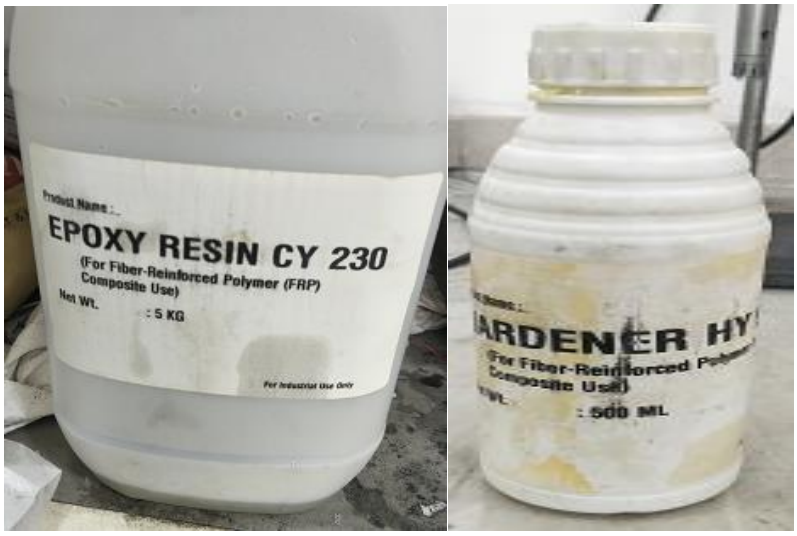

Figure 3.6: Resin and hardener used for making epoxy.

3.4 PREPARATION OF SELF-HEALING MICROCAPSULES

For the preparation of micro-capsules, procedure of *In-situ* polymerization, reported by *Samadzadeh et al. (2011)* has been used. Generally nano-particles are dispersed in a liquid monomer or comparatively low molecular weight precursor as well as in their solution. When a homogeneous mixture is formed, originator is added and exposed to suitable source of heat, light, etc. The procedure used for preparation of micro-capsules is detailed below:

Step 1: Take 260ml of deionized or distilled water.

Step 2: Add 10ml of 5 wt% dodecyl sulphate solution in water.

Step 3: Mix it with homogenizer at speed of 10,000 rpm for 2-3 minutes.

Step 4: After 2-3 minutes of homogenizing, add 5gm of urea and homogenize for 30 seconds. Add 0.5gm of ammonium chloride and homogenize for 30 seconds then 0.5gm of resorcinol and again homogenize the sample for 10-12 minutes.

Figure 3.7: (a) Homogenizing of sample, (b) After homogenization.

Step 5: After completion of homogenization adjust pH of the solution using 1wt% of hydrochloric acid to approximately 3. This would help in controlling the morphology of the polymer shells (urea-formaldehyde shells).

Step 6: After adjusting pH, homogenized sample was assembled with mechanical mixer on digital water bath apparatus (Figure 3.8). Both water bath and mechanical mixer work simultaneously at a temperature of 25^0C with the speed of mixer set to 200 rpm.

Step 7: At the agitation rate of 200 rpm the sample was subjected to 10 min of agitation and then 50ml of tung-oil is added to the sample to form a blend and permitted to stabilize for 15 min.

Step 8: In the stabilized solution, add 13gm of 37wt% aqueous solution of formaldehyde. Then raise the water bath temperature to 60 ^{0}C for 4 h at 400 rpm to enable the polymerization reaction between urea and formaldehyde and solution is covered (Figure 3.9).

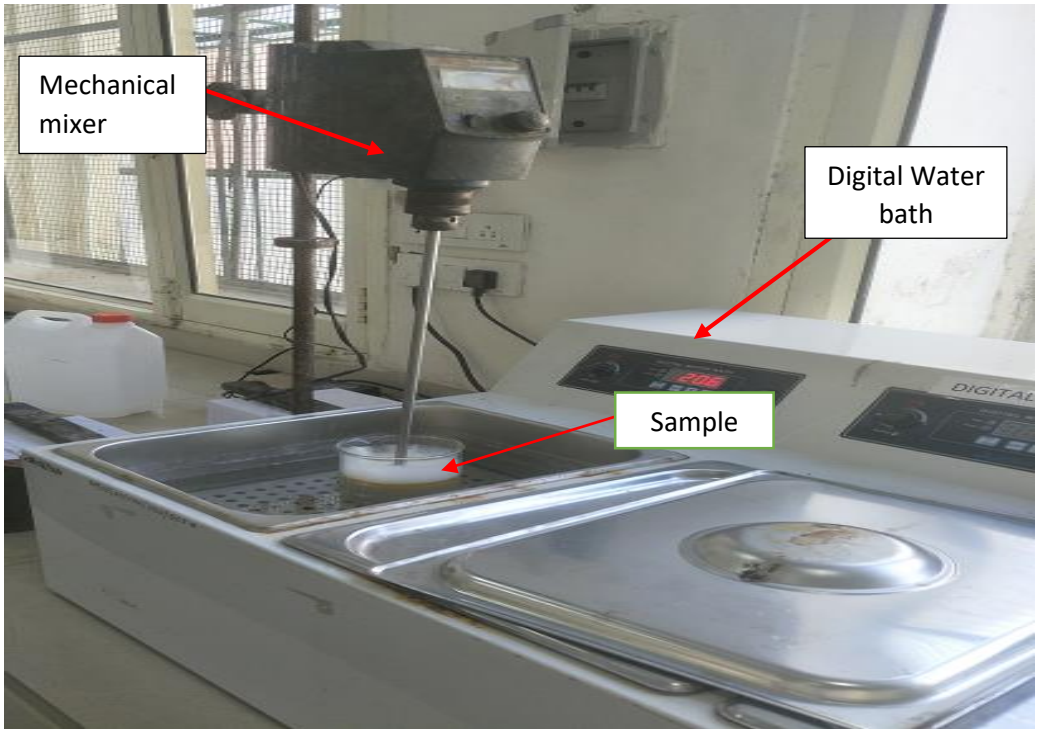

Figure 3.8: Mechanical mixer assembled with digital water bath apparatus.

Figure 3.9: Covered solution for the polymerization reaction between Urea-Formaldehyde.

Step 9: After 4 h of reaction, the solution was cooled down to room temperature, while maintaining at same speed of the mixer of 400 rpm. It takes approximately 6 h to cool down to room temperature.

Step 10: To extract microcapsules from the mixture, mixture with coarse filter paper was vacuum filtered and then washed with acetone and deionized water.

Step 11: Extracted capsules were air dried for 48 hours and then dried out in vacuum-oven at 50^0C for 24 h (Figure 3.10) and were ready to be used for coatings of rebar.

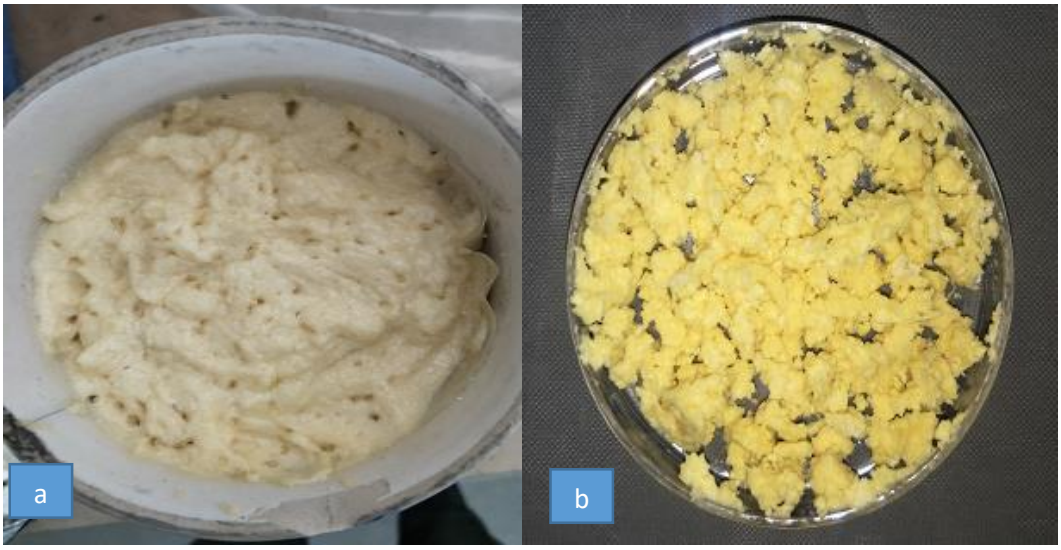

Figure 3.10: Tung-oil microcapsules; (a) Air dried microcapsules, (b) Oven dried microcapsules.

3.5 PREPARATION OF COATINGS AND TESTING

Four kinds of epoxy coatings were prepared as four different coatings evaluated on plain rebar and rebar in concrete. The various epoxy coatings were: plain epoxy coatings, Micro-encapsulated based epoxy coatings, Nano-clay mixed epoxy coatings and Micro-encapsulated with Nano-clay epoxy coatings were prepared. Plain epoxy is non-self-healing coating and rest of the coatings prepared were self-healing coatings.

3.5.1 Plain Epoxy Coating (PC)

For the epoxy coating, the resin and hardener were mixed in the ratio of 10:1 and mechanically mixed at 500 rpm for 10 minutes. Mild steel rebar of length 305 mm with diameter of 12 mm was coated with plain epoxy using a small brush. Samples were cured for 4-5 days before corroding or casting them. Coated rebar shown in Figure 3.11.

3.5.2 Tung-Oil Micro-Encapsulated Epoxy Coating (MC)

For the MC, epoxy was prepared as mentioned in section 3.5.1 and then tung-oil based microcapsules prepared (Section 3.4) were slowly added to the emulsion with the proportion of

10wt% of the epoxy product. Micro-encapsulated solution was stirred for 3 to 5 minutes at 500 rpm and the rebar was coated (Section 3.5.1). Coated rebar shown in Figure 3.11.

3.5.3 Nano-clay Epoxy Coating (NC)

For NC, epoxy with nano-clay was prepared as mentioned by *Singh et al. (2017)*. Nano-clay (Cloisite® 15-A) was heated at 120 ^{0}C for 5 to 6 h to eliminate all the moisture content present. Dried nano-clay was dispersed in epoxy resin by 2wt% and homogenized using a shear homogenizer at 20,000 rpm for 10 minutes. Ultrasonication using a probe sonicator was further done for 10 minutes at 80% amplitude. During ultrasonication, the temperature of beaker was controlled by ice bath. After ultrasonication, sample was cooled for 5-10 minutes to reduce its temperature to 40 ^{0}C before adding hardener in it. Hardener was added (resin to hardener ratio 10:1) and sample was stirred using a mechanical stirrer for 10 minutes at 500 rpm for uniform mixing. After the completion of the product rebar coated (Section 3.5.1) and coated rebar shown in Figure 3.11.

3.5.4 Tung-Oil Micro-Encapsulated with Nano-Clay Epoxy Coating (MNC)

For MNC, first nano-clay and epoxy product being prepared as mentioned in Section 3.5.3 then after completion of the product, 10wt% of the emulsion tung-oil microcapsules were deliberately added to the emulsion and stirring was continual for 4-5 minutes at 500 rpm until the solution becomes uniform. After the completion of the stirring, rebar were coated and cured as Section 3.5.1. (Figure 3.11).

3.5.5 Damage Induced to Coatings

Coatings were damaged to evaluate the performance of healing efficiency of the coatings. The damage was induced using a blade to make a cut of 2.5 cm (1 in.) in the middle of rebar (Figure 3.9) with uniform pressure applied. All four types of coated bars were subjected to a simulated damage to initiate corrosion. Four samples were prepared with damage, damaged plain epoxy coating (PC-D), damaged tung-oil micro-encapsulated epoxy coating (MC-D), damaged nano-clay epoxy coating (NC-D) and damaged tung-oil micro-encapsulated nano-clay coating (MNC-D). Tung-oil micro-encapsulated coated rebar was left for 4 to 5 days to initiate healing after damage and then subjected to accelerated corrosion, to allow for sufficient time for the self-healing due to tung-oil microcapsules. Damage induced rebar is shown in Figure 3.12.

Figure 3.11: Coated rebar; (a) PC, (b) MC, (c) NC, (d) MNC.

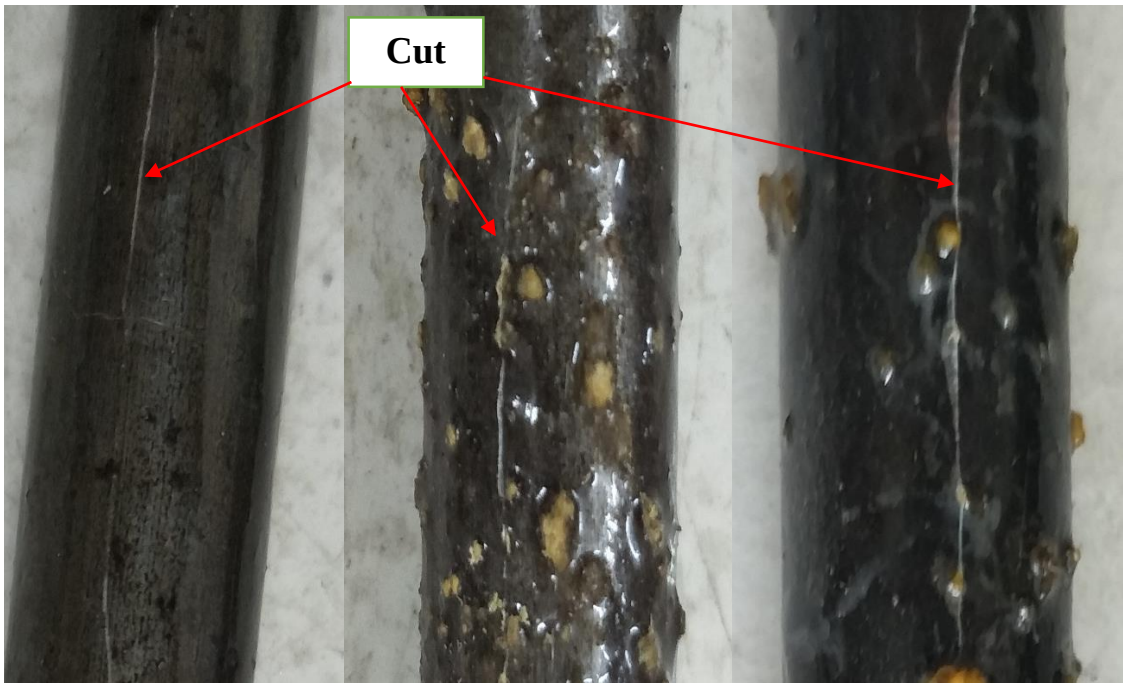

Figure 3.12: Coated rebar subjected to damage initiation.

3.5.6 Accelerated Impressed Current Corrosion

The four types of coated rebar, four types of damage induced coated rebar and one uncoated rebar as control specimen were subjected to accelerated impressed current corrosion as plain bars and bars reinforced in concrete beams. For the corrosion of coated plain rebar, a container was taken with an approximate width of less than 1ft and cut it from one side for easy assembling (Figure 3.13). The mild steel rebar was placed at the middle of the container with the projection of minimum 25-30mm on both sides. Ends were sealed with the clay so that there is no substantial environmental difference to minimize corrosion at the junction. A stainless steel wire mesh was enfolded around rebar and connected to negative terminal of a constant voltage source to act as cathode. One end of the rebar was connected to positive terminal (acting as anode) of Direct Current (DC) supply and filled with 3.5% NaCl solution acting as electrolyte to facilitate corrosion. Constant voltage of 1V was induced and corrosion current was noted in all coated rebar, with and without initial damage. Similarly, reinforced beams were prepared for corrosion by wrapping stainless steel wire mesh around the beam with sack in between. Anode and cathode connected to DC supply (Figure 3.14) to induce corrosion and constant voltage of 15V was induced and corrosion current was noted in all coated bars reinforced in concrete.

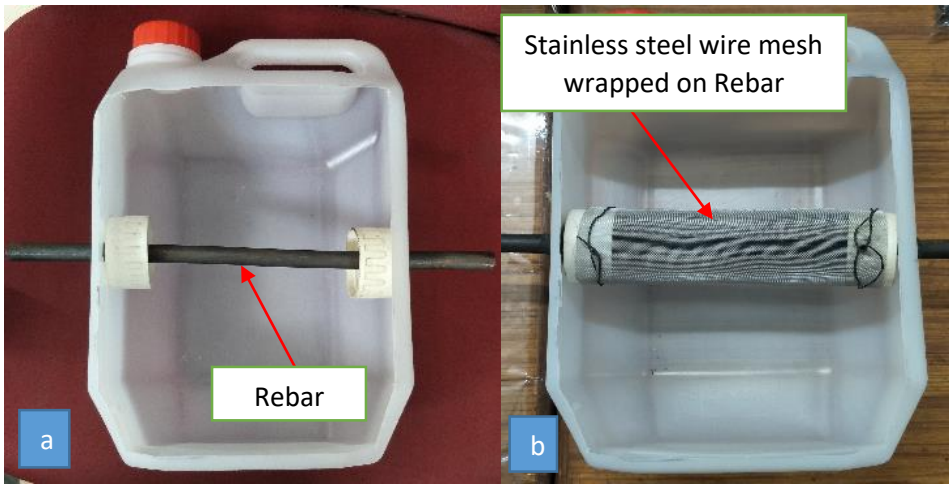

Figure 3.13: Assembling of sample for corrosion of plain bars, (a) Rebar in container, (b) Wire mess wrapped around rebar.

3.5.7 Ultrasonic Guided Wave Measurement

The rebar experiencing corrosion were also subjected to ultrasonic guided wave testing using specific L (0, 7) mode at 1MHz *(Sharma et al. 2011)*, which could effectively pick up pitting effect of corrosion using a conventional ultrasonic testing system and set-up for UGW testing is

shown in Figure 3.14. Identical samples were tested as mentioned in Section 3.5.6. Ultrasonic testing system consists of a pulser-receiver device (DPR 500), cylindrical contact transducers and CPU with Data Acoustic Card (DAC). One end of the bar was connected to transducers through which guided waves were generated in rebar and other end of the bar was connected to transducer which received the generated waves. Monitoring of the deterioration of the rebar in the form of pitting was noted using mode L (0, 7) with varying the exciting frequency and readings were taken at every interval of 24hr throughout the impressed current corrosion duration for all types of coatings i.e. damaged and undamaged with plain bars and bars reinforced in concrete.

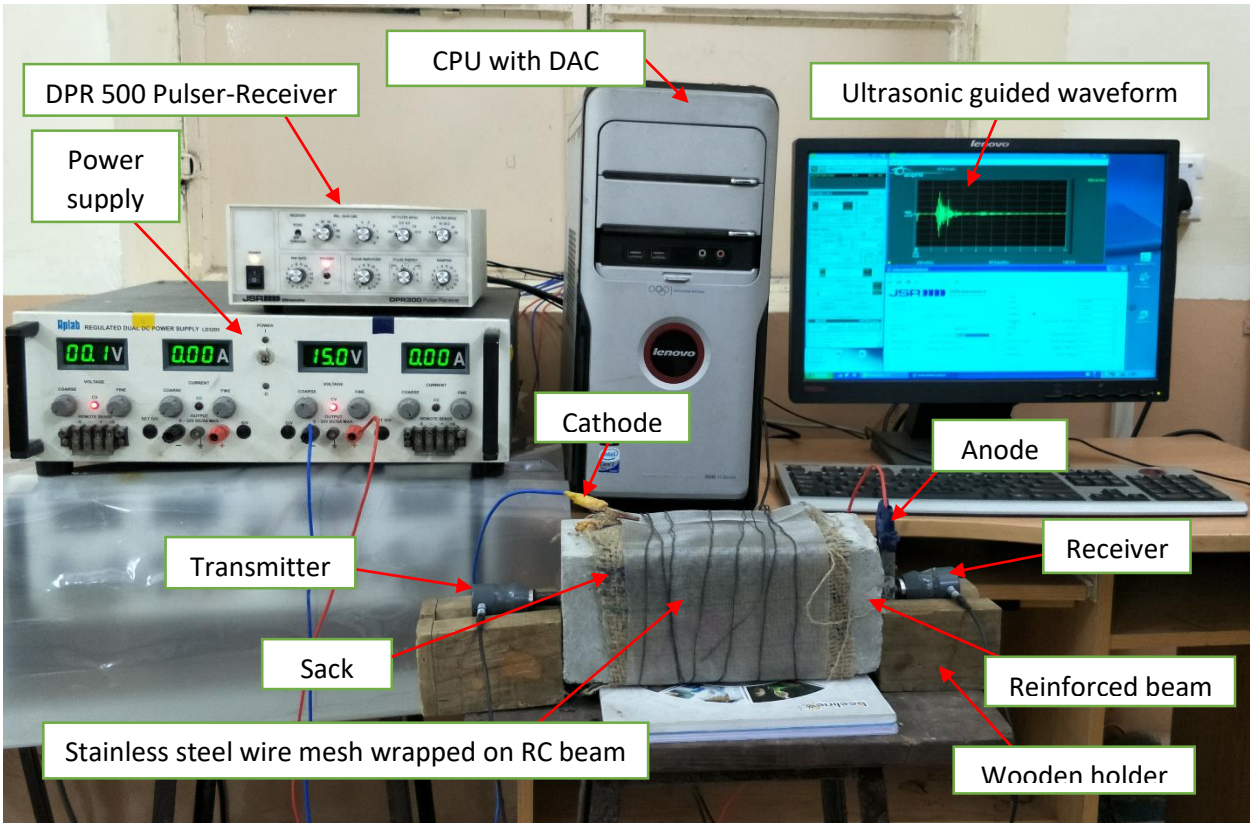

Figure 3.14: Set-up for ultrasonic guided wave testing for RC beams.

3.6 DESIGN MIX PROPORTIONS AND CONCRETE SAMPLES

For the casting of specimens, M20 grade concrete was used with design mix of 1:1.45:2.91 ratio of cement, sand and aggregates and water to cement ratio of 0.45. Size of stone aggregates was limited to maximum 10mm. The concrete prepared was used for casting of:

- Cubes of standard size of 150mm for 7 and 28 days compressive strength testing.
- Cylinders of 100mm×200mm (diameter × length) for 28 days pullout strength testing.

- Reinforced beams of 100mm×100mm×250mm for 28 days accelerated corrosion testing.

3.6.1 Compressive Strength

Concrete cubes were tested on Universal Testing Machine (UTM) of capacity 1000kN on 7^{th} day and 28^{th} day for compressive strength of concrete at the load rate of 5kN/second. Averages of 7 and 28 days compressive strength of concrete were obtained as 17.5kN/m^2 and 28kN/m^2, respectively. These values of compressive strength are within acceptable limits.

3.6.2 Pullout Strength

All four types of coated bars and one uncoated bar were subjected to pullout strength testing. In the reinforced concrete section, rebar takes all the tensile loads and is transferred by the bond between concrete and steel. After coating the rebar, the interface between steel and concrete changes and so does its properties. Pullout testing of rebar was done to measure the bond strength between the steel and concrete after rebar coatings. A 100mm × 200mm (diameter × length) cylindrical specimens were cast with a rebar of 12mm diameter and length 305mm at the middle of its cross-section. Rebar was placed at a cover of 25mm from the bottom and is projected out at the other end by 130mm. After 28 days of curing prepared samples were tested on UTM of capacity 1000kN (Figure 3.15) at the rate of 0.5kN/second till failure. Three samples of each type were tested.

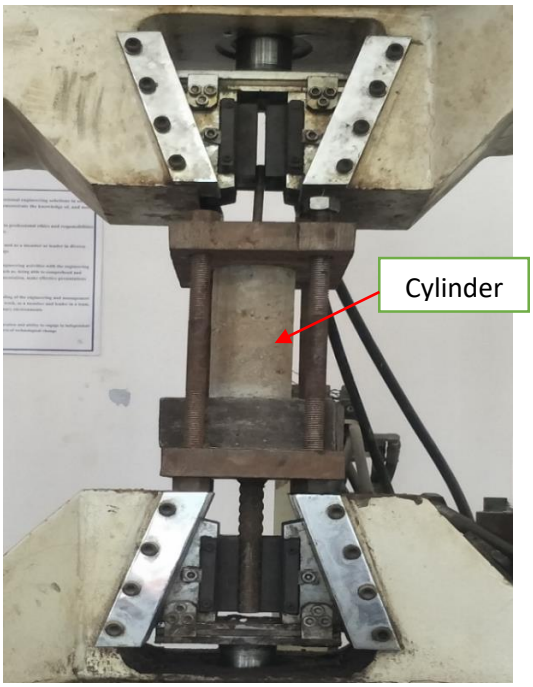

Figure 3.15: Setup of pullout testing of rebar on UTM.

3.6.3 Reinforced Beams for Corrosion Testing

The coated rebar; damaged and undamaged, and uncoated rebar were also cast in concrete to study the consequence of self-healing coatings on rebar undergoing actual corrosion in concrete. RC beams of size 100mm × 100mm × 250 mm length with a single rebar of 12mm diameter and 300mm length in the middle of beam with the projection of 25mm on the both sides were casted and subjected to corrosion. The effectiveness of coatings was measured by non-destructive techniques i.e. corrosion current and ultrasonic guided waves (Figure 3.14).

3.7 DESTRUCTIVE TESTING

After completion of the corrosion, all the corroded rebar were exposed to destructive testing of mass loss and residual tensile strength of the rebar. Corroded bars were removed and cleaned with an iron brush and washed with acetone to remove all the corroded product and then residual mass was weighed on the digital weighing balance. For the residual strength of the rebar, corroded bars were tested on UTM and the residual tensile strength was measured.

3.8 CHARACTERIZATION FOR MICROCAPSULES

Scanning Electron Microscopy (SEM) was used for the characterization of tung-oil based self-healing microcapsules prepared in the Section 3.4. It was conducted to study the micro structures i.e. shape or morphology of the microcapsules prepared.

3.9 CLOSING REMARKS

The chapter discuss about the experimental program and methodology involving synthesis of self-healing microcapsules using tung-oil and methodology of preparing different types of coatings. The experimental details of various tests and methodology to monitor and evaluate the corrosion of rebar with destructive and non-destructive testing are also detailed.

CHAPTER 4
RESULTS AND DISCUSSION

4.1 GENERAL

The effectiveness of different types of epoxy based coatings on rebar in air and in concrete were subjected to accelerated corrosion. The effectiveness has been quantified using visual inspection, corrosion current and ultrasonic guided waveform. All coated bars: damaged and undamaged, and uncoated bars were studied and compared with respect to corrosion initiation and progression. Pullout strength of all four types of coatings were compared among themselves and with uncoated bar. Micro-structure of the self-healing microcapsules prepared were investigated using SEM images.

4.2 PLAIN MILD STEEL BARS

The effectiveness of different types of epoxy based coatings vis-à-vis corrosion initiation has been studied by visual inspection, corrosion current and ultrasonic guided wave changes as the rebar undergoes accelerated corrosion.

4.2.1 Visual Inspection

Visual inspection of undamaged and initially damage induced coated bars has been studied.

4.2.1.1. Undamaged Coated Rebar

Coated rebar were directly subjected to corrosion and were visually monitored at regular intervals during accelerated corrosion testing. Accelerated corrosion testing was stopped when the ultrasonic peak to peak voltage of the waveform either vanished or after 60 days of corrosion.

A) PC Rebar (Plain Epoxy Coating)

Within 2 days of accelerated corrosion, bubbles were formed on the surface of the rebar (Figure 4.1) which were filled with air. On the 6^{th} day, the air bubbles burst and initiation of corrosion could be seen simultaneously. On the 10^{th} day, the rebar rust product cracked the epoxy layer and corrosion was accelerated at higher rate. Once epoxy layer was cracked, the corrosion products get a path to travel from anode to cathode easily and then the corrosion rate was almost constant throughout the whole remaining period of corrosion. Corrosion cracks widened within 15

days and on 18th day the ultrasonic peak to peak voltage of the waveform for the PC rebar vanished and corrosion test was stopped.

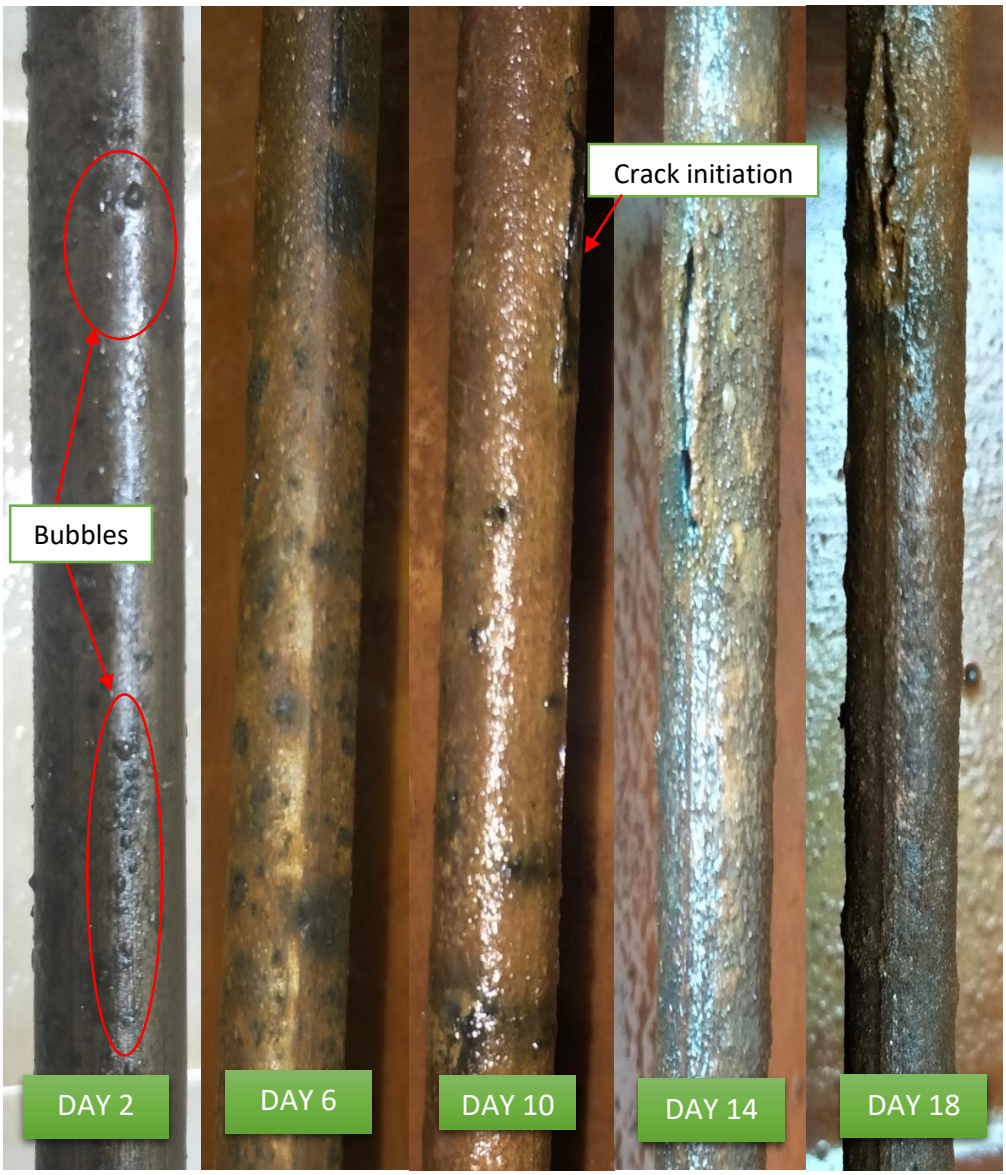

Figure 4.1: Visual observation of PC bars.

B) NC Rebar (Nano-clay Epoxy Coating)

In NC rebar, no significant observations and formation of bubbles was seen for the first 15 days (Figure 4.2), which points to the inhibition of corrosion by addition of nano-clay to epoxy layer coating on the rebar. Bubbles start appearing on the 15th day, accumulation of corrosion products was observed and on the 25th day, the bubbles busted and corrosion accelerated. This continued till the 35th day, cracked bubbles were observed leading to accelerate corrosion rate and

on the 41st day, ultrasonic guided wave peak to peak voltage almost vanished and bar was removed from the corrosion testing. There are two things to note: presence of nano-clay in epoxy, in general leads to a poorer surface texture and with nano-clay, the cracks take longer time to propagate.

Figure 4.2: Visual observation of NC bars.

C) MC Rebar (Tung-Oil Micro-Encapsulated Epoxy Coating)

Figure 4.3 shows the effect of progressive corrosion on tung-oil based self-healing microcapsules coatings on rebar. In 10 days, bubbles were seen to be forming on the surface of coated rebar and were air filled. On the 20th day, it was observed that the bubbles were not air filled but hard. This is probably due to self-healing polymerized material inside the bubbles. This means that polymerization reaction of tung-oil is under process (forms solid film in the presence of oxygen) which would delay the corrosion of the rebar by making an impermeable layer. These polymerized bubbles do not burst during the entire period of accelerated corrosion which was 60

days. Even after 60 days of corrosion ultrasonic peak to peak voltage for MC coated rebar did not vanished completely. This shows a significant self-healing effect of microcapsules on the inhibition of corrosion which continued for 60 days. On the 60th day very few spots from where rust travels from anode to cathode and impermeable layer breaks were observed (Figure 4.3).

Figure 4.3: Visual observation of MC bars.

D) MNC Rebar (Tung-Oil Micro-Encapsulated with Nano-Clay Epoxy Coating)

From Figure 4.4 it can be seen that due to the presence of nano-clay, bubble formation is very less or negligible in the initial stages as compared to the tung-oil based micro-encapsulated coating or plain epoxy coating. The corrosion pattern was almost same as MC coated rebar i.e. when bubbles are formed they are filled with the polymerized tung-oil, which delays the corrosion by making an impermeable layer. It is observed that may be due to nano-clay, microcapsules

uniformity of corrosion inhibition is not preserved as in MC coated bars and more spots were subjected to corrosion (Figure 4.4, Day 60) as compared to MC rebar. The ultrasonic voltages did not completely dropped even after 60 days but corrosion test was stopped after this time.

Figure 4.4: Visual observation of MNC bars.

Visual Inspection of the Coatings

- Amongst all the four coatings, MC and MNC coated bars showed the best inhibition of corrosion damage. These coatings can significantly delay the corrosion by making an impermeable layer due to the polymerization reaction of tung-oil microcapsules.
- Epoxy mixed with nano-clay was also effective in delaying the corrosion significantly due to the water repellent nature of clay materials and increased obstructions in the path of corroding agent. However, at longer time periods, more corroded spots, as compared to MC coated bars would be observed. Moreover nano-clay disperses in epoxy matrix will

very significantly improve the mechanical strength, modulus and toughness of the epoxy coatings.

- The best effect of delaying corrosion was observed in tung-oil micro-encapsulated bars. This is probably due to self-healing effect of tung-oil microcapsules which blocks the entry of for corrosion agents.

4.2.1.2 Effect of Initial Damage on Coated Rebar

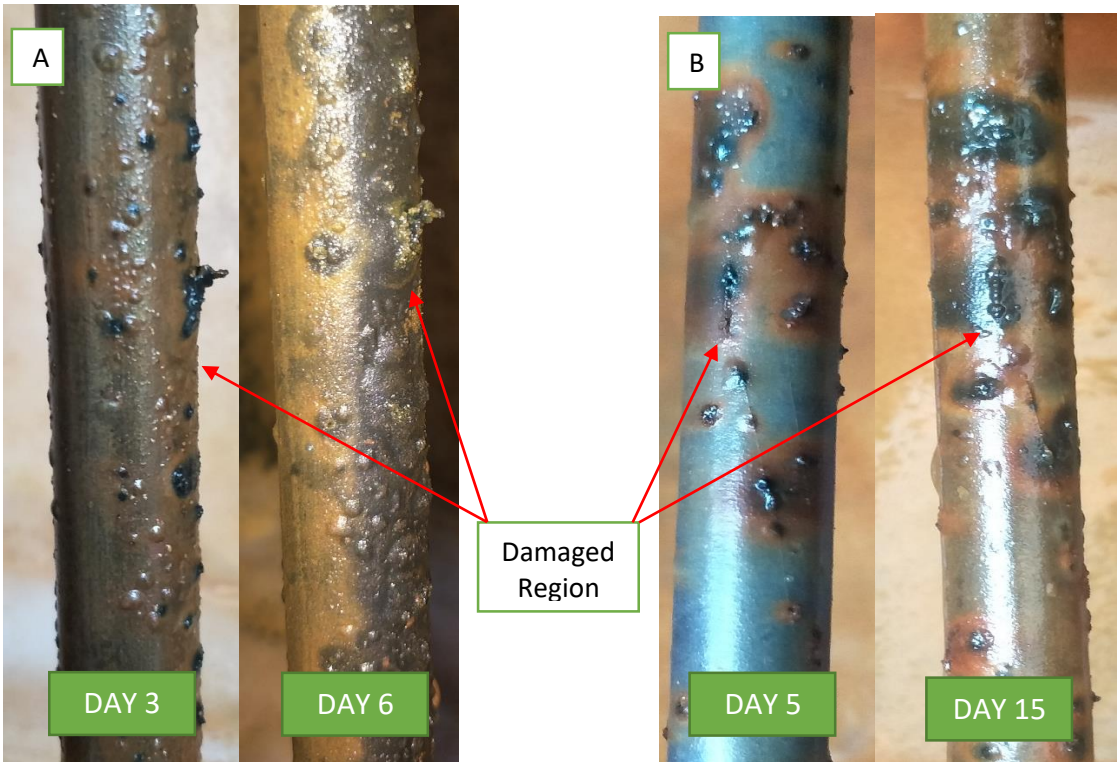

Figure 4.5: Visual observation, (A) PC-D rebar, (B) NC-D rebar.

A cut is made by blade on PC-D rebar and NC-D rebar. As shown in Figure 4.5, the corrosion initiation in the region surrounding the cut was initiated in the form of bubbles which ruptured much earlier than the bubbles on the rest of rebar. Formation of bubbles is an indication of breaking of passive layer and busting points towards the rust product accumulation, the initial damage act as a week point for further damage progression of PC and NC coated rebar.

In micro-encapsulated bars with initial damage, the phenomenon of self-healing by tung-oil microcapsules was observed. The site of initial damage even after 20 days, the cracks were not visible but covered by microcapsules (Figure 4.6). Corrosion does not affect the rebar even after

60 days and the rebar looks similar to healthy coated rebar after 60 days. This is observed in MC-D as well as MNC-D coated bars. This observation justifies the healing mechanism proposed in this work by tung-oil microcapsules and was beneficial in impeding corrosion successfully. These phenomenon are be further verified quantitatively by non-destructive testing in the form of corrosion current and ultrasonic guided voltages.

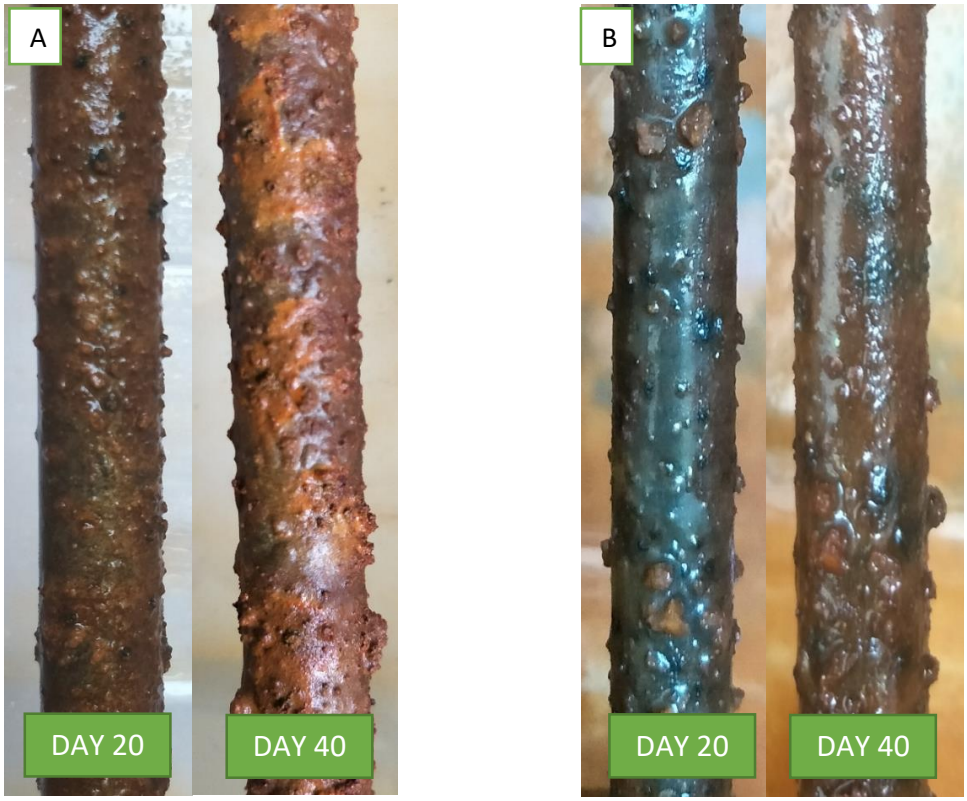

Figure 4.6: Visual observation, (A) MC-D rebar, (B) MNC-D rebar.

4.2.2 Corrosion Current

Corrosion currents for all coated: damaged and undamaged rebar were evaluated to study the effect and initiation of corrosion and point of break of passive layers on bars.

A) Control Rebar

Figure 4.7 shows the variation of corrosion current at constant voltage of 1V in control rebar (uncoated rebar). It is observed that corrosion current suddenly jumps after 8 to 10 h of corrosion, pointing towards the breakdown of passive layer and initiation of corrosion. Further, corrosion rate became almost constant with little fluctuations and on 10^{th} day, corrosion test was stopped since the ultrasonic peak to peak voltage vanished completely.

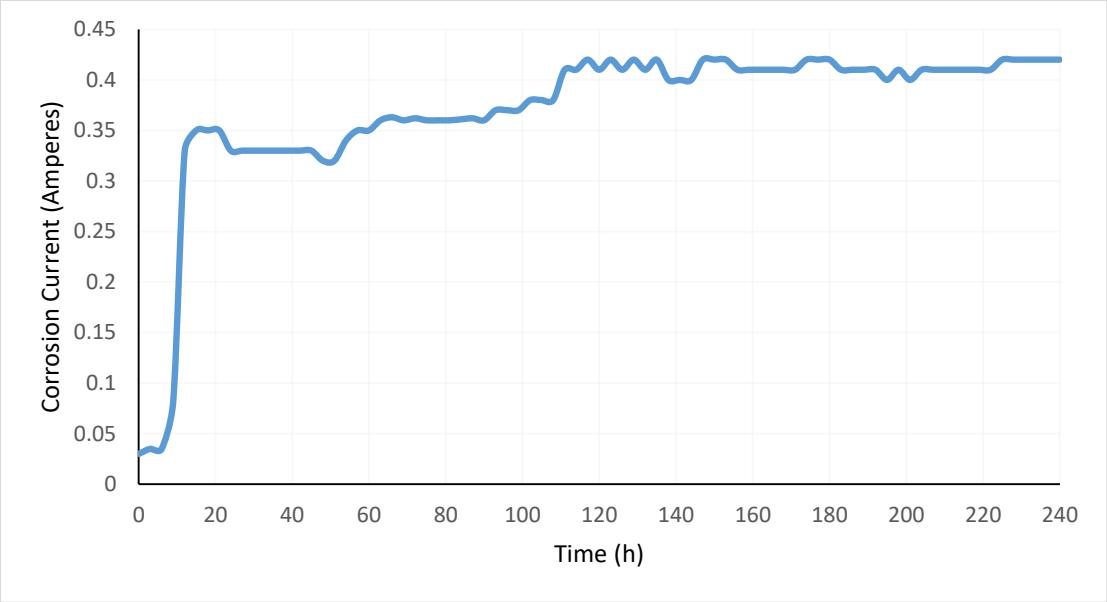

Figure 4.7: Variation in corrosion current in control rebar.

B) Coated Rebar

Figure 4.8, shows the variation of corrosion current for all coated rebar as well as control rebar. The following were observed:

- Passive layer of control bar breakdown within 8-10 h of corrosion whereas passive layer of the PC breakdown on 5th day of accelerated corrosion. It is due to busting of bubbles, which points towards the significant delay in corrosion by plain epoxy.
- In PC after 5 days pitting proceeds and on 18th day, pitting of the rebar reaches to level wherein peak to peak voltage in ultrasonic voltages completely diminishes.
- NC bar shows better corrosion prevention than PC bar. NC bar passive layer breaks down on 8th or 9th day and also the rate of corrosion is much less than PC bar, pointing towards better inhibition by nano-clay mixed epoxy in comparison to plain epoxy coating.
- In NC bar on 25th -26th day, corrosion current suddenly increases, indicating the bursting of bubbles. It was observed that whenever any bubble busted, a jump in current readings was seen. This continued till 41 days as against 18 days in plain epoxy coated bar.
- In MC coated rebar, corrosion initiated on the 5th day by breakdown of passive layer, but interestingly immediately self-healing effect comes into play between day 5-10 days by the polymerization reaction of the tung-oil microcapsules preventing further corrosion. Tung-oil provides an impermeable layer between anode and cathode restricting the flow of

electrons and delay corrosion significantly. This impermeable layer is very firm and it holds corrosion for the entire period of corrosion revelation thereafter as shown by red line in Figure 4.8 from 20-60 days.

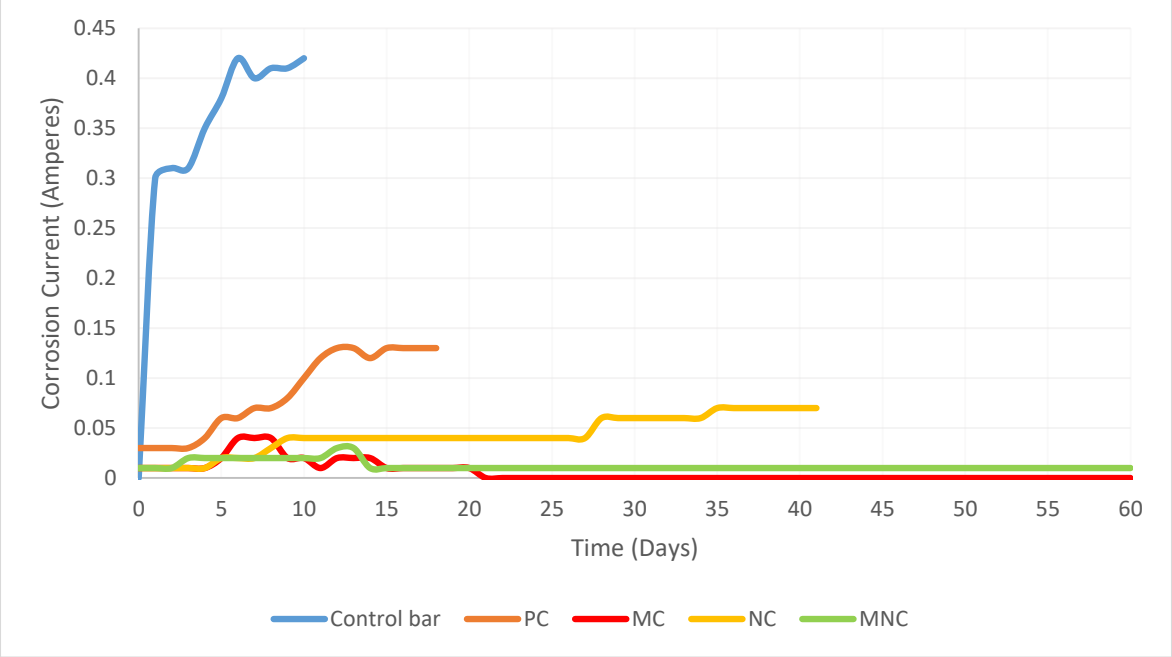

Figure 4.8: Variation in corrosion current in coated bars and control bar.

- MNC behaves almost similar to MC bar. After the breakdown of passive layer on the 10th day, the broken passive layer is not healed everywhere by the tung-oil microcapsules which leads to corrosion of rebar but at very low rate.

Hence it can be concluded that the micro-encapsulation is extremely effective in preventing corrosion further once the passive layer breaks, and healing starts by polymerization and reduces the rate of corrosion significantly in comparison to plain epoxy coating and nano-clay based epoxy coating.

C) Coated Rebar with Initial Damage

- From Figure 4.9, it can be observed that PC-D rebar completely corroded in 15 days, as shown by rise a in corrosion current due to breakdown of passive layer from 5th day onwards, presence of initial damage accelerates corrosion. Bubbles bursts at various locations and current keeps on increasing and reaches a maximum of 0.14A on the 15th day.

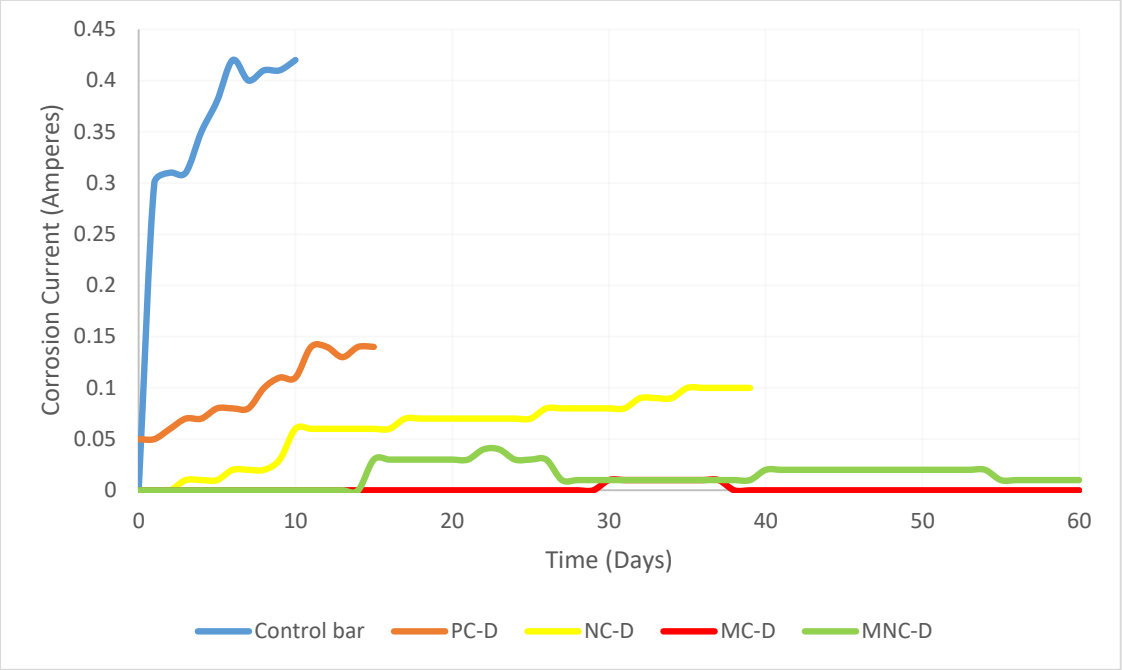

Figure 4.9: Variation in corrosion current in initially damaged coated bars and control bar.

- In NC-D bar, nano-clay platelets were successfully able to reduce the bubble formation but at the damaged region, corrosion accelerated on 10th day of corrosion which further keeps on increasing and nano-clay was not able to restrict after damage initiation.
- Clay is a ceramic and therefore its presence (2 wt %) in epoxy will tends to reduces current because of its non-conductivity to current. Note this effect is independent of corrosion.
- MC-D coated bar did not show any corrosion current until 29 days of exposure indicating that the damage initiated self-healing in the coating when it was left for 5 days for polymerization reaction or healing process after damage which restricts the corrosion for very long time. Microcapsules block the path of electrons and no current reading was seen on the DC power supply. Pointing towards successful self-healing by tung-oil microcapsules of initial damage.
- In MNC-D, on 14th day the passive layer breaks and current flows which was reduced by healing mechanism on 26th day. On 40th day again increase in current is observed which remains constant for long time and reduces at later stages, probably due to healing effect.
- The initially damaged coated bars showed higher current than in comparison to coated rebar without damage (Figure 4.10 and Figure 4.11). Initial damage facilitated the healing process of tung-oil microcapsules in both MC and MNC bars.

- The addition of nano-clay is to significantly reduce crack propagation in matrix (epoxy) and then in undamaged specimen, NC offers better corrosion protection as compared to PC. But in damaged specimen, crack have already been introduced by the researcher in the epoxy, hence the advantage of clay is lost when NC and PC are compared. Same observation will be valid for damaged and undamaged MC and MNC comparison, concluded that damage particularly reduce performance of nano-clay coatings but it is still more effective than PC.

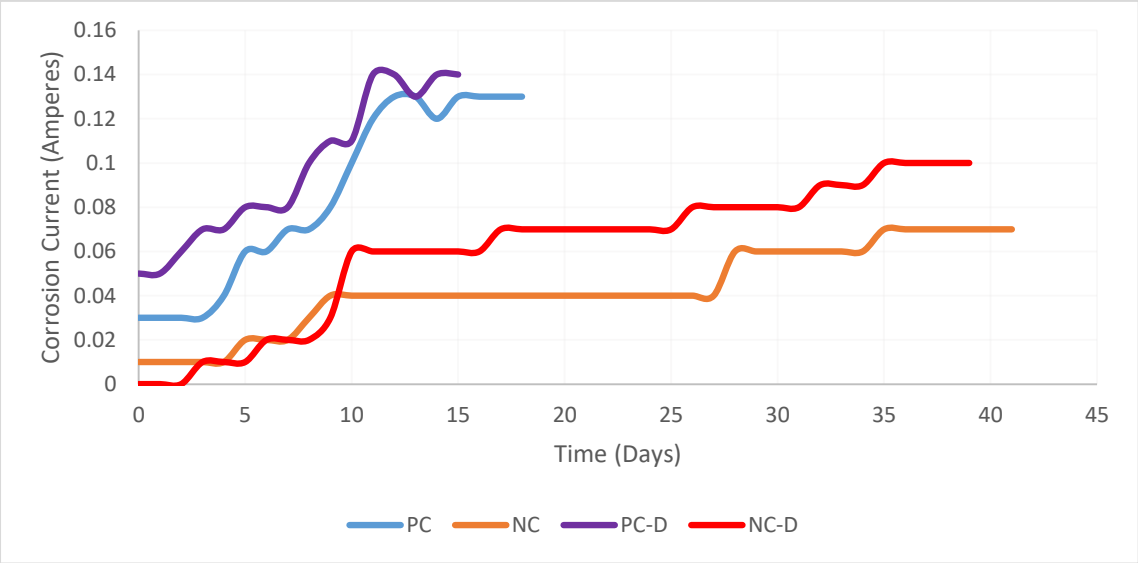

Figure 4.10: Variation in corrosion current in PC and NC rebar with or without damage.

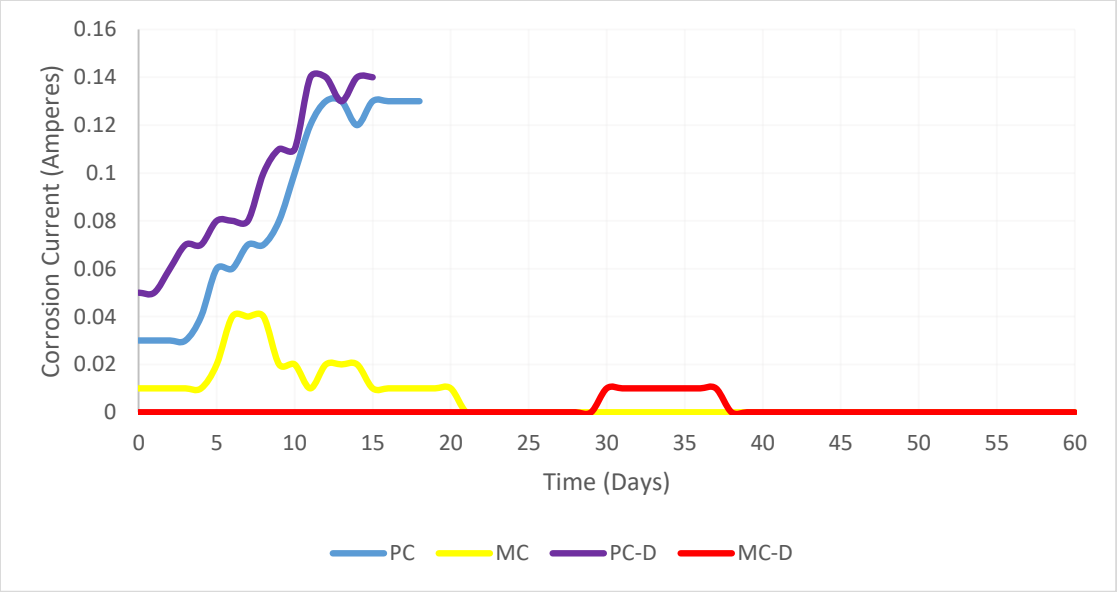

Figure 4.11: Variation in corrosion current in PC and MC rebar with or without damage.

4.2.3 Ultrasonic Guided Waves (UGW)

From the ultrasonic guided wave signatures peak to peak voltage was calculated and expressed as ratio with healthy bar value. The ultrasonic signatures obtained for all coated bars without damage and control bar are shown in the succeeding section. Signature behavior is similar for all the types of bars except the duration of the fall of signals. Therefore only undamaged coatings signature were shown (Figure 4.12 - 4.16) to understand the significance of UGW signatures.

Figure 4.12 shows the ultrasonic signatures obtained for a control bar without any coating subjected to successive days of corrosion. The ultrasonic peak obtained diminishes with increasing corrosion level, since the bar undergoes degradation in the form of pitting which reduces the signal transmission and the ultrasonic pulse received at the other end diminishes with increasing corrosion. The pulses vanished after 10 days of corrosion test.

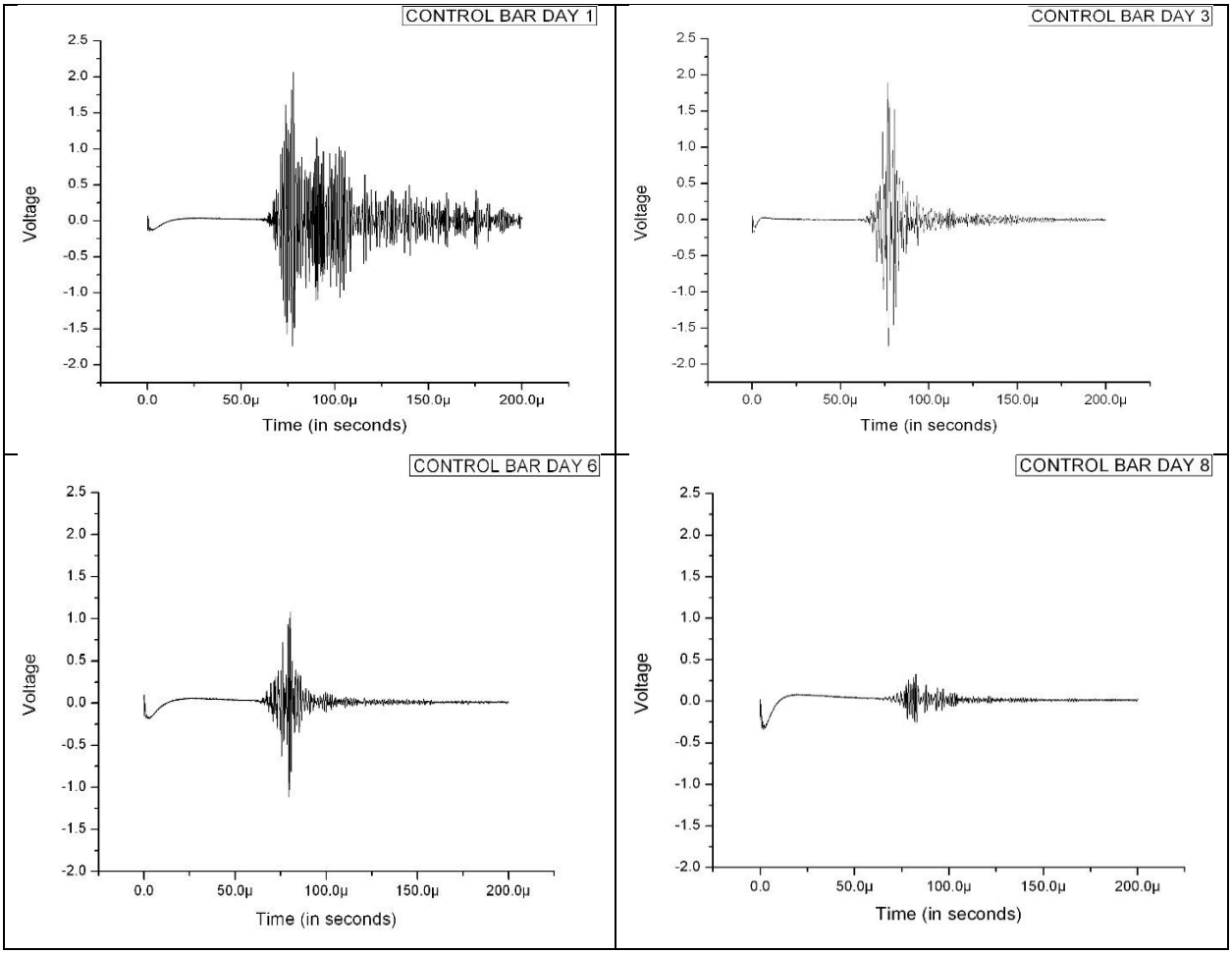

Figure 4.12: UGW signatures at different phases of corrosion of control rebar.

Figure 4.13 shows similarly the ultrasonic signals received, vanishes after 18 days at same degree/level of corrosion. It shows that epoxy coating is able to delay the corrosion by 8 days in comparison to plain rebar.

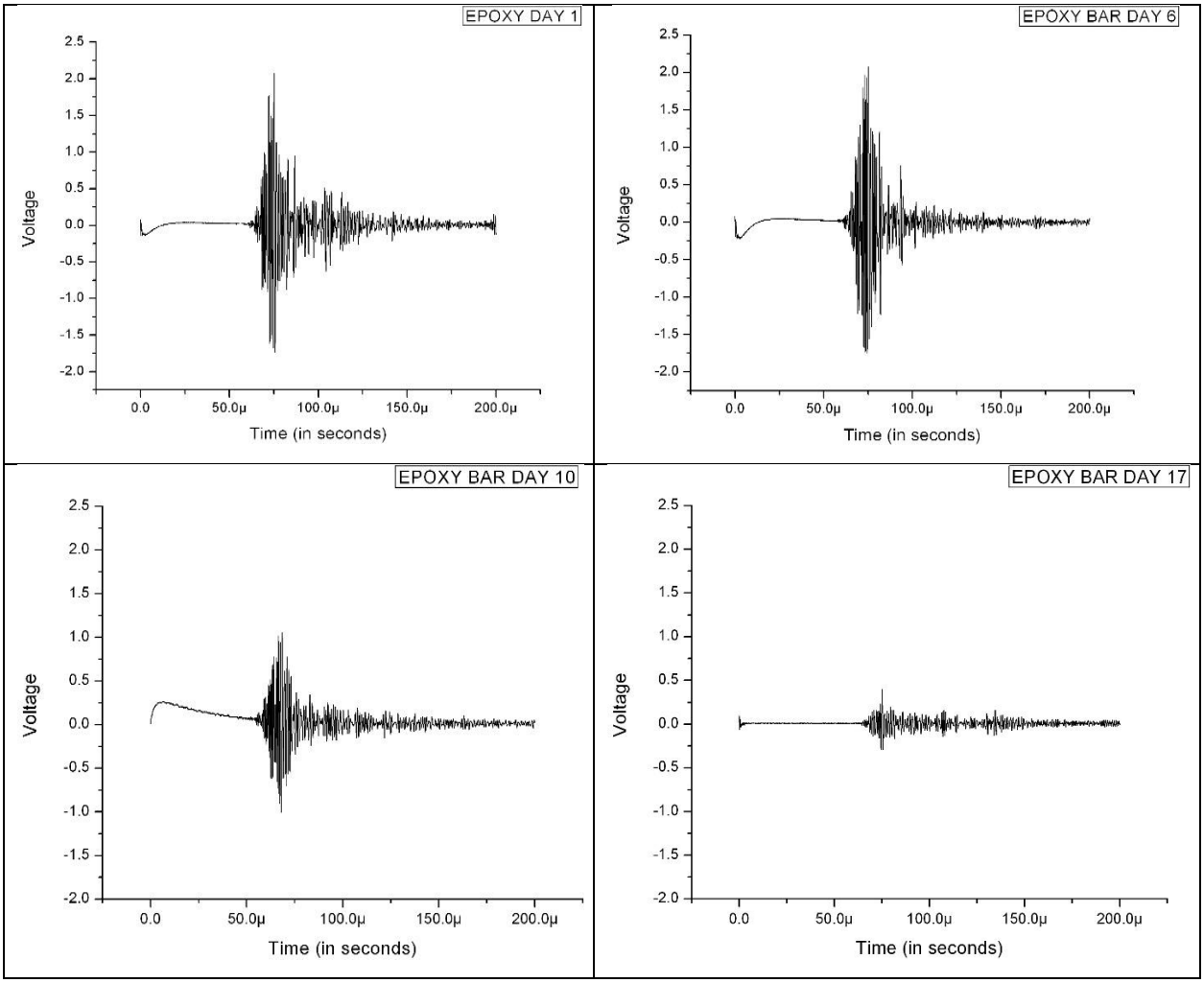

Figure 4.13: UGW signatures at different phases of corrosion of PC rebar.

Figure 4.14 showing the ultrasonic signatures obtained for a rebar coating with nano-clay, shows the effectiveness of nano-clay in inhibiting corrosion till 41 days in comparison to 10 days and 18 days in plain and epoxy coated rebar, respectively.

The best results of corrosion inhibition was displayed by tung-oil microcapsules coated rebar (Figure 4.15, 4.16) both MC and MNC bars. The corrosion was significantly low even after 60 days of corrosion in both bars. MC bars showing the self-healing characteristics performed the best and it elaborates the effectiveness of microcapsules in self-healing of coated rebar (Figure 4.18).

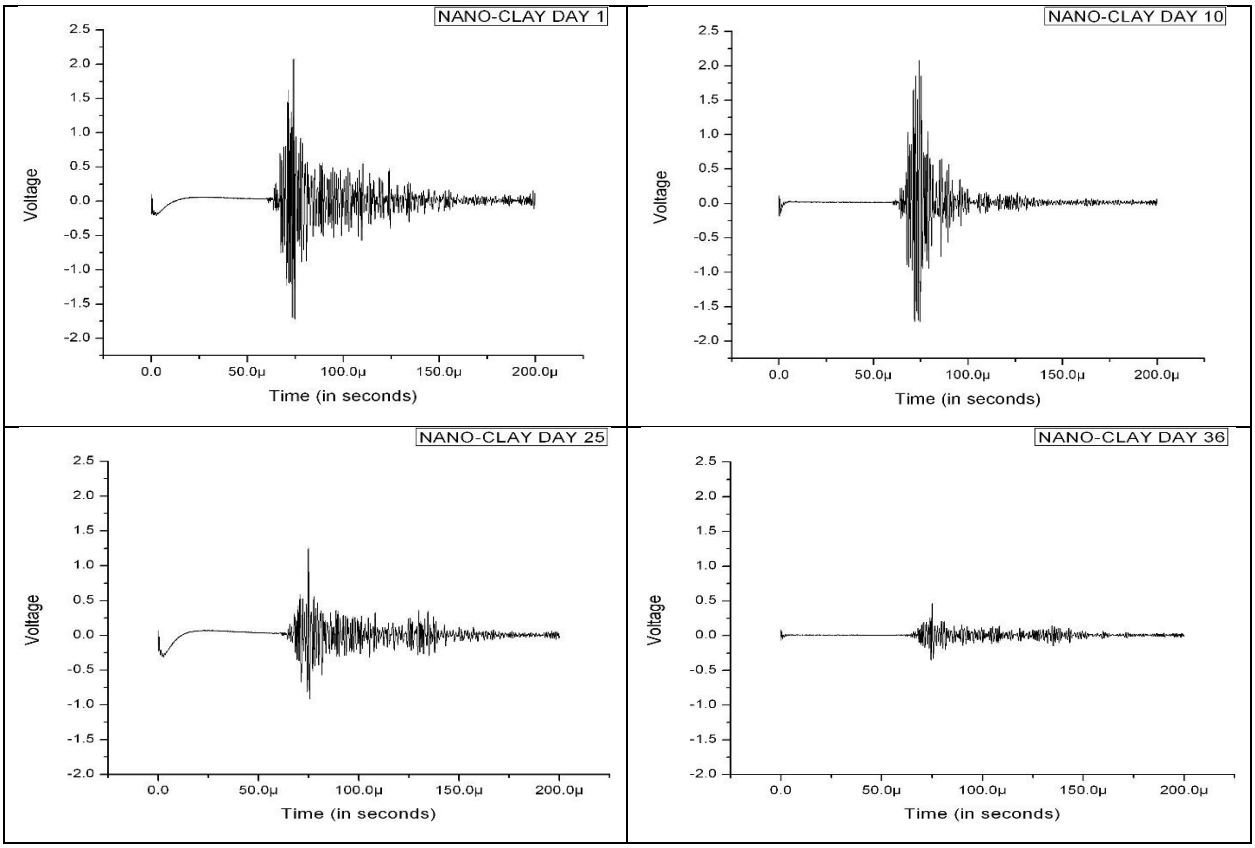

Figure 4.14: UGW signatures at different phases of corrosion of NC rebar.

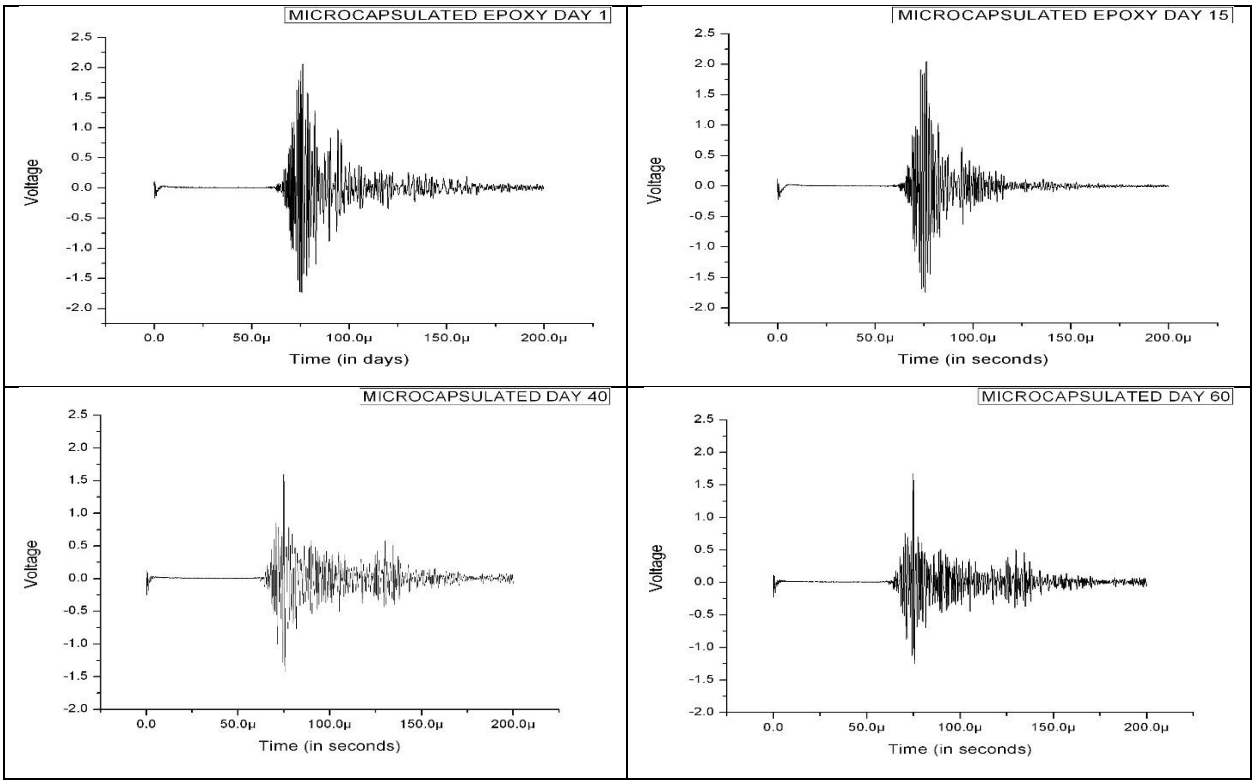

Figure 4.15: UGW signatures at different phases of corrosion of MC rebar.

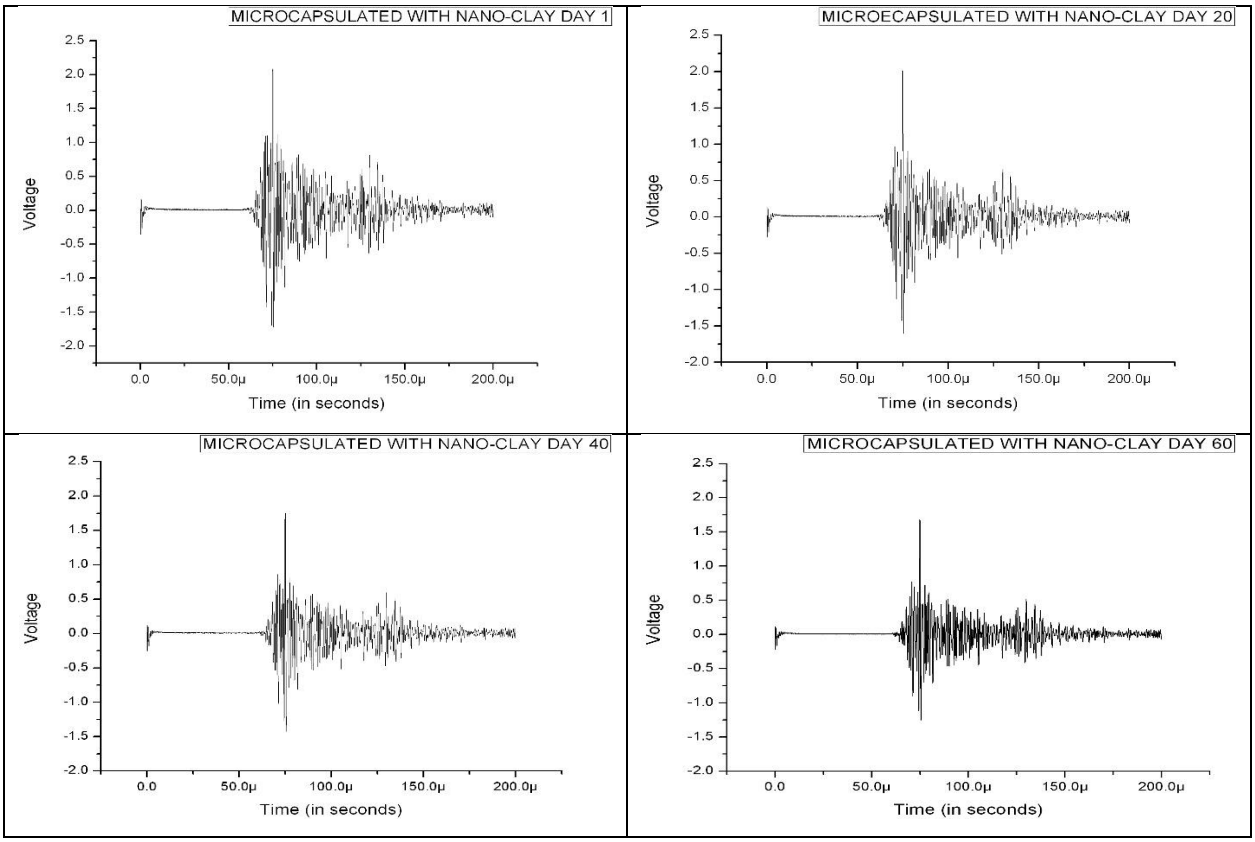

Figure 4.16: UGW signatures at different phases of corrosion of MNC rebar.

A) Coated Rebar

- Continued from Section 4.2.2 discussion, the PC bars show drop after 5 days, as against 1st day drop in control bar (Figure 4.17) showing better performance than control bar. The signals vanished on 10th and 18th day in control bar and PC bar respectively, indicating the effectiveness of epoxy coatings in delaying corrosion.
- NC coated rebar showed better performance than PC rebar. Voltage drops was observed after 11 days and was significantly slow as compared to PC (5 days). Because of less bubbles formation and busting, less spots are available for corrosion initiation and hence rate of corrosion was very low.
- The corrosion continued till 41 days as against 18 days of PC bar showing significant protection offered by NC coated rebar to corrosion inhibition.
- MC rebar performance was best as compared to NC and PC bars. Rate of voltage drop was insignificant 30-35 days, and later very small drop is observed till 60th day and voltage

reduced from 3.82V to 3.125V only pointing towards the significant healing by tung-oil microcapsules.

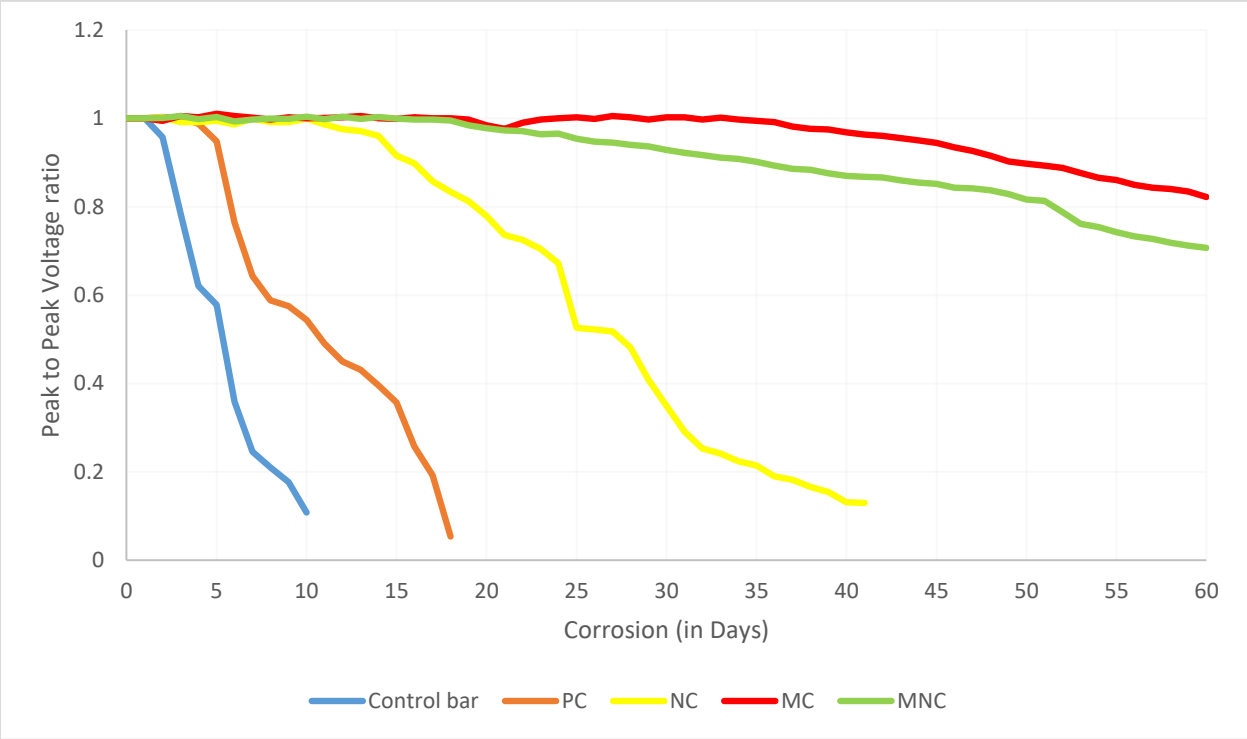

Figure 4.17: Peak to peak voltage ratio-corrosion time variation in coated bars and control bar.

- MNC rebar performance almost similar to MC rebar but a layer more drop in voltage as compared to MC rebar was noted. But its performance was much better than PC rebar and NC rebar.
- Hence UGW have the capability of picking up healing provided by microcapsules to corrosion inhibition.

B) Coated Rebar with Initial Damage

- From Figure 4.18, it is observed that PC-D rebar holds corrosion exposure for 15 days compared with 10 days of control rebar. As discussed in Section 4.2.2, initial damage presence accelerates corrosion due to which peak to peak voltage vanished in 15 days.
- NC-D performed better than PC-D rebar. Voltage starts drop after 10 days and rate was significantly low as compared to PC rebar, pointing towards the better corrosion inhibition continues for 38 days compared to 15 days of PC rebar.

- MC-D and MNC-D rebar performed almost similar. There is no significant drop of voltage observed for both. MC-D performed best among all but MNC-D performance much better than PC-D and NC-D rebar. This implies that the dominated role in reducing corrosion is due to tung-oil encapsulation as compared to the nano-clay rebar.

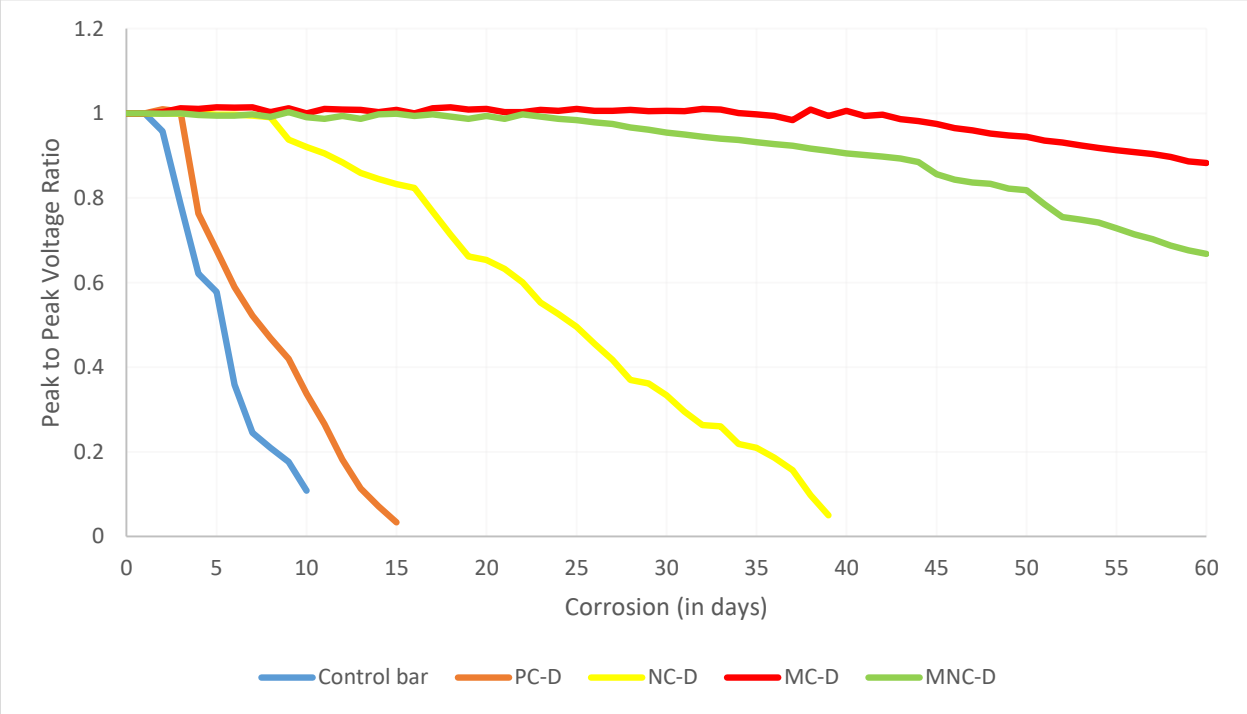

Figure 4.18: Peak to peak voltage ratio-corrosion time variation in damaged coated bars and control bar.

- Comparison of coatings with or without damage are shown in Figure 4.19 & 4.20. In PC bars with initial damage showing a rapid reduction in voltage than undamaged PC bars. Initiation of corrosion is earlier in PC-D rebar and ultrasonic signals vanish earlier in PC-D rebar as compared to PC rebar. Similar observation made with NC coated bars with and without damage. The comparison of PC with NC-D coated bars shows better performance of NC-D bars than PC bars.
- From Figure 4.20, it was observed that MC and MC-D rebar performance was much better than PC rebar. MC-D and MC rebar performance is almost similar pointing towards the successful self-healing effect of tung-oil microcapsules. MC and MC-D rebar uphold in corrosive environment for 60 days compared to 15 days and 18 days for PC-D and PC rebar respectively.

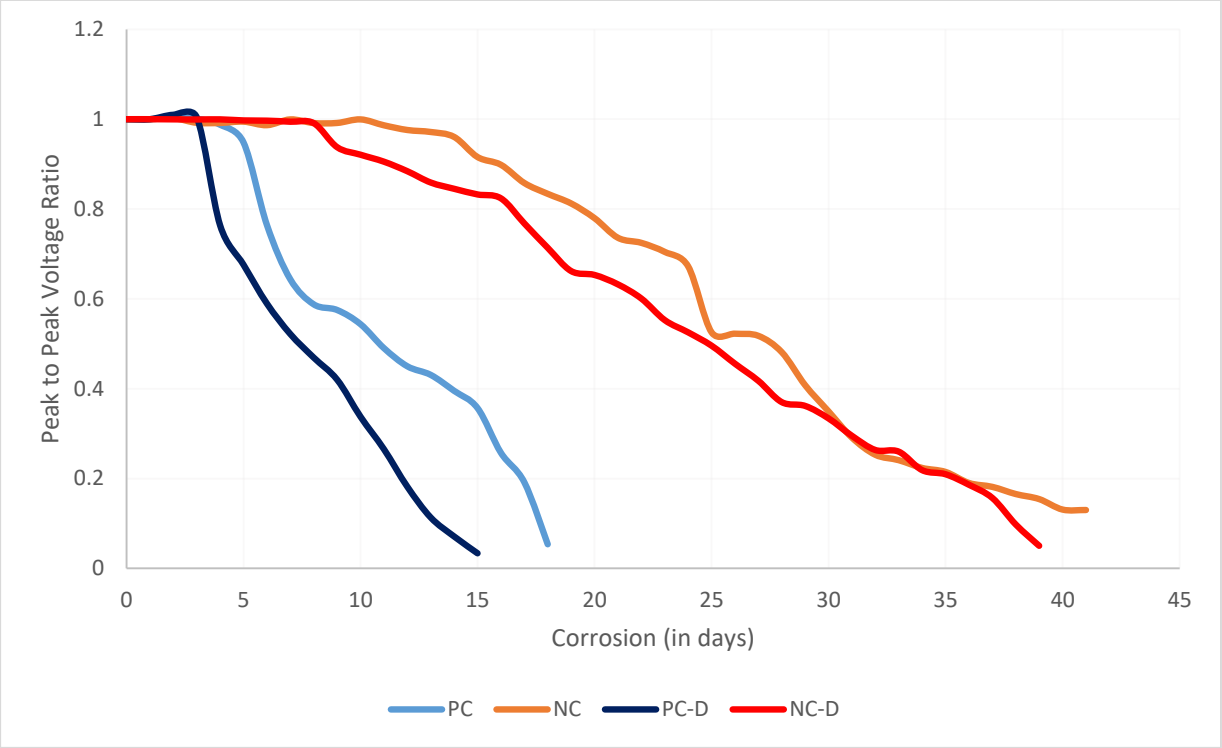

Figure 4.19: Peak to peak voltage ratio-corrosion time variation in PC and NC rebar with or without damage.

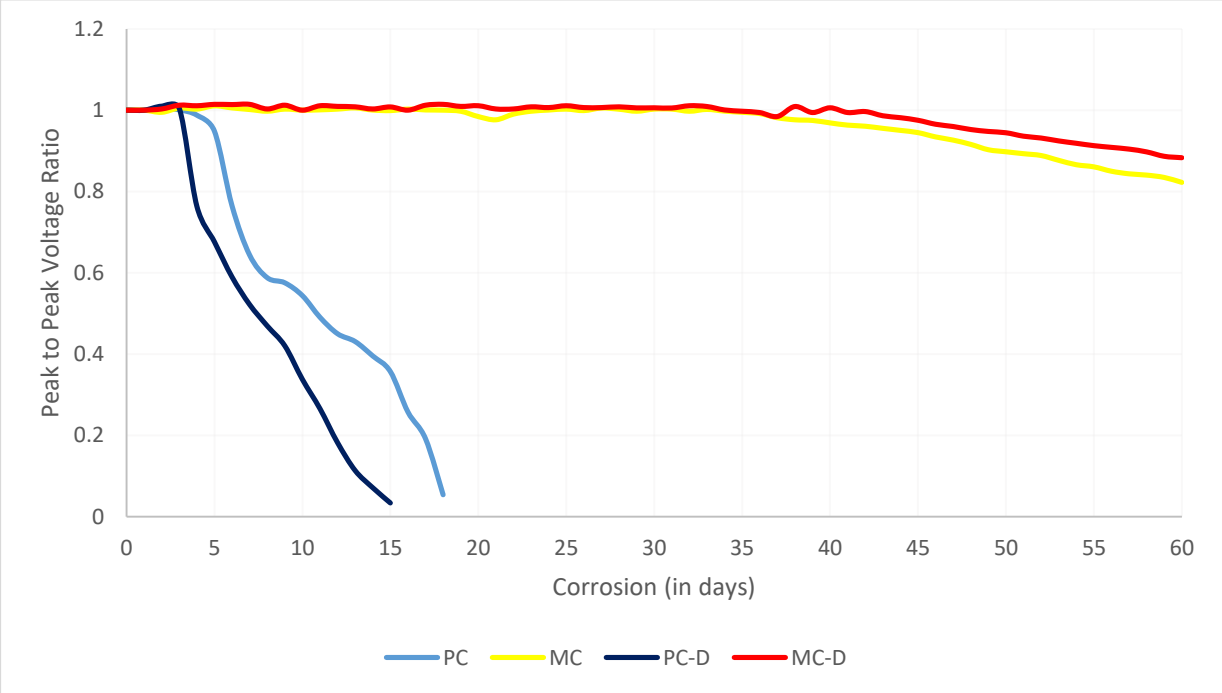

Figure 4.20: Peak to peak voltage ratio-corrosion time variation in PC and MC rebar with or without damage.

4.3 REINFORCED CONCRETE BEAMS

The effectiveness of different types of epoxy based coatings vis-à-vis corrosion initiation has been studied by corrosion current and ultrasonic guided wave changes as the bar reinforced in concrete undergoes accelerated corrosion. In visual inspection red brownish product observed on all beams, there is no such evidence found through which comparison of all the types of coted RC beams can done.

4.3.1 Corrosion Current

Corrosion current for all coated bars in concrete with initial damage and without damage has been evaluated to study the effect on corrosion rate in concrete.

A) Coated Rebar in RC beams

- Figure 4.21 shows the deviation of corrosion current at constant voltage of 15V in all coated bars as well as control reinforced beam. It was perceived that in control beam current initiates indicated by jump after 8 days in corrosion current pointing towards the breakdown of passive layer. After 16 days corrosion current was stopped since the ultrasonic peak to peak voltage vanished completely with days indicating damage of rebar due to corrosion.

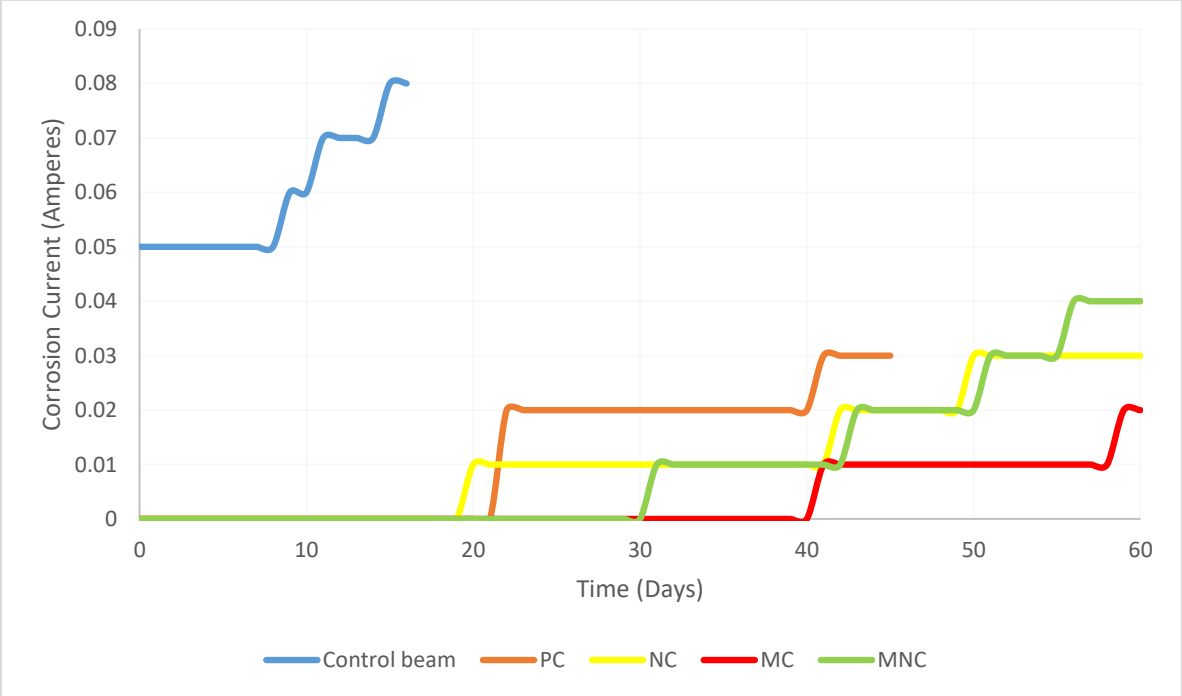

Figure 4.21: Variation in corrosion current in different beams.

- From Figure 4.21, in beams with PC rebar corrosion current initiated after 21 days as compared to 8 days in control beam with respect to corrosion delay, pointing towards the effectiveness of PC rebar over uncoated rebar. Rate of corrosion is much lower in PC rebar beam and corrosion continues till 45 days.
- In beams with NC coated rebar, better corrosion prevention is observed than PC beam. Breakdown of passive layer is observed on the 20th day but the rate of corrosion current is lower than PC beam pointing towards better inhibition by nano-clay in comparison with plain epoxy coated rebar beam.
- In MC and MNC beams no breakdown of passive layer was observed till 40 days and 30 days respectively indicating self-healing capability of microcapsules. MC rebar beam observed most promising corrosion inhibition out of all, NC, MC and MNC rebar beams and holds corrosion till 60 days.

B) Coated Rebar with Initial Damage in RC Beams

- From Figure 4.22, it was observed that beams with PC-D rebar holds corrosion for 38 days and rise in corrosion current observed after 19 day indicating breakdown of passive layer whereas effect of presence of initial damage was not much observed.

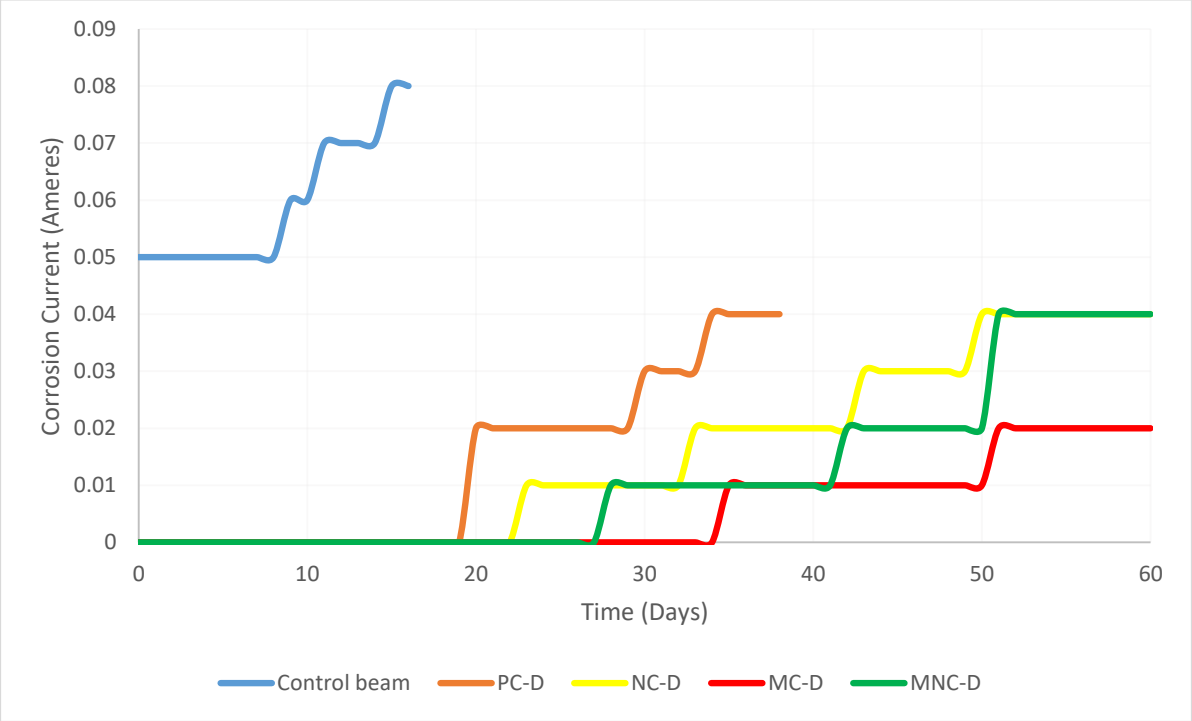

Figure 4.22: Variation in corrosion current in different beams.

- In NC-D beams, corrosion current observed was lower than the PC-D beams pointing towards the better corrosion prevention by nano-clay.
- MC-D and MNC-D beams performed good in comparison with PC-D and NC-D. MC-D performed outstanding among all whereas corrosion continued till 60 days for all NC-D, MC-D and MNC-D since ultrasonic guided waves are not completely vanished.

4.3.2 Ultrasonic Guided Waves (UGW)

From UGW signatures peak to peak voltage was calculated and expressed as ratio with healthy bar value. Signatures obtained for all the beams signifies similar consequence as discussed in Section 4.2.3 for plain mild steel rebar except duration of fall of pulses which were discussed by the peak to peak voltage ratio graphs.

A) Coated Rebar in RC Beams

- Continued from discussion 4.3.1, Figure 4.23 represents peak to peak voltage ratio with corrosion for coated rebar beams as well as control RC beam. PC rebar beams shows voltage drop after 10 days as against 4 days drop in control beam, indicating the effectiveness of PC beam in delaying corrosion.
- NC beams holds corrosion better than PC beams, the corrosion continued till 60 days in NC beams since ultrasonic peak to peak voltage did not vanished completely.

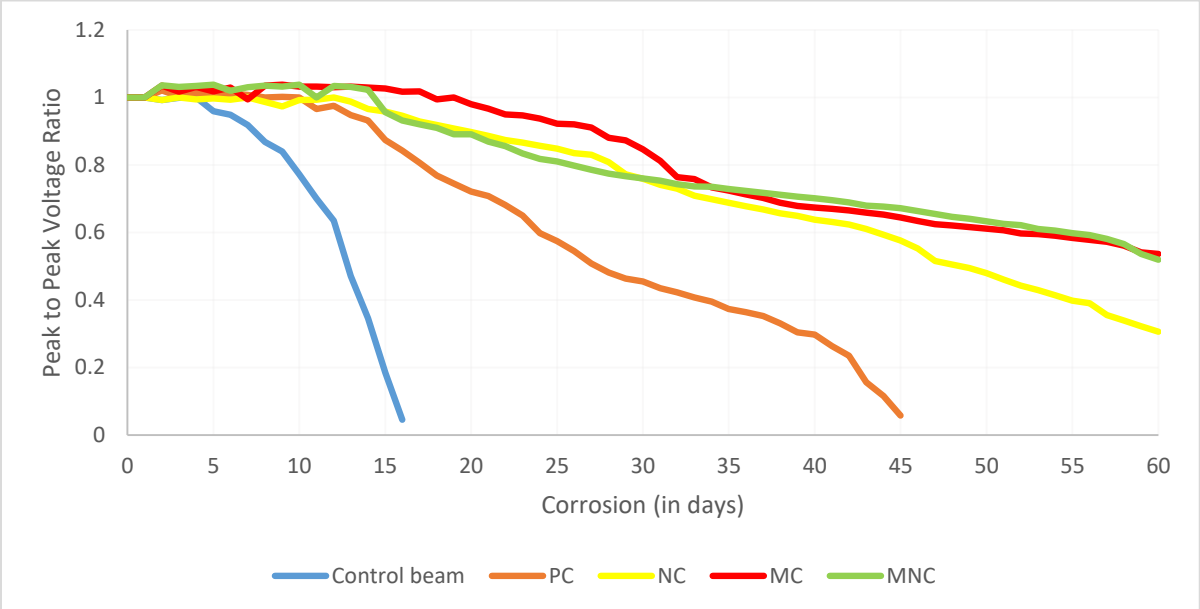

Figure 4.23: Peak to peak voltage ratio-corrosion time variation in coated RC beams and control beam.

- Both MC and MNC coated beams holds corrosion till 60 days, in MNC beam voltage drops between 15-30 days at constant rate then later on rate of drop in voltage reduces whereas MC beams holds corrosion better than MNC beams till 30 days then a constant rate of reduction was observed signifies self-healing effect performance in corrosion inhibition..

B) Coated Rebar with Initial Damage in RC Beams

- From Figure 4.24, it was observed that PC-D beam also performed better than control beam, drop observed on 6th day of corrosion and after 30 days of corrosion rate of voltage drop was high which completely vanished ultrasonic signals on 38th day.
- NC-D, MC-D and MNC-D rebar beams behaves similarly till 20 days. Later on rate of voltage drop was different for all of them, highest for NC-D. All three coated rebar beams holds corrosion exposure for 60 days since ultrasonic voltage does not vanished completely indicating the effectiveness of coatings in comparison with plain epoxy coated rebar beams.

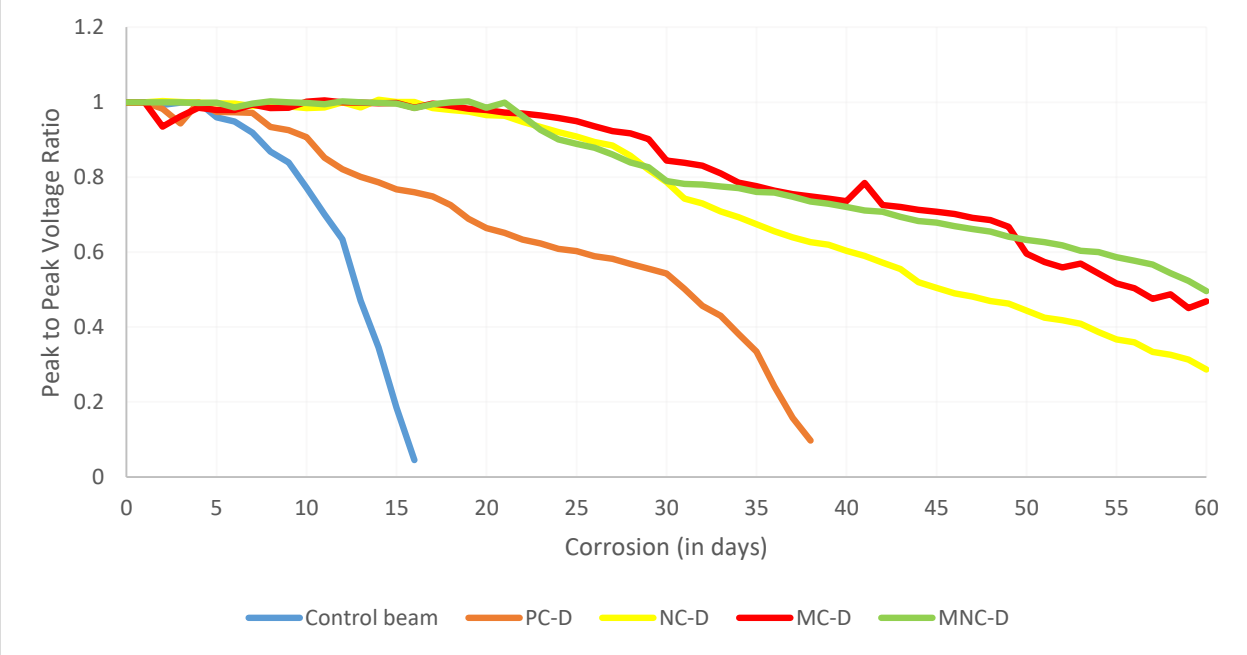

Figure 4.24: Peak to peak voltage ratio-corrosion time variation in coated RC beams and control beam.

4.4 DESTRUCTIVE TESTING

After completion of accelerated corrosion testing all the corroded samples were removed and cleaned to remove all the corrosion product. Then mass loss due to corrosion and residual

strength of corroded bars measured for both damaged and undamaged conditions of plain mild steel rebar and rebar of RC beams.

4.4.1 Corroded Samples Images

Samples used for the corrosion testing of plain mild steel rebar were imaged to observe the condition of the rebar after corrosion. Bars removed from corrosion, washed and cleaned to remove corrosion product and imaged. In Figure 4.25, uncoated rebar before corrosion and after corrosion is being displayed. After 10 days of corrosion of uncoated plain rebar the diameter of the rebar is significantly and uniformly reduced throughout the section which was subjected to corrosion.

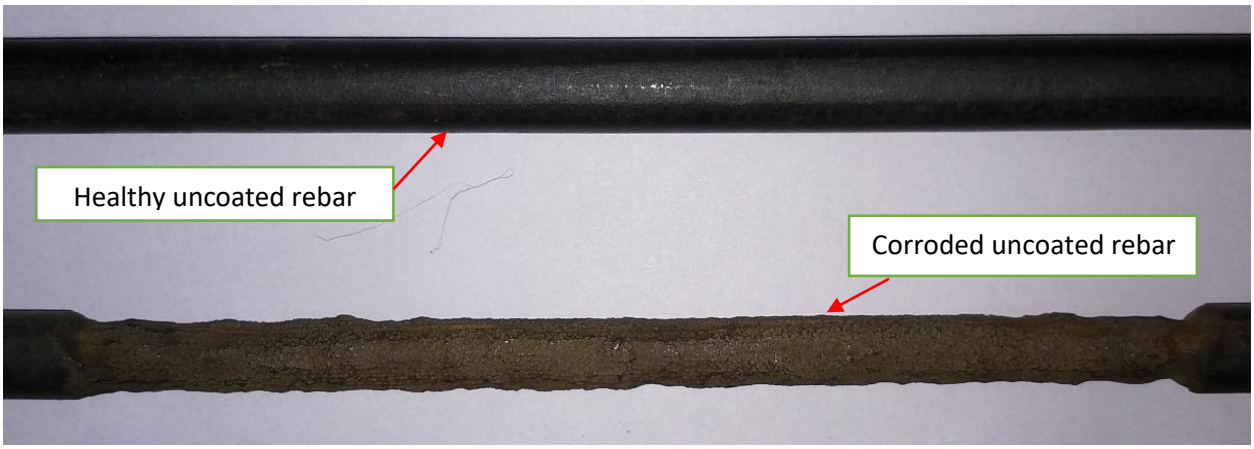

Figure 4.25: Uncoated rebar before corrosion and after 10 days of accelerated corrosion of plain mild steel rebar.

In Figure 4.26, all coated rebar conditions displayed after corrosion, in which pitting due to corrosion can see evidently. From Figure 4.26, in PC rebar it is observed that the reduction of the diameter is noticeable almost throughout the rebar section but pitting was more where bubbles busted earlier (Section 4.2.1). In NC rebar, it can be observed that only the locations where bubbles busted were subjected to pitting, rest of the surface of rebar was negligibly affected by corrosion or very less pitting of rebar observed indicating better performance than PC rebar.

From Figure 4.26, in corroded MC rebar it is observed that the pitting due to corrosion was least among all. Corrosion only affect the surface of the rebar and due to self-healing microcapsules pitting was not boosted further. In the pits of MC rebar, self-healing microcapsules product was found which could be the reason to restrict corrosion pitting of rebar to next level. In corroded MNC rebar displayed image it was observed that pitting due to corrosion is present on various locations and more as compared to MC rebar due to less uniformity of self-healing microcapsules.

Pitting holes still not as much big as observed in PC and NC rebar pointing towards more effectiveness than both.

Figure 4.26: Corroded plain mild steel rebar, (A) PC rebar after 18 days, (B) NC rebar after 41 days, (C) MC rebar after 60 days, (D) MNC rebar after 60days of corrosion.

4.4.2 Mass Loss

Mass loss after corrosion testing was measured with the aid of weighing balance. Mass loss of all samples subjected to accelerated corrosion for plain mild steel rebar discussed in the Table 4.1 and mass loss of all samples of accelerated corrosion for bars in RC beams is discussed in Table 4.2.

Table 4.1: Mass loss for undamaged and damaged coated rebar and for control rebar.

Sample Type	Mass Loss in Sample 1 (grams)	Mass Loss in Sample 2 (grams)	Mass Loss in Sample 3 (grams)	Average Mass Loss (grams)
Control bar	63	76	67	68
PC bar	35	37	32	35
NC bar	22	25	24	24
MC bar	12	13	10	12
MNC bar	15	16	15	15
PC-D bar	34	38	37	36
NC-D bar	24	23	21	23
MC-D bar	10	12	14	12
MNC-D bar	14	13	14	14

From Table 4.1, average loss of mass is maximum for control bar, 25% mass loss observed in control bar from healthy sample whereas 12% mass reduction marked for PC rebar. In NC rebar it is 9% and in MC rebar it is 4% of healthy samples. From the results it can be clearly concluded that the tung-oil microencapsulated coatings were most effective for corrosion inhibition.

From the Table 4.1 it is observed that when epoxy is introduced to an uncoated rebar mass loss due to corrosion is almost 48% reduced (PC rebar) and when tung-oil microcapsules were introduced in epoxy coating loss of mass due to corrosion is approximately reduced to 82% in comparison with uncoated rebar. Pointing towards the effectiveness of MC coatings due to self-healing effect. Similarly, initially damage induced coatings displayed almost similar loss of mass due to corrosion.

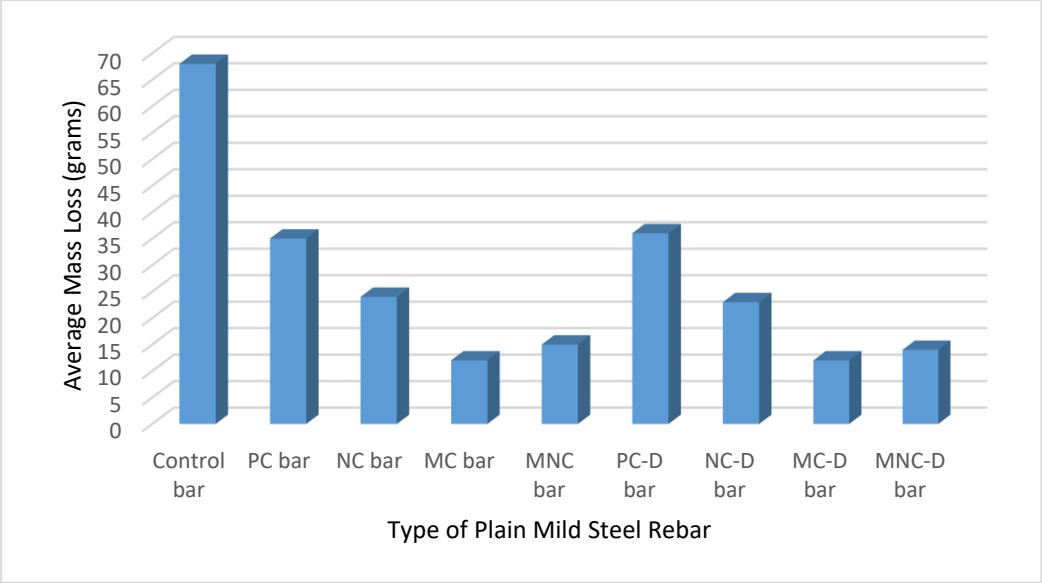

Figure 4.27: Average mass loss of corroded plain mild steel rebar.

Table 4.2: Mass loss for undamaged and damaged coated RC beams and for control beam.

Sample Type	Mass Loss in Sample 1 (grams)	Mass Loss in Sample 2 (grams)	Average Mass Loss (grams)
Control beam	18	22	20
PC beam	08	10	09
NC beam	06	11	8.5
MC beam	03	04	3.5
MNC beam	03	05	4
PC-D beam	09	08	8.5
NC-D beam	06	08	07
MC-D beam	04	04	04
MNC-D beam	03	04	3.5

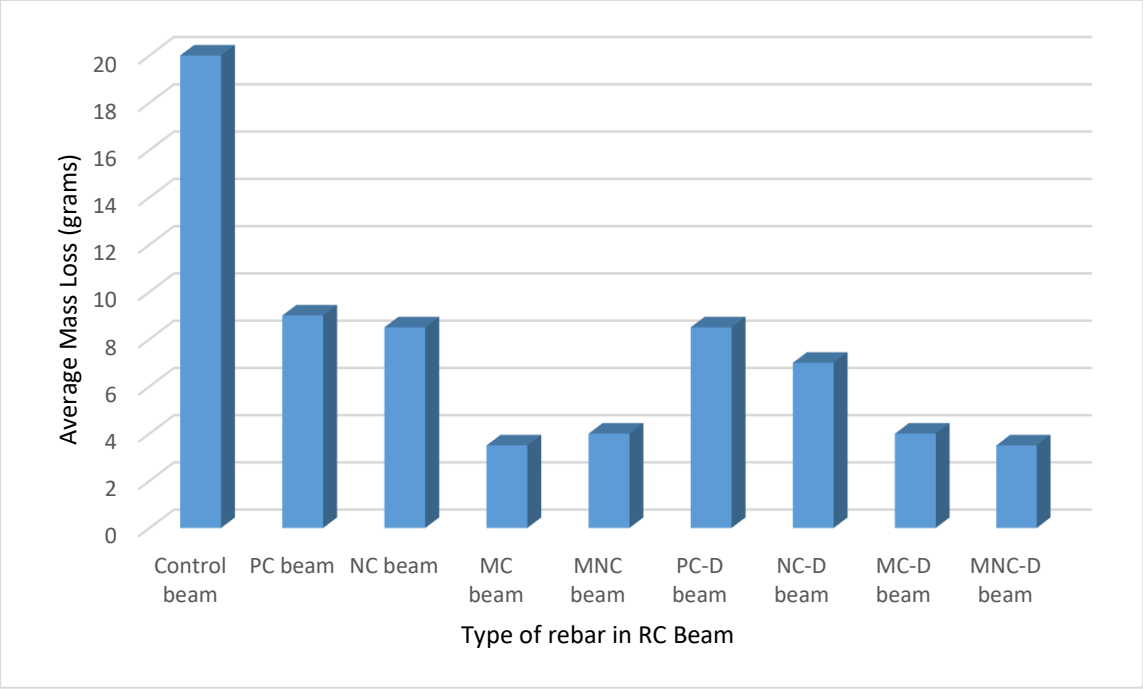

Figure 4.28: Average mass loss of corroded bars in RC beam.

In Table 4.2, average loss of mass is displayed for all bars corroded in RC beams. Loss of mass for control beam rebar is 7% in comparison with healthy rebar whereas in PC beam rebar it is observed as 3-4%. In NC beam and in MC beam rebar it is observed to be 2-3% and 1-2% respectively indicating that the MC beams are most effective for corrosion inhibition.

Mass loss due to corrosion in reinforced beams is not very effective since very less mass loss difference observed for all different types of coatings. Loss of mass in MC beam rebar is 60% less as compared to loss of PC beam rebar whereas in NC beam rebar only 10% increment in mass loss due to nano-clay as compared to PC beam and initially damage induced beams also have similar pattern of mass loss due to corrosion.

4.4.3 Residual Strength of Rebar

Residual tensile strength of rebar measured after corrosion testing. After weighing and cleaning corroded samples were tested on UTM for its residual tensile strength. Samples corroded in accelerated corrosion testing of plain mild steel rebar is discussed in Table 4.3 and samples corroded in accelerated corrosion testing of rebar in RC beams is discussed in Table 4.4.

Table 4.3: Residual strength for undamaged and damaged coated rebar and for control rebar.

Sample Type	Peak Load of Sample 1 (kN)	Peak Load of Sample 2 (kN)	Peak Load of Sample 3 (kN)	Average Residual Tensile Peak Load (kN)
Control bar	40	42	39	41
PC bar	24	27	23	25
NC bar	41	29	35	35
MC bar	68	67	72	69
MNC bar	57	49	62	56
PC-D bar	19	21	23	21
NC-D bar	40	43	39	41
MC-D bar	72	75	70	72
MNC-D bar	69	71	72	71

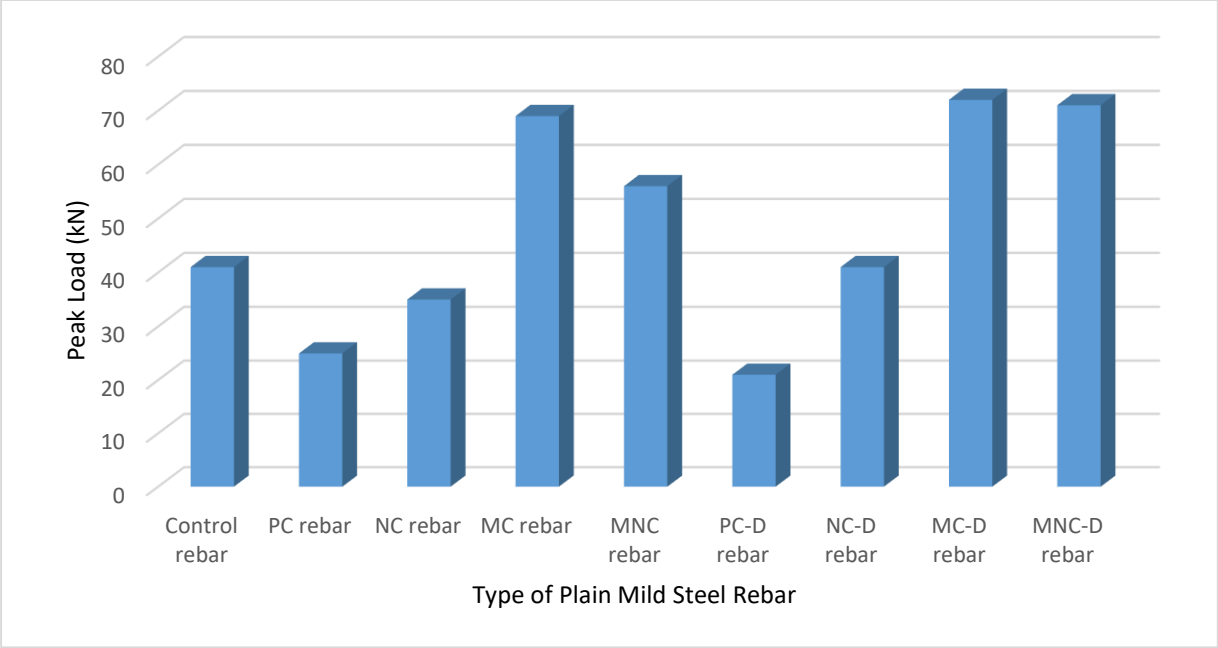

Figure 4.29: Residual tensile strength of corroded plain mild steel rebar.

From Figure 4.29, it was observed that residual tensile strength for PC rebar is less than control rebar since in control bar uniform reduction in surface area whereas in PC rebar continuous pitting on particular location or spots leads weak point for tensile strength. Residual strength of tung-oil micro-encapsulated coated rebar is highest since least pitting holes present in MC rebar.

Tensile strength of uncoated corroded rebar 65% less in comparison with healthy rebar whereas tensile strength of MC rebar is 27% less in comparison with healthy rebar pointing towards the effectiveness of MC rebar over uncoated rebar. Highest decrement of 77% is observed for PC rebar. In damaged induced rebar also strength parameters follows the almost similar manner indicating that microcapsules induced coatings were most effective to corrosion inhibition.

Table 4.4: Residual strength for undamaged and damaged coated rebar in RC beams and for control beam.

Sample Type	Peak Load of Sample 1 (kN)	Peak Load of Sample 2 (kN)	Average Residual Tensile Peak Load (kN)
Control beam	96	92	94
PEC rebar	82	87	84.5
NCEC rebar	76	79	77.5
MCEC rebar	88	93	90.5
MCNC rebar	89	88	88.5
Dam PEC rebar	85	87	86
Dam NCEC rebar	75	73	74
Dam MCEC rebar	83	91	87
Dam MCNC rebar	88	86	87

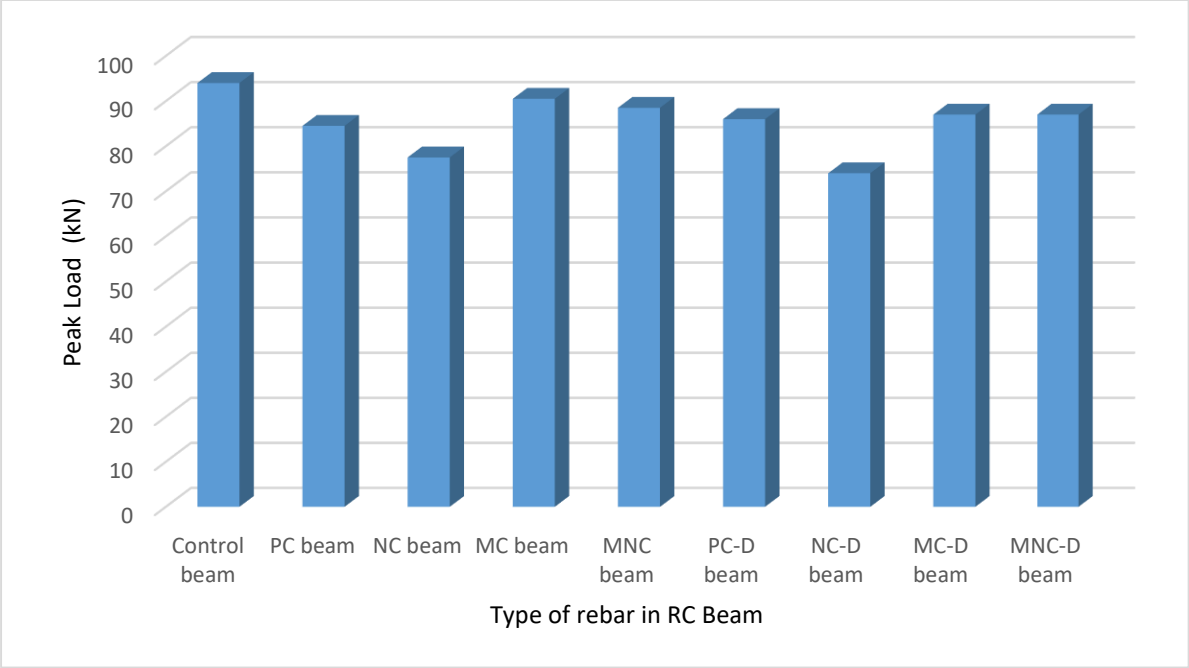

Figure 4.30: Residual tensile strength of corroded bars in Reinforced beam.

From Figure 4.30, it is observed that residual tensile strength of control beam rebar is more than PC beam rebar since control beam rebar reduction in surface area is more uniform than PC rebar. Tensile strength of nano-clay based coated rebar is lowest in the test for both damaged and undamaged condition. While performance of corroded MC and MNC rebar in tensile strength is quite good in comparison with PC and NC beam rebar.

4.5 PULLOUT STRENGTH TESTING

Rebar pullout strength testing used to assess the reinforced mild steel rebar and concrete interface reliability, which may be changed by the introduction of coatings for mild steel rebar. Interface of steel and concrete is filled by coating and changes in the behavior is evaluated by pullout testing shown in Table 4.5.

From Figure 4.31, the pullout strength of uncoated rebar is more than the PC and NC coated rebar since PC and NC coatings introduce glossy or smooth surface in comparison with uncoated rebar. Introducing microcapsules into coatings makes surface of rebar rougher than PC and NC coatings leads to little increment in pullout strength of rebar. But variations of all coatings and uncoated rebar is not much different indicating that the provided thickness of the coatings hardly affect the performance of bond strength criteria.

Table 4.5: Pullout strength of coated bars and uncoated bar (kN).

Sample Type	Sample 1	Sample 2	Sample 3	Average
Uncoated rebar	31	30	31	31
PC rebar	29	28	30	29
NC rebar	28	28	30	29
MC rebar	33	31	32	32
MNC rebar	33	35	30	33

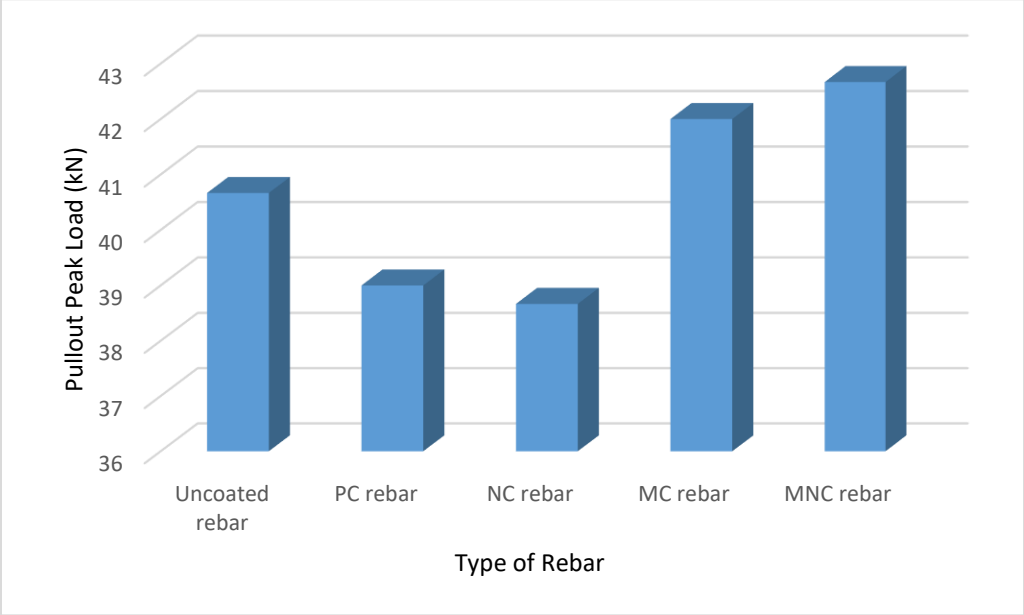

Figure 4.31: Average pullout strength of coated bars and uncoated bar.

4.6 MICRO-STRUCTURE STUDY

Tung-oil based self-healing microcapsules were characterized using scanning electron microscopy (SEM). In SEM the microstructure of the microcapsules prepared were studied. Urea-Formaldehyde shell (U-F shell) can see in the SEM image (Figure 4.32) which is shell for the tung-oil. The shape of the microcapsules are irregular but all the microcapsules were unbroken before use and they performed well when needed for self-healing.

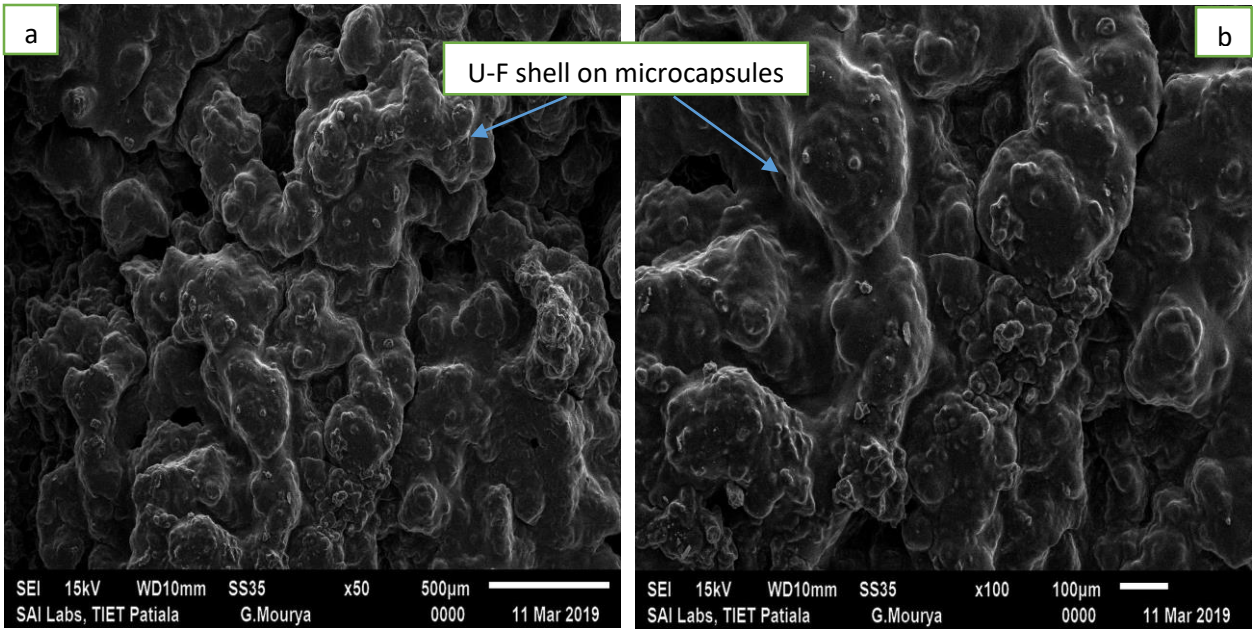

Figure 4.32: SEM images of tung-oil based micro-capsules at different magnification, a) at 500µm, b) at 100µm.

4.7 CLOSING REMARKS

The chapter discusses the results attained from the experiments conducted for the comparisons of effectiveness of all types of coatings on rebar in air and rebar in concrete. Highlights from all results been discussed, and it is clear from the results that tung-oil based micro-encapsulated coatings are most effective coating among all. Observation of pullout strength testing and SEM images of tung-oil based microcapsules were discussed in detail.

CHAPTER – 5

CONCLUSION AND FUTURE RECOMMENDATIONS

5.1 GENERAL

Self-healing methods have very high potential for implementation in construction industry. Use of micro-encapsulated self-healing agents extends the life of structures since healing agents remains non-reactive inside the shell and become reactive when triggered by damage, leads to improve the effectiveness of usage. In the present study, tung-oil based micro-encapsulated self-healing capsules and nano-clay based epoxy coatings has been used to delay the corrosion in reinforcing steel bars and their vis-à-vis performance is compared with their effectiveness in inhibiting corrosion.

5.2 CONCLUSION AND MAJOR FINDINGS

Based on the type of coatings used, method of testing and exposure to the rebar the following conclusions were stated as under:

5.2.1 Visual Inspection

- Air filled bubbles formed in PC rebar coatings, which once burst accelerates the corrosion.
- Bubbles formation reduced by the introduction of nano-clay in epoxy, NC rebar coatings leads to a poorer surface and water repellent nature.
- Bubbles formation in MC rebar coatings were air filled before self-healing effect and after self-healing polymerization reaction bubbles were filled by the polymerized material of tung-oil microcapsules leads to restrict the corrosion initiation.
- In MNC coated rebar, introduction of nano-clay leads to less bubble formation and self-healing effect was observed when bubbles filled with the polymerized material also non-uniformity of microcapsules observed in MNC coated rebar.
- Initial damage act as a week point for PC and NC coated rebar whereas for MC and MNC coated rebar initial damage does not affect the performance of rebar justifies the healing mechanism proposed in this work by tung-oil microcapsules.
- Tung-oil micro-encapsulated coated rebar found in best condition after a particular exposure of accelerated corrosion indicating self-healing effect due to microcapsules works appropriately.

5.2.2 Corrosion Current

- The increase in corrosion current at constant voltage indicates increase in corrosion rate.
- PC coated rebar significantly delay initiation of corrosion as compared with control rebar.
- In PC coated rebar passive layer breakdown was earlier than NC coated rebar since due to the nano-clay cracks take longer time to propagate. Introducing nano-clay in epoxy almost doubles the life of coated rebar.
- Micro-encapsulation of tung-oil works wonders in preventing the corrosion completely. They come into action when the passive layer breaks and healing starts by polymerization. It reduces the rate of corrosion significantly in comparison to PC coatings and NC coatings.
- Initially damage induced coatings lower the performance of PC and NC coated rebar whereas no effect on the performance of MC and MNC coated rebar is observed.
- In RC beams, coated rebar reported delay in the breakdown of passive layer. With MC coated bars, the initiation of corrosion is delayed best in comparison to plain epoxy and nano-clay based epoxy coatings.

5.2.3 Ultrasonic Guided Waves

- Ultrasonic voltage peak vanished for PC and NC coated rebar in 18 days and 41 days respectively, whereas voltage peak diminishes very little in 60 days of accelerated corrosion of MC and MNC coted rebar.
- Rate of voltage drop is lowest in MC coated rebar. Performance of coatings is in the order of MC, MNC, NC and then PC.

5.2.4 Destructive Testing

- Mass loss in plain rebar corrosion is 25% for control rebar and only 4% for the MC coated rebar indicating MC epoxy coating as most effective coating in comparison with PC, NC and MNC. Mass loss in beams with MC coated bar is least in comparison with all other coatings pointing towards the effectiveness of tung-oil based coatings.
- By introducing tung-oil microcapsules into the epoxy mass reduction in MC bar is 65% less comparison to plain epoxy based coated bar.
- Residual tensile strength is less for PC and NC rebar as compared to control rebar since continuous pitting in rebar due to corrosion is concentrated on single location leads to develop weak points.

- In control rebar residual strength is 40% more than the plain epoxy coated rebar.
- By introducing tung-oil microcapsules into the epoxy residual strength in MC bar is 63% more comparison to plain epoxy based coated bar and 40% more comparison to control rebar.
- Residual tensile strength is highest for tung-oil based coatings since self-healing mechanism restrict the corrosion and further pitting of rebar.

5.2.5 Pullout Strength

- The pullout strength of rebar follows MNC rebar, MC rebar, uncoated rebar, NC rebar and PC rebar in which maximum for MNC coated rebar and minimum for PC coated rebar.
- Variations in pullout strength for all coatings and uncoated rebar is not much different indicating that the provided thickness of the coatings barely affect the bond strength performance.
- Epoxy coated bars with different damage will definitely affect the pull-out strength when they are embedded in concrete and corroded but this is not studied in this work and this is the future scope of work.

5.3 RECOMMENDATIONS FOR FUTURE WORK

- In proposed coatings the effect of the different coating thicknesses on the corrosion inhibition can studied further.
- Different self-healing agents may use for the better compatibility with nano-clay coatings for hybrid coatings.
- Microscopic study on the effect of nano-clay presence on the uniformity of the microcapsules in the coatings.
- Study on large scale for the behavior of coatings under corrosion in the RC beams.

REFERENCES

- Achal, V., Mukherjee, A., & Reddy, M. S. (2010). Microbial concrete: way to enhance the durability of building structures. *Journal of materials in civil engineering*, *23*(6), 730-734.

- Ahn, T. H., & Kishi, T. (2008). The effect of geo-materials on the autogenous healing behavior of cracked concrete. In *Concrete Repair, Rehabilitation and Retrofitting II* (pp. 143-144). CRC Press.

- Al-Ansari, M., Abu-Taqa, A. G., Hassan, M. M., Senouci, A., & Milla, J. (2017). Performance of modified self-healing concrete with calcium nitrate microencapsulation. *Construction and Building Materials*, *149*, 525-534.

- ASCE, A Comprehensive Assessment of America's Infrastructure 2017.

- Bekas, D. G., Tsirka, K., Baltzis, D., & Paipetis, A. S. (2015). Self-healing materials: a review of advances in materials, evaluation, characterization and monitoring techniques. *Composites Part B: Engineering*, *87*, 92-119.

- Broomfield, J.P. (2007). Corrosion of Steel in Concrete: Understanding, Investigation and Repair, 2nd edition, New York: Taylor & Francis.

- Chen, Y., Xia, C., Shepard, Z., Smith, N., Rice, N., Peterson, A. M., & Sakulich, A. (2017). Self-healing coatings for steel-reinforced concrete. *ACS Sustainable Chemistry & Engineering*, *5*(5), 3955-3962.

- Clear, C.A. *The Effects of Autogenous Healing upon the Leakage of Water through Cracks in Concrete*; Cement and Concrete Association: Slough, UK, 1985; p. 28.

- Dong, B., Wang, Y., Fang, G., Han, N., Xing, F., & Lu, Y. (2015). Smart releasing behavior of a chemical self-healing microcapsule in the stimulated concrete pore solution. *Cement and Concrete Composites*, *56*, 46-50.

- Dong, B., Ding, W., Qin, S., Han, N., Fang, G., Liu, Y., & Hong, S. (2018). Chemical self-healing system with novel microcapsules for corrosion inhibition of rebar in concrete. *Cement and Concrete Composites*, *85*, 83-91.

- Du, W., Yu, J., Gu, Y., Li, Y., Han, X., & Liu, Q. (2019). Preparation and application of microcapsules containing toluene-di-isocyanate for self-healing of concrete. *Construction and Building Materials*, *202*, 762-769.

- Edvardsen, C. Water permeability and autogenous healing of cracks in concrete. *ACI Mater. J.* **1999**, *96*, 448–454.

- Fayala, I., Dhouibi, L., Nóvoa, X. R., & Ouezdou, M. B. (2013). Effect of inhibitors on the corrosion of galvanized steel and on mortar properties. *Cement and Concrete Composites*, *35*(1), 181-189.

- García-Alonso, M. C., Escudero, M. L., Miranda, J. M., Vega, M. I., Capilla, F., Correia, M. J., & González, J. A. (2007). Corrosion behaviour of new stainless steels reinforcing bars embedded in concrete. *Cement and concrete research*, *37*(10), 1463-1471.

- Hassan, M. M., Milla, J., Rupnow, T., Al-Ansari, M., & Daly, W. H. (2016). Microencapsulation of calcium nitrate for concrete applications. *Transportation Research Record*, *2577*(1), 8-16.

- Homma, D., Mihashi, H., & Nishiwaki, T. (2009). Self-healing capability of fiber reinforced cementitious composites. *Journal of Advanced Concrete Technology*, *7*(2), 217-228.

- In, C. W., Holland, R. B., Kim, J. Y., Kurtis, K. E., Kahn, L. F., & Jacobs, L. J. (2013). Monitoring and evaluation of self-healing in concrete using diffuse ultrasound. *NDT & E International*, *57*, 36-44.

- Jacobsen, S.; Sellevold, E.J. Self-healing of high strength concrete after deterioration by freeze/thaw. *Cem. Concr. Res.* **1995**, *26*, 55–62.

- Jonkers, H. M., Thijssen, A., Muyzer, G., Copuroglu, O., & Schlangen, E. (2010). Application of bacteria as self-healing agent for the development of sustainable concrete. *Ecological engineering*, *36*(2), 230-235.

- Jonkers, H. M., & Schlangen, E. (2007). Self-healing of cracked concrete: a bacterial approach. *Proceedings of FRACOS6: fracture mechanics of concrete and concrete structures. Catania, Italy*, 1821-1826.

- Kim, D. M., Yu, H. C., Yang, H. I., Cho, Y. J., Lee, K. M., & Chung, C. M. (2017). Microcapsule-type self-healing protective coating for cementitious composites with secondary crack preventing ability. *Materials*, *10*(2), 114.

- Kuang, Y., & Ou, J. (2008). Self-repairing performance of concrete beams strengthened using super-elastic SMA wires in combination with adhesives released from hollow fibers. *Smart Materials and Structures*, *17*(2), 025020.

- Lau, K., Sagüés, A. A., & Powers, R. G. (2007). Long-term corrosion behavior of epoxy coated rebar in Florida Bridges. *CORROSION/2007, paper*, (07306).

- Li, V.C.; Lim, Y.M.; Chan, Y.-W. *(*1998) Feasibility study of a passive smart self-healing cementitious composite. *Compos. Part B Eng.*, *29*, 819–827.

- Li, W., Jiang, Z., & Yang, Z. (2017). Acoustic characterization of damage and healing of microencapsulation-based self-healing cement matrices. *Cement and Concrete Composites*, *84*, 48-61.

- Miller, T. H., Kundu, T., Huang, J., & Grill, J. Y. (2013). A new guided wave–based technique for corrosion monitoring in reinforced concrete. *Structural Health Monitoring*, *12*(1), 35-47.

- Nishiwaki, T.; Koda, M.; Yamada, M.; Mihashi, H.; Kikuta, T. (2012) Experimental study on self-healing capability of FRCC using different types of synthetic fibers. *J. Adv. Concr. Technol.*, *10*, 195–206.

- Qian, S.Z.; Zhou, J.; Schlangen, E. *(*2010) Influence of curing condition and pre-cracking time on the self-healing behavior of Engineered Cementitious Composites. *Cem. Concr. Compos. 32*, 686–693.

- Restuccia, L., Reggio, A., Ferro, G. A., & Tulliani, J. M. (2017). New self-healing techniques for cement-based materials. *Procedia Structural Integrity*, *3*, 253-260.

- Şahmaran, M.; Keskin, S.B.; Ozerkan, G.; Yaman, I.O. Self-healing of mechanically-loaded self-consolidating concretes with high volumes of fly ash. *Cem. Concr. Compos.* **2008**, *30*, 872–879.

- Sakai, Y.; Kitagawa, Y.; Fukuta, T.; Iiba, M. (2003) Experimental study on enhancement of self-restoration of concrete beams using SMA wire. In Proceedings of Conference on Smart Structures and Materials, San Diego, CA, USA.

- Samadzadeh, M., Boura, S. H., Peikari, M., Ashrafi, A., & Kasiriha, M. (2011). Tung oil: An autonomous repairing agent for self-healing epoxy coatings. *Progress in Organic Coatings*, *70*(4), 383-387.

- Sangadji, S.; Schlangen E. (2012) self-healing of concrete structures Novel approach using porous network concrete. Journal of Advanced concrete technology vol. 10, 185-194.

- Sharma, A., Sharma, S., Sharma, S., & Mukherjee, A. (2015). Ultrasonic guided waves for monitoring corrosion of FRP wrapped concrete structures. *Construction and Building Materials*, *96*, 690-702.

- Sharma, A., Sharma, S., Sharma, S., & Mukherjee, A. (2018). Monitoring invisible corrosion in concrete using a combination of wave propagation techniques. *Cement and Concrete Composites*, *90*, 89-99.

- Sharma, S., & Mukherjee, A. (2011). Monitoring corrosion in oxide and chloride environments using ultrasonic guided waves. *Journal of Materials in Civil Engineering*, *23*(2), 207-211.

- Sharma, S., & Mukherjee, A. (2013). Nondestructive evaluation of corrosion in varying environments using guided waves. *Research in Nondestructive Evaluation*, *24*(1), 63-88.

- Sharma, S., & Mukherjee, A. (2015). Monitoring freshly poured concrete using ultrasonic waves guided through reinforcing bars. *Cement and Concrete Composites*, *55*, 337-347.

- Shirehjini, F. T., Danaee, I., Eskandari, H., & Zarei, D. (2016). Effect of Nano clay on corrosion protection of Zinc-rich epoxy coatings on steel 37. *Journal of Materials Science & Technology*, *32*(11), 1152-1160.

- Singh, K., Nanda, T., & Mehta, R. (2017). Compatibilization of polypropylene fibers in epoxy based GFRP/clay nanocomposites for improved impact strength. *Composites Part A: Applied Science and Manufacturing*, *98*, 207-217.

- Song, Y.K.; Jo, Y.H.; Cho, S.Y.; Yu, H.C.; Ryu, B.C.; Lee, S.I.; Chung, C.M. (2013), Sunlight-induced self-healing of a microcapsule-type protective coating. ACS Appl. Mater. Interfaces 5, 1378–1384.

- Ter Heide, N.; Schlangen, E. Self-healing of early age cracks in concrete. In Proceedings of 1st International Conference on Self-Healing Materials, Noordwijk aan Zee, The Netherlands, 18–20 April 2007.

- Tsangouri, E., Aggelis, D. G., Van Tittelboom, K., De Belie, N., & Van Hemelrijck, D. (2013). Detecting the activation of a self-healing mechanism in concrete by acoustic emission and digital image correlation. *The Scientific World Journal*, *2013*.

- Van Tittelboom, K., & De Belie, N. (2013). Self-healing in cementitious materials—A review. *Materials*, *6*(6), 2182-2217.

- Wang, X., Xing, F., Zhang, M., Han, N., & Qian, Z. (2013). Experimental study on cementitious composites embedded with organic microcapsules. *Materials*, *6*(9), 4064-4081.
- White, S. R., Sottos, N. R., Geubelle, P. H., Moore, J. S., Kessler, M., Sriram, S. R., & Viswanathan, S. (2001). Autonomic healing of polymer composites. *Nature*, *409*(6822), 794.

- Weishaar, A., Carpenter, M., Loucks, R., Sakulich, A., & Peterson, A. M. (2018). Evaluation of self-healing epoxy coatings for steel reinforcement. *Construction and Building Materials*, *191*, 125-135.

- Xue, C., Li, W., Li, J., Tam, V. W., & Ye, G. (2018). A review study on encapsulation-based self-healing for cementitious materials. *Structural Concrete*.

- Yang, H.I.; Kim, D.M.; Yu, H.C.; Chung, C.M. (2016), Microcapsule-type organogel-based self-healing system having secondary damage preventing capability. ACS Appl. Mater. Interfaces 8, 11070–11075.

- Yang, Z.; Hollar, J.; He, X.; Shi, X.; *(*2011) A self-healing cementitious composite using oil core/silica-gel shell microcapsules. *Cem. Concr. Compos*, *33*, 506–512.

Thesis

ORIGINALITY REPORT

14%	3%	10%	7%
SIMILARITY INDEX	INTERNET SOURCES	PUBLICATIONS	STUDENT PAPERS

PRIMARY SOURCES

1	Submitted to Thapar University, Patiala Student Paper	1%
2	www.mdpi.com Internet Source	1%
3	Yixi Chen, Chris Xia, Zachary Shepard, Nicholas Smith, Nicholas Rice, Amy M. Peterson, Aaron Sakulich. "Self-Healing Coatings for Steel-Reinforced Concrete", ACS Sustainable Chemistry & Engineering, 2017 Publication	1%
4	Biqin Dong, Weijian Ding, Shaofeng Qin, Ningxu Han, Guohao Fang, Yuqing Liu, Feng Xing, Shuxian Hong. "Chemical self-healing system	1%